Dissertation

Kaempferol ameliorates calcium oxalate crystal-induced renal injury and crystal deposition by attenuating oxidative stress and inflammation through the downregulation of the AR/NOX2 signaling pathway

submitted by

Xifeng SUN

for the Academic Degree of

Doctor of Medical Science (Dr. scient. med.)

at the

Medical University of Graz

Department of Urology

under the Supervision of

Prof. Dr. Georg HUTTERER

2022

Declaration of Academic Integrity

I hereby confirm that the present diploma thesis is the result of my own independent scholarly work. I also confirm that in all cases, where material from the work of others (in books, articles, essays, dissertations, and on the internet) is acknowledged, quotations and paraphrases are clearly indicated. No material other than that cited in the reference list has been used. I have read and understood the Medical University's regulations and procedures concerning plagiarism.

Graz, 01.12.2022

Disclosures

All parts of this thesis have been published in Yuan P, Sun X, Liu X, Hutterer G, Pummer K, Hager B, et al. Kaempferol alleviates calcium oxalate crystal-induced renal injury and crystal deposition via regulation of the AR/NOX2 signaling pathway. Phytomedicine. 2021; 86:153555. (1).

All co-authors have explicitly agreed to the use of their data in this thesis.

Obtained permission of reproduction: Yes. As the author of this Elsevier article, I retain the right to include it in a thesis or dissertation.

Contribution in the published paper: Doctoral student Xifeng Sun carried out experiments, collected the data, analyzed the data, and drafted the original manuscript.

Acknowledgements

Doctoral student Xifeng Sun received funding from the Chinese Scholarship Council (CSC,

no. 202107710003), the National Natural Science Foundation of China (No.81670645), and the Medical University of Graz through the Doctoral School “Sustainable Health Research Doctoral School, SHR”.

Sincere thanks to the Doctoral Program in Medical Science and the Doctoral School “Sustainable Health Research Doctoral School, SHR” at the Medical University of Graz.

Thanks

Time flies, the thesis has come to an end. I would like to express my great appreciations to all the people who helped me during my doctoral study and life in Graz. Firstly, I would like to thank my supervisor **Assoz. Prof. Georg Hutterer**, and I am grateful for giving the opportunity to become one of the members in your group. I sincerely thank for your significant guidance and support in daily life, and evaluable revisions and recommendations in the thesis. Secondly, I would like to thank the two reviewers **Prof. Christian Seitz** and **Prof. Alexander Kirsch** for reviewing my thesis and making great and helpful suggestions for revisions. And I sincerely thank **Prof. Sebastian Mannweiler** for becoming the chairperson of my final comprehensive oral examination board. Then I would like to thank the members of Dissertation Committee **Prof. Richard Zigeuner** and **Assoz. Prof. Martin Pichler**, making much effort to evaluate my thesis. A great thank to two directors **Prof. Sascha Ahyai** and **Prof. Karl Pummer** of department of urology, creating a nice platform for us to work and study. I also express my true gratitude to **Dr. Boris Hager**, providing the initial project plan and support for my doctoral study. My doctor’s life will not go so well without the help of **Prof. Andrea Berghold**, **Ms. Petra Seidler**, **Ms. Veronika Rechberger** and **Ms. Miriam Sedej**. Moreover, I would like to

thank **Dr. Peng Yuan, Dr. Xiao Liu, Prof. Zhangqun Ye,** and **Prof. Zhiqiang Chen** for the project cooperation.

Finally, I would show my deepest thanks to my family, girlfriend, and friends. Your silent support, understanding and love make me concentrate on my doctoral study.

Thank all you for reading my thesis.

Conflicts of interest

None.

Table of Contents.

Abbreviations 6
Graphical abstract 9
Abstrakt 10
Abstract 12
1. Introduction 14
2. Materials and methods 34
2.1. Animal procedures 34
2.2. Cell Culture and treatment 36
2.3. Measurement of renal function and acute kidney injury 37
2.4. Renal histology 37
2.5. Cell viability assay 38
2.6. Crystal adhesion assay 39
2.7. Real-time quantitative Polymerase Chain Reaction (RT-qPCR) 40
2.8. Western blot (WB) assay 41
2.9. Immunofluorescence (IF) assay 42
2.10. Chromatin Immunoprecipitation (ChIP) assay 43
2.11. Luciferase reporter assay 43
2.12. Measurement of ROS and H2O2 levels 44
2.13. Measurement of SOD, MDA, and glutathione (GSH) levels 44
2.14. Statistical analysis 44
3. Results 45
3.1. Effects of kaempferol on renal tubular damage and CaOx crystal deposition in mice 45
3.2. Effects of kaempferol on cell deaths induced by CaOx crystals, and crystal adhesions to HK-2 cells 50
3.3. Effects of kaempferol on OS and inflammation led by CaOx crystals in HK-2 cells and in mice 54
3.4. Possible mechanisms on how kaempferol inhibited NOX2 expression via mediating AR expression 63
3.5. Kaempferol ameliorates CaOx crystal deposition, tubular injury, and OS and

inflammation induced by CaOx crystals by regulating the AR/NOX2 pathway in mice kidney 68
3.6. Kaempferol suppressed cell injury, crystal-cell adhesion, OS, and inflammation induced by CaOx crystals by downregulating AR/NOX2 pathway in HK-2 cells 76
4. Discussion 82
Bibliography 94
Attachment 115

Abbreviations

AR: androgen receptor

ARE: androgen receptor element

BMPs: bone morphogenetic proteins

BUN: blood urea nitrogen

CaOx: calcium oxalate

CaP: calcium phosphate

CAT: catalase

CCK-8: Cell Counting Kit-8

ceRNA: competing endogenous RNA

CHIP: Chromatin Immunoprecipitation

CMC-Na: sodium carboxymethylcellulose

CNPs: Calcifying nanoparticles

COM: calcium oxalate monohydrate

Cr: creatinine

CSF-1: colony-stimulating factor 1

Cyp D: cyclophilin D

DAPI: 4',6-diamidino-2-phenylindole

DC: dendritic cell

DCFH-DA: 2,7-Dichlorodi-hydrofluorescein diacetate

DHT: dihydrotestosterone

DMSO: dimethyl sulfoxide

ERβ: estrogen receptor beta

EREs: estrogen response elements

ESWL: extracorporeal shock wave lithotripsy

GA: glyoxylic acid

GSH: glutathione

HE: hematoxylin–eosin

hRIFs: human renal interstitial fibroblasts

HK-2: Human renal cortex proximal tubule epithelial cells

IαI: Inter-alpha-inhibitor

IC50: 50% inhibitive concentration

IFN-γ: interferon-γ

IHC: Immunohistochemistry

iNOS: inducible NOS

KSF: kidney stone former

LDH: lactate dehydrogenase

LNCaP: Lymph Node Carcinoma of the Prostate

LncRNA: long non-coding RNA

LPS: lipopolysaccharide

MCP1: monocyte chemoattractant protein-1

MDA: Malondialdehyde

MPT: mitochondrial permeability transition

MSX2: msh homeobox 2

NB: Nanobacteria

NC: Normal control

NFκB-p65: nuclear factor kappa B-p65

NGAL: neutrophil gelatinase-associated lipocalin

NOX: nicotinamide adenine dinucleotide phosphate (NADPH) oxidase

OPN: osteopontin

OS: oxidative stress

PAS: periodic acid schiff

PBS: phosphate buffer saline

PCNL: percutaneous nephrolithotomy

ROS: reactive oxygen species

RPs: Randall's plaques

RT-qPCR: Real-time quantitative Polymerase Chain Reaction

RUNX2: Runt-related transcription factor 2

SD: Standard deviation

SEM: Scanning electron microscopy

SOD: Superoxide dismutase

TP: testosterone propionate

WB: Western blot

Graphical abstract

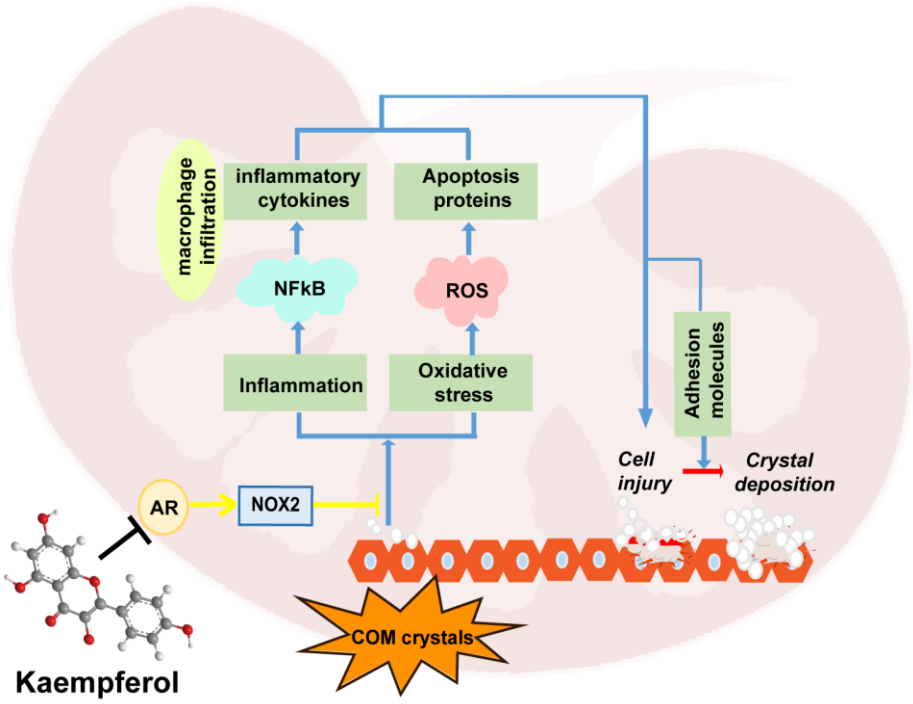

Abstrakt

Hintergrund

Oxidativer Stress (OS) und Entzündungen gelten als entscheidende Faktoren für den Prozess der Bildung von Urolithiasis.

Methoden

Wir verwendeten Mäusemodelle und menschliche Nieren-2 (HK-2) -Zellen, um die Rolle und den Mechanismus von Kaempferol in CaOx-Kristall-induzierten Nierenkristallablagerungen und -verletzungen zu untersuchen. Die Kristallablagerung in der Niere wurde durch pathologische Untersuchung bewertet und Nierenverletzungen durch histologische Färbung und Serumneutrophil-Gelatinase-assoziiertes Lipocalin, Harnstoffstickstoff und Kreatinin nachgewiesen. Die Kristalladhäsion an HK-2-Zellen wurde durch Mikroskopie beobachtet, und die Zellverletzung wurde durch Durchflusszytometrie nachgewiesen. Die oxidative Spannung wurde durch Durchflusszytometrie, Fluoreszenzbildgebung und Mikroplatten gemessen. Immunhistochemie -Färbung, Fluoreszenzfärbung, Western Blot und Polymerasekettenreaktion wurden verwendet, um die Genexpressionen zu bewerten. Der Mechanismus, wie der Androgenrezeptor (AR) Nicotinamid -Adenin -Dinukleotid -Phosphatoxidase 2 (NOX2) reguliert, wurde durch Chromatin -Immunpräzipitation und Luciferase -Reporter -Assay geprägt.

Ergebnisse

Kaempferol verringerte die CaOX-Kristallablagerung in der Mäusekidney- und

Kristalladhäsion an HK-2-Zellen. Kaempferol unterdrückte kristallinduzierte Zellverletzungen, Entzündungen und OS in In-vivo und in vitro. Darüber hinaus inhibierte Kaempferol die Nieren -AR -Expression, und AR könnte direkt an den NOX2 -Promotor binden, um die NOX2 -Expression auf Transkriptionsebene zu fördern. Kaempferol spielte eine Schlüsselrolle bei der Hemmung der kristallinduzierten Nieren-OS und einer entzündlichen Verletzung und der Kristallablagerung, indem der AR/NOX2-Signalweg herunterreguliert wurde.

Fazit

Insgesamt legt diese Arbeit nahe, dass Kaempferol durch die Hemmung des OS und der Entzündung durch Herunterregulierung des AR/NOX2-Signalwegs die Nierenkristall-induzierte Verletzung und Kristallablagerung hemmen könnte. Kaempferol kann potenzielle vorbeugende und therapeutische Wirkungen für die CaOx -Urolithiasis haben.

Abstract

Background

Oxidative stress (OS) and inflammation are thought to be crucial contributors to the process of forming urolithiasis.

Methods

We used mice models and human kidney-2 (HK-2) cells to explore the role and mechanism of kaempferol in CaOx crystal-induced renal crystal deposition and injury. The crystal deposition in kidney was evaluated by pathologic examination, and renal injury was detected by histological staining and serum neutrophil gelatinase-associated lipocalin, urea nitrogen and creatinine. Crystal adhesion to HK-2 cells was observed by microscopy, and cell injury was detected by flow cytometry. Oxidative stress was measured by flow cytometry, fluorescence imaging and microplate. Immunohistochemistry staining, fluorescence staining, western blot and polymerase chain reaction were used to assess the gene expressions. The mechanism of how androgen receptor (AR) regulates nicotinamide adenine dinucleotide phosphate oxidase 2 (NOX2) was dissected via chromatin immunoprecipitation and luciferase reporter assay.

Results

Kaempferol decreased CaOx crystal deposition in mice kidney and crystal adhesion to HK-2 cells. Kaempferol suppressed crystal-induced cell injury, inflammation, and OS in *in vivo* and *in vitro*. Moreover, kaempferol inhibited the renal AR expression, and AR could directly bind to the NOX2 promoter to promote NOX2 expression at the transcriptional

level. Kaempferol played a key role in inhibiting crystal-induced renal OS and inflammatory injury, and crystal deposition by downregulating the AR/NOX2 signal pathway.

Conclusion

All in all, this work suggests that kaempferol could inhibit renal crystal-induced injury and crystal deposition by inhibiting OS and inflammation by downregulating the AR/NOX2 signal pathway. Kaempferol may have potential preventive and therapeutic effects for CaOx urolithiasis.

Keywords

Androgen receptor; Calcium oxalate crystal; Inflammation; Kaempferol; NOX2; Oxidative stress; Urolithiasis.

1. Introduction

Urolithiasis is a general urological disease, and about 1-15% of the world's population suffer from urolithiasis in a lifetime, and the prevalence and incidence rates of urolithiasis are both increasing across gender, races, and age worldwide especially in many developed countries, resulting in corresponding heavy medical burden (2, 3). In China, urolithiasis has a lifetime prevalence of up to 15.5%, and leads to heavy socioeconomic and healthcare burden (4, 5). Without timely treatments, kidney stone may result in ureter blockage, hematuria, painful urination, frequent urinary tract infections, backache and vomiting, which may eventually lead to permanent functional damage to kidney function (6). Urolithiasis has a 50% recurrence rate within 5-10 years and up to 75% within 20 years (7). Previous researches revealed that the urolithiasis occurrence rate was increasing because of many factors including dietary habits and lifestyle changes, and global warming (6, 8). But exact factors contributing to the growth of urolithiasis have not been clarified. Because of the high incidence in working-age adults, urolithiasis has become a public health problem with a far-reaching influence on the population and society (9, 10).

There are five primary types of kidney stone based on the different compositions, containing calcium oxalate (CaOx), calcium phosphate (CaP), uric acid, magnesium ammonium phosphate (struvite) and cystine with approximate percentages of 64%, 16%, 9%, 10%, 1% (11-13). Calcium-containing calcareous stones CaOx and CaP are radio-opaque (14). Kidney stones are considered to form above the basis of Randall's plaques (RPs) whose main composition is CaP, which starts from the basement membrane

of thin limb of the Henle loops at the renal papillary surfaces (15). CaOx and uric acid stones represent higher incidence rates in male, while CaP and struvite stones show higher incidence rates in female (13, 16). But the relevant precise mechanisms of gender difference in urolithiasis are still unclear.

Apart from stone types, the formation of urolithiasis is a complicated and multi-step process, containing supersaturation of urine, and nucleation, growth, aggregation and retention of crystals (14). Stone formation is believed to have a strong relationship with systemic disorders, including metabolic syndrome, hypertension, cardiovascular diseases, diabetes, and obesity (17-21). The traits of metabolic syndrome is correlated to significantly increased risks of hypocitraturia, hyperoxaluria, hyperuricosuria, hypercalciuria, and higher rate and recurrence rate of kidney stone or multiple stones (22). Moreover, proinflammatory adipocytokines and macrophages in metabolic syndrome mice model significantly facilitates the formation of renal crystals (23). Conversely, kidney stone formers (KSF) have a higher risk of chronic kidney disease and hypertension (24-26). Various promoters and inhibitors have been revealed to play important regulatory roles in the formation process of urolithiasis. Hyperoxaluria, phosphaturia and hyperuricosuria are promoters, and can increase the kidney stones formation risk (27, 28). Inter-alpha-inhibitor (IαI) is a protease inhibitor, and was revealed to suppress the formation of CaOx crystal (29). Previous studies also demonstrated that cell injury of renal tubular epithelium in turn promote CaOx crystal adhesion, and the CaOx crystal or excessive oxalate ion exposure was able to worsen renal injury (30-32). Taken together, cell injury has an important part in the formation process of CaOx urolithiasis.

Although evidence of the formation processes of kidney stone have been revealed, precise formation and development mechanisms are still to be determined. Over time, various theories and different strategies have been proposed and applied in treating and managing KSF, with recent developments of technology. Research directions show several different mechanisms of the formation of kidney stones. Urine supersaturation and crystallization are the two most important initial steps for renal crystal deposition. RPs are considered the formation origin of CaOx stones. The microbiome such as intestinal microbiota, nanobacteria and urease-producing bacteria, have potential to have profound influences on the urinary tract, positive or negative, based on the metabolic properties and possible mechanisms. Sex hormones are crucial factors in developing urolithiasis and can be potential new drug targets to inhibit urolithiasis. The immune responses, especially macrophage polarizations, play critical roles in the CaOx crystal formation in kidney. Vascular calcification has been suggested to have a close link with kidney stone formation. Knowing knowledge of various aspects of urolithiasis is helpful to discover novel problems, explore new research directions, and deepen understanding of the formation and development of urolithiasis for primary care and urologists.

Firstly, urine supersaturation is important force for renal crystal deposition, and primarily results from associated acquired or inherited disorders with damaged renal functions. In the first place, urine supersaturation is mainly influenced by concentrations of specific substances and urine pH, and CaOx, CaP, uric acids, amino acids, purines, and drugs such as atazanavir, sulfamethoxazole, ceftriaxone and amoxicillin are main specific substances (33, 34). Then, stone formation and development process is impacted by

various regulatory molecules, including receptors, promoters, and inhibitors.

Many promoters have been revealed to take crucial part in cell-crystal interactions, and are very important part in renal crystal formation processes (10, 35). In a recent study, alterations of proteins in CaOx monohydrate (COM) treatment model were analyzed, and over 1,100 proteins in HK-2 cells with COM treatment were identified to be differentially expressed (36). Proteins and glycosaminoglycan such as osteopontin (OPN), Annexin II, heat shock protein 90, hyaluronan, nucleolin, and CD44, have been revealed to be stone formation promoters (37-40). Several molecular components and structures, such as the phosphatidylserine component of the lipid bilayers and the acidic side chains of proteins, take an important part in cell-crystal attachment (41). A previous study found that first-time KSF had enhanced serum 1,25(OH)2D and calcium level compared with healthy individuals, indicating that kidney stone formation may be a consequence of elevated vitamin D and calcium levels (42). High level of serum calcium is a promoter of stone formation, which can be modulated by the calcium sensor receptors (43). Moreover, phosphate and urate ions were found to enhance the process of heterogeneous nucleation and increase the crystal attachments to tubular cells (44, 45). Urine pH is a crucial promoter for forming stones (46). Low pH can result in CaOx crystallization and then precipitation of crystal (47). High-alkaline can enhance CaOx crystals nucleation and precipitation (48). Recently, proteins lysozyme and lactoferrin were found to increase the development of COM crystals by promoting the advancement rate of surface layers (49).

A number of inhibitors exist in normal urine, and are competitive and cooperative, consequently inhibiting crystallization, crystal development and attachment to the tubular

cell (50, 51). Inhibitors are mainly categorized into 3 groups: Metallic cations, anions, and macromolecules. In the majority of urolithiasis patients, the levels of citrate excretion are decreased, and citrate anions can be able to decrease the growth of crystals effectively when their concentration is above 0.1 mM (52, 53). Alkali supplement is widely applied for treating recurrent hypocitraturic urolithiasis patients to recover citrate levels back to normal (54, 55). Hydroxycitrate, one of structural analogs of citrate, is also recently found to have excellent ability in inhibiting crystal formation and growth by combining with calcium (56, 57). Metallic ions such as magnesium were found to suppress the development and aggregation of crystal, and have synergy with citrate in an acidic environment (58, 59). Macromolecules are considered the most efficient inhibitors of growth of crystal. For example, it was revealed that some subunits of the serum IαI, nephrocalcin, Tamm-Horsfall protein, OPN, and urinary prothrombin fragment 1 could suppress the development, aggregation, and adhesion of crystal to the renal tubular cell (14, 53, 59).

Above all, it is a competitive relationship between saturation states, promoters and inhibitors, which eventually decides the patterns of crystal formation in urolithiasis patients and healthy people (60). In states of saturation, excessive promoters and decreased inhibitors can promote crystal formation and growth, and finally stones occur.

In 1937, RPs were firstly reported by Alexander Randall (61), and are mineralized regions containing CaP, located at the tissue under the epithelial of the papillary tips and surrounded by the Bellini ducts openings (62). Scanning electron microscopy (SEM) test results have found that RPs contained tubules obstructed by CaP plugs and calcified

tubules (63). RPs consist of CaP and an organic matrix which contain various lipids and proteins, and also can contain exosomes, membrane bound vesicles, collagen fibers, or extracellular matrix components (64). RPs are widely considered the origin of kidney stones (65). A study previously revealed that kidney stone was the overgrowth on RPs, and the stone overgrowth part did not contain fibrillar collagen, a unique organic composition, which was the biggest difference (66). In addition, a recent study using a murine RPs model found that supplementation of vitamin D and intake of calcium significantly promoted the formation of RPs (67). But the specific and complete mechanisms of RPs formation are still unknown.

Recent researches have demonstrated that long non-coding RNA (lncRNA) MALAT1 and H19 regulated the osteogenic differentiations of human renal interstitial fibroblasts (hRIFs) and played a role in the process of RPs formation (68, 69). lncRNA MALAT1 is a competing endogenous RNA (ceRNA) by sponging miR-320a-5p, and enhances Runt-related transcription factor 2 (RUNX2) expression, and then promotes the osteogenic phenotypes of hRIFs (69). It was reported that lncRNA H19 was significantly increased in RPs, promoting hRIFs osteogenic differentiation through the activation of Wnt/β-catenin signal pathway (68). lncRNA H19 also can be a promoter in the induction of OS and cell injury by the CaOx crystal deposition to renal tubular epithelial cells through interacting with miR-216b, and perform the function through the HMGB1/TLR4/NF-κB signal (70).

Studies have been provided novel insights of the pathogenesis of RPs-regulated kidney stones formation, although what provokes the formation of RPs is yet unknown. Therefore, studies exploring the precise mechanisms of RPs formation, and exact role of RPs in the

process of stones formation are urgently needed in the future.

More and more evidence have suggested that the renal and urinary microbiome has important effects on the health of urinary system, because of metabolic activities and other aspects (71).

Urease-producing bacteria, such as *Morganella morganii, Serratia, Pseudomonas aeruginosa, Staphylococcus aureus, Klebsiella pneumonia* and *Proteus mirabilis*, are reported to be strongly associated with formation of struvite stones and higher recurrence rate (72, 73). The produced urease can degrade urea and increase the generation of ammonia and carbon dioxide, thereby alkalizing urine and precipitating phosphate compounds.

Up to date, acidification of urine and urease inhibitors are suggested and administered for preventing or dissolving struvite stone and for preventing the encrustation in patients infected with urease-producing bacteria, while the long-term use is limited because of the possible invalidity and toxicity (74). Also, non-urease-producing bacteria (e.g., *Enterococcus spp.* and *Escherichia coli*) can cause secondarily infected stones (75, 76).

More than 30 years ago, nanobacteria (NB) were separated from kidney stones (77-79), but the exact properties and the involved mechanisms are still unclear. Diameters of NB were reported to be 60 - 160 nm, and NB infection was found in apatite kidney stone patients (80). It was revealed that NB were able to grow in normal RPMI-1640 or DMEM by self-proliferation (81). Although the highest immunopositivity was detected in apatite-based kidney stones, the NB presence did not have significant associations with the stone types (81). In a previous research, it was reported that NB existed in 97.2% (70/72)

kidney stones (82). Because NB are able to generate sufficient CaP to induce calcification and then stone formation, NB is thought to take crucial part in calcium nucleation, which is strongly supporting the suggestions that NB are actually living organisms (83-85).

On the contrary, accumulating evidence suggests that NB, also named 'Nanobes', 'nanobacteria-like particles' or 'Calcifying nanoparticles (CNPs)', display biomimetic functions and are just nanoparticles containing minerals and proteins (77, 79). As the precise definitions and nature of CNPs are still unclear and controversial, the functions of NB in kidney stones have been widely researched (86). CNPs were found and detected in RPs, and were tested to have cytotoxicity to HK-2 cells and 3T6 fibroblasts (79). It was indicated that CNPs could promote the generation of reactive oxygen species (ROS) via activating the JNK signal pathway, inhibit mitochondrial membrane potentials and increase cell apoptosis of cells via upregulating the expressions of Bax and downregulating the expressions of Bcl-2, and result in cell autophagy via upregulating the expressions of microtubule-related proteins such as Beclin-1 and LC3-II (79). CNPs can contribute to cell injury of tubular cells in the process of stone formation. It was indicated that malonaldehyde (MDA) level and catalase (CAT) level were markedly increased in renal tubular cells with CNP treatment compared with control group, which suggested that CNPs could promote the generation of OS especially lipid peroxidation and finally lead to the damages to HK-2 cells (87).

Based on currently reported results, NB are located in the kidney, and are isolated from RPs and most kidney stones, existed in urine, and take a crucial part in the initiation of stones via promoting calcium nucleation and crystal formation. Further future studies

should be undertaken to resolve the question of whether NB are alive or not, and to demonstrate the exact mechanisms of how NB induce nucleation and stones formation.

The intestinal microbiota is a thriving research area with wide interest worldwide, and has been suggested to take a significant part in the pathogenesis of urinary stone diseases (88-90). *Oxalobacter formigenes* have potential probiotic properties and can degrade oxalate in the intestinal tract, making it the most well-researched Gram-negative anaerobic bacterium for preventing formation of CaOx kidney stones (90).

Stern et al. performed a pilot study, and indicated significant gut microbiome differences in urolithiasis formers (91). The findings demonstrated that the genus *Bacteroides* was markedly richer in urolithiasis patients, while the genus *Prevotella* were significantly richer in the normal control group. Involved with 24-h urine analysis of KSF, this study indicated that the genus *Escherichia* also showed a negative correlation with citrate levels, and the genus *Eubacterium* were negatively correlated with oxalate level (91). Ticinesi et al. found that faecal microbial diversity was less in urolithiasis patients, and three taxa (*Dorea, Enterobacter, Faecalibacterium*) expressions significantly decreased in the faecal samples of stone formers (89).

Studies have identified both secretory and absorptive pathways for oxalate in the distal and proximal segment of the colon, mediated by neurohormone which can directly regulate serum oxalate level (92, 93). It is also assumed that the intestinal tract significantly takes part in the processes of oxalate level balance and oxalate homeostasis, and the intestinal tracts are the areas in which oxalate degrading bacteria reside, especially *Oxalobacter formigenes* because they require a strictly anaerobic environment to live (94). A reasonable

assumption of the roles of the microbiome in preventing kidney stones formation is bacteria with special functions, for example the oxalate degrading bacteria (*Bacillus sp., Porphyromonas gingivalis, Bifidobacterium sp.*, and *Oxalobacter formigenes*), play important functions in the human intestinal tract, making use of oxalate to be the source of energy and thriving in oxalate ion environment, and inhibit the renal CaOx crystallization and growth (95-97). The activities of oxalate degrading bacteria mediate oxalate elimination in the intestinal tract and have a marked influence on the homeostatic oxalate level in urine and plasma, which can finally have an influence on CaOx stone formation (98).

However, a previous work found that the abundance of *Oxalobacter formigenes* was not markedly different between stone formers and control group through metagenome analysis of gut microbiota, but expressions of oxalate-degrading related genes were significantly decreased in a few species of bacteria in urolithiasis patients and the cumulative abundances were negatively correlated with oxaluria (89). Regrettably, observation and intervention studies have given conflicting results, making it contradictory in its role of the microbes in kidney stones formation (99).

It is still unclear how the microbiota may be incorporated in the novel gut-kidney axis, even though personal dietary habits and composition are widely considered to be decisive factors in the composition of the intestinal microbiome. For example, nutritional imbalances, like low fruit and vegetable intake, low calcium, high animal proteins, poor hydration, and high salt, are recognized as the primary risks for CaOx kidney stones diseases (100, 101). On the contrary, adequate water intake, adequate dairy consumption,

normal fruit and vegetable intake, low salt intake and low animal protein intake are thought to be effective diet and non-drug prevention of urolithiasis (102, 103).

Up to date, the precise causative mechanisms of gut microbiota dysbiosis in kidney stones diseases are still not clear, and the exact correlations of urinary excretion level of oxalate and abundances of oxalate degrading bacteria is under study (78, 96, 104).

Macrophage recruitment and accumulation, and inflammation or anti-inflammation are primary immune response alterations found in urolithiasis, which have been widely revealed to take critical part in CaOx crystal formation and growth in kidney (105). Infiltrating monocytes can be differentiated into different macrophage phenotypes with a number of histological phenotypes, presentations and clinical manifestations, displaying protective or pathogenic properties in the development process of renal stone diseases (105).

Firstly, increased macrophage recruitment could improve the growth of COM crystal via interacting CD44 with fibronectin (FN) and OPN, whose expressions are increased in tubular cells after induction by COM crystals (106). Furthermore, various regulators have been identified to be secreted by macrophages by classical pathways, and these regulators can lead to interstitial inflammation in kidney, especially IL-8, monocyte chemoattractant protein-1 (MCP1) and macrophage inhibitory protein-1 (107, 108). These special chemokines could promote the recruitment of different immune cells, such as T cells, dendritic cells (DC), neutrophils, macrophages, and monocytes, into corresponding inflammation position (109, 110). It is reported that after exposure to COM crystals macrophage-secreted exosomes take an important part in the formation and growth

processes of renal stones (107, 108, 111). Previous studies have identified various proteins in macrophage exosomes after the induction of COM, and proteins are usually involved primarily in various immune responses, for example cell migration, interferon-γ (IFN-γ) regulation, Fcγ receptor-mediated phagocytosis, and T-cell activation and homeostasis (107).

Other evidence also have reported that polarizations of M1 and M2 macrophage play crucial roles in renal CaOx crystal formation and growth (112-114). However, it is controversial if inflammation regulated by M1 macrophage can promote kidney stone formation by decreasing stone inhibitors and increasing stone promoters. It was indicated that M1 macrophage might result in acute tissue damage, leading to the promotion of RP formation and crystal development (64). Interestingly, it was demonstrated that urinary variables changes were not found in M1 macrophage-regulated acute renal damage animal model induced by lipopolysaccharide (LPS), which suggested no significant correlation between increased renal crystal deposition and dysfunction (115). Also, M2 macrophages are anti-inflammatory and have the ability of phagocytizing and then degrading fragments of renal CaOx stone via clathrin related mechanisms (110, 114, 115).

Given the crucial roles of immune responses in deposition and development of CaOx crystal, immunotherapy has been attempted in order to prevent stone recurrence in special population via the regulation of the related immune responses, so as to inhibit renal inflammation and promote the degradation of CaOx crystals and then inhibit kidney stone development (116). Therefore, further investigations of immunotherapy targets for kidney stone diseases are required to contribute to the application of clinical immune-treatment.

Interestingly, a few studies have revealed a close association between idiopathic kidney stones formation and vascular calcification (117-121). Vascular calcification is thought to be dynamic processes in vascular smooth muscle cells which are acquiring an osteogenic phenotype, which has similarities with the association of CaP deposition with collagen (122-124). After exposure to high levels of calcium and phosphate, the osteogenic transformations will be triggered in vascular smooth muscle cells (124, 125). In these processes, WNT signal pathways and bone morphogenetic proteins (BMPs) were activated through upregulating RUNX2 and msh homeobox 2 (MSX2) transcription factor expressions (126). Reactive oxygen species (ROS) can regulate this transformation (127, 128), and the transformed cells can produce matrix proteins (124, 129).

Furthermore, some studies have supported that renal tubular epithelial cells have the osteogenic capacities (130). The basal levels of osterix (also genetically named Sp7, also a transcription factor), BMP2 and RUNX2 are higher in genetic hypercalciuric rat model in which intrarenal CaP depositions are usually produced (131). Madin–Darby canine kidney cells can form basal-side CaP microliths when growing as a monolayer (132, 133), and exposure to high concentrations of oxalate, CaP or CaOx crystal can result in activating NADPH oxidase and producing ROS in these cells (134-139), eventually leading to the osteogenic phenotype. It was demonstrated that genes which encode osteogenic phenotype markers vimentin, fibronectin, cadherin, osteoprotegrin, matrix-gla-protein, osteonectin, osteocalcin, collagen, BMP receptor type 2, BMP2, BMP7, RUNX2, osterix and OPN were related to epithelial transformations and bone morphogenesis, and they were overexpressed in hyperoxaluric rats (140). All in all, multiple lines of evidence support that

abnormal urine conditions including high renal OS, hypocitraturia, hypercalciuria and hyperoxaluria can activate the renal epithelial cell transformation into osteoblastic phenotype. The dedifferentiation state improves CaP crystal depositions and formation of RPs (141).

Very importantly, previous epidemiological study has demonstrated that CaOx urolithiasis incidence in male is significantly higher compared with female at a ratio of about 2 to 1, which suggests sex hormones take a crucial part in CaOx stones (6); but precise mechanisms are still not clear. Several works have found that androgen increases but estrogen decreases oxalate excretion in urine, oxalate level in plasma and CaOx crystals deposition in kidney, and the enhanced androgen signal pathways are responsible for the correlation between gender and urolithiasis (142-145). Renal subunit p22-PHOX, epithelial nicotinamide adenine dinucleotide phosphate oxidase (NADPH), and hepatic glycolate oxidase can be directly upregulated by androgen receptor (AR) signal at the transcriptional level to promote the biosynthesis of oxalate, resulting in urolithiasis in the end (146, 147). It was found that testosterone could contribute to urolithiasis development via inducing apoptosis and necrosis of renal tubular cells by activating HIF-1α/BNIP3 signaling (148). It was found that testosterone could contribute to urolithiasis through the increased adhesions of COM crystals to cell by overexpression of surface α-enolase (149). It was indicated that AR suppressed macrophage recruitment and inhibited the phagocytic capability of macrophages for COM crystal through decreasing the colony-stimulating factor 1 (CSF-1) signal with an upregulation of miR-185-5p (150). This suggests that AR signaling can be crucial in developing urolithiasis.

In recent ideas, AR is a novel potential target and can be thought as a newly developed treatment option for suppressing urolithiasis. Finasteride is one of the 5α-reductase inhibitors, and has been found to effectively protect the formation of kidney stones induced by testosterone via recovering apical surface expressions of α-enolase and adhesion of COM crystals to cells at a basic level, and inhibit the induced COM crystallization *in vitro* (151). Recently, dimethylcurcumin (ASC-J9), a novel AR degradation enhancer, has been found to inhibit formation process of CaOx crystals through suppressing oxalate biosynthesis and renal tubular epithelial cell damage induced by ROS by using a mice experiment (150). Conversely, estrogen can act as an inhibitor against urolithiasis. A study has indicated that estrogen can lead to the cellular proteome changes in tubular cells, which can decrease the expressions of CaOx crystals receptor surfaces like α-enolase and annexin A1, decrease the production of intracellular ATP, and promote the proliferation of renal cells and healing of renal tubular cells and tissues *in vitro* (152). More evidence revealed that estrogen receptor beta (ERβ) signal could decrease oxalate biosynthesis in the liver through upregulating glyoxylate aminotransferase, and also indicated that ERβ could inhibit OS induced by oxalate OS through inhibiting the NADPH oxidase subunit 2 (NOX2) at the transcriptional level via directly bound to estrogen response elements (EREs) of the NOX2 5′ promoter, playing a suppressive role on the deposition of CaOx crystals in mice model (153).

All these findings partially explain higher incidence of urolithiasis in males than females. AR-directed treatment can be studied as a potentially therapeutic option for CaOx stones disease. But all the studies were conducted in exclusively animal models and cell lines *in*

vivo or *in vitro*. Future validations and related clinical studies are needed. ASC-J9 and finasteride have been indicated to inhibit various AR-regulated diseases, such as liver cancer and prostate cancer (154-156). Further studies are needed before applying these two medicines to clinical practice in the prevention and therapy of urolithiasis, researching the possible adverse effects like erectile dysfunction (157).

As for the association between renal OS and cell injury in the processes of crystal formation, both clinical and experimental evidence has shown the production of ROS and the development of OS in KSF. Khan et al. revealed that decreased antioxidative capacity can lead to enhanced crystal deposition, resulting in OS and urolithiasis, and the ROS production and NADPH oxidase (NOX) involved pathways were crucial modulators of CaOx kidney stone formation (158). Microstructural change in tubular cell in primary stages of renal stones formation was measured, and it was found that the internal structures of mitochondria were in the processes of destruction, vacuolization and calcification (159). OPN is considered as an organic matrix component of renal calcium-containing stones, and it is basic in renal stone formation and can promote the initial development of renal stones (160, 161). By using immune transmission electron microscopy to observe ultrastructure, OPN expression was detected on the luminal sides of renal tubular cells, and crystal nuclei with cell debris and collapsed mitochondria were measured in the tubular lumens (162).

Injury of tubular cells is thought to be a crucial risk for the initial stage of process of renal stones formation (163). Exposure to CaOx crystals can induce OS, for example enhanced arachidonic acid level released by phospholipase A2, upregulated lipid peroxidation, and enhanced generation of free radicals (137, 164). Evidence demonstrated

that compounds like superoxide dismutase (SOD), vitamin E, and green tea, can decrease the levels of OS and was correlated with decreased cell damage of tubular cells and crystals deposition (165, 166).

Exposure of tubular epithelial cell to crystal results in upregulated synthetic levels of prostaglandin E2, MCP1, heparin sulfate, bikunin and OPN, which is believed to be involved in the inflammation responses and production of extracellular matrix (167). Previous studies revealed that pretreated tubular cell with a NADPH oxidase inhibitor could result in decreased productions of ROS, MCP1 and OPN, and results in decreased oxalate and CaOx crystal-induced cell injury (168). It was demonstrated the good preventive effect of citrate and vitamin E, two scavengers of free radicals, in reducing free radical induced by the shock wave (169). These results revealed the excellent capability for the therapeutic application of scavengers of free radical and antioxidants to reduce the recurrence rate of stones and kidney injuries after shockwave lithotripsy, which usually induces generations of ROS and results in renal OS injury (170). Umekawa et al. indicated that the deposition of CaOx crystal was decreased in hyperoxaluric rat kidneys after the angiotensin II type I receptor blocker candesartan treatment, with lower expression of OPN and significantly reduced levels of MDA in comparison with untreated group (171).

Mitochondrial collapse can lead to increased levels of OS, which is considered to involve in the primary phases of urolithiasis (172). Mitochondria is the primary source of intracellular ROS because mitochondria is the site of aerobic metabolism, and increased mitochondrial ROS production is induced by cell injury or increased stress (171). After CaOx crystals adhere to renal tubular cells, cyclophilin D (Cyp D) in mitochondria is

activated by superoxide which is produced by NADPH oxidase. Promotion of the mitochondrial permeability transition (MPT) leads to OS, mitochondrial collapse, activated apoptotic pathway, and increased OPN expression in the primary processes of renal CaOx formation (173). The activation of Cyp D induces the MPT acceleration, induces mitochondrial collapse and changes the mitochondrial transmembrane potentials. In the processes of mitochondrial collapse, cytochrome c is secreted into the cytosol and then combines to apoptotic protease-activating factor 1 to activate caspase-3 and -9 and initiate cell apoptosis, and finally ROS are secreted into the cytosol, inducing renal tubular cells injury (174). Inhibitors of Cyp D, cyclosporin A and NIM811, successfully inhibited the MPT acceleration, and reduced OPN expression and renal calcification (175). Inhibiting the activation Cyp D can prevent renal calcium crystal formation by suppressing the activation of mitochondrial collapse, OS, and apoptosis, suggesting that inactivating Cyp D by pharmacological approach may provide novel treatment options for urolithiasis.

All in all, during the interactions between cell and crystal, renal tubular cell damage is caused and aggravated by OS and inflammation (176-178). OS has a correlation with excessive ROS production, which is mediated by NOX (179). NOX, as a family of isoenzymes consisting of DUOX1, DUOX2, NOX1, NOX2, NOX3, NOX4 and NOX5, has been found to be located in plasma membranes throughout human body (180). The NOX family activation is regulated by a few important signal pathways, while it has been demonstrated that increased NOX2 expression could promote inflammation and OS in the kidney (181-183).

Also, increasing evidence suggests that the androgen and AR signal are associated to the

progress of CaOx urolithiasis. *In vitro*- and *in vivo* researches have demonstrated that an AR overexpression or testosterone supplements are able to lead to more renal crystal formation or urolithiasis (143, 184, 185). Injury of tubular cells induced by crystal may be mediated by AR signal, and inflammation and OS are involved in this process (186). Studies have demonstrated that the AR can increase endogenous hepatic oxalate synthesis, and renal recruitment, infiltration and differentiations of macrophages induced by crystal or oxalate via various signal pathways (147, 150).

Despite of the dramatical advance of minimally invasive surgical techniques for treating urolithiasis, medication treatment always has its position in the prevention of high recurrence rates of this disorder (187). Plant-derived natural compounds have their specific compositions, and have been used for their pharmacological properties. Kaempferol (3,4′,5,7-trihydroxyflavone) is one of the most common flavonoids and has a wide distribution in vegetables and fruits with various beneficial pharmacological effects like anti-inflammatory, anti-oxidant, anti-apoptotic, and immunomodulatory properties (188, 189). Several studies reported that kaempferol could selectively regulate the expression levels of sex hormone receptors, like the progesterone and estrogen receptor, which might further exert some biological effects like anti-cancer activity in various malignant diseases (190-192).

However, the precise functional roles of kaempferol in CaOx urolithiasis is yet unknown. In this work, we verified the inhibitory effects of kaempferol on the expression of AR, and subsequently we revealed the potential mechanisms of AR/NOX2 signal. This study indicated kaempferol had protective effects on renal crystal formation and tubular cell

injury induced by CaOx crystals through the antioxidant and anti-inflammatory functions via downregulating the AR/NOX2 pathways.

2. Materials and methods

2.1. Animal procedures

All animal experiments followed the guideline of the National Institutes of Health's *Guide for the Care and Use of Laboratory Animals* and were approved by the Animal Experiment Ethics Committee of Tongji Hospital, Tongji Medical College, Huazhong University of Science and Technology (Institutional Review Board ID: TJ-A20180205).

C57BL/6 male mice weighted 18-22g and aged 6-8 weeks, which were acquired from Tongji Hospital Experimental Animal, Tongji Medical College, and were used in all experiments. Mice had totally free accesses to water, and were fed standard chow. After a one-week-adaption, mice were divided into different groups. Details of the protocols for animal experiments are as follows:

There were three independent animal experiment protocols.

(1) Eligible mice were assigned into 5 groups (n=8 per group):

Normal control (NC) group: no special intervention and treatment.

Glyoxylic acid (GA) group: treated with GA at the dose of 100 mg/kg by the intraperitoneal injection once a day on 4th-10th day.

GA + vehicle group: received GA (described as GA group), and 200 μL 0.5% sodium carboxymethylcellulose (CMC-Na) by the oral gavage one time per day for 10 days.

GA + kaempferol (25 mg/kg) group: received GA (described as GA group), and the treatment of kaempferol (25 mg/kg) by the oral gavage one time per day for 10 days.

GA + kaempferol (50 mg/kg) group: received GA (described as GA group), and the simultaneous treatment of kaempferol (50 mg/kg) by the oral gavage one time per day for 10 days.

(2) Eligible mice were assigned into seven groups (n=8 per group):

NC group: without special intervention and treatment.

Testosterone propionate (TP) group: treated with TP at the dose of 3 mg/kg by the leg subcutaneous injection on the 4th, 6th and 8th day.

TP + vehicle group: received TP (described as TP group), and 200 μL 0.5% CMC-Na by the oral gavage one time per day for 10 days.

TP + kaempferol (25 mg/kg) group: received TP (described as TP group), and the treatment of kaempferol (25 mg/kg) by the oral gavage one time per day for 10 days.

TP + kaempferol (50 mg/kg) group: received TP (described as TP group), and the treatment of kaempferol (50 mg/kg) by the oral gavage one time per day for 10 days.

kaempferol (25 mg/kg) group: with treatment of kaempferol (25 mg/kg) by the oral gavage one time per day for 10 days.

kaempferol (50 mg/kg) group: with treatment of kaempferol (50 mg/kg) by oral gavage one time per day for 10 days.

(3) Eligible mice were assigned into five groups (n=8 per group):

NC group: without special intervention and treatment.

GA group: received GA (described as GA group)

GA + TP group: received both GA and TP (described as GA and TP groups)

GA + TP + kaempferol (25 mg/kg) group: received both GA (described as GA group) and TP (described as TP group), as well as treatment of kaempferol (25 mg/kg) by the oral gavage one time per day for 10 days.

GA + TP + kaempferol (50 mg/kg) group: received both GA (described as GA group) and TP (described as TP group), as well as the treatment of kaempferol (50 mg/kg) by the oral gavage one time a day for 10 days.

During animal experiments, GA (Sigma-Aldrich, USA) was used to establish a mouse renal CaOx crystal model, which was prepared as the solution via being dissolved into sterile distilled water to achieve 10 mg/mL concentration before intraperitoneal injection. Kaempferol was provided by Nanjing Zelang Medical Technology Co., Ltd. (Nanjing, China), and was prepared as a solution by dissolving it into 100-200 µl 0.5% CMC-Na (Sigma-Aldrich, USA) to achieve a final concentration of 5 mg/mL. Testosterone propionate (TP, Aladdin, China), which was dissolved in 100 µl corn oil (Aladdin, China) to achieve a final concentration of 0.75 mg/mL, was used to promote AR expression in mice kidneys. After 10-days of intervention, retro-orbital blood was collected and stored at -80ºC on the 11^{th} day. Afterwards, all mice were sacrificed followed by the excision of two kidneys. One kidney was fixed in paraformaldehyde for pathological examinations whereas the other was immediately stored at -80ºC for further assays.

2.2. Cell Culture and treatment

Human renal cortex proximal tubule epithelial (HK-2) cells were acquired from the Type Culture Collection of the Chinese Academy of Sciences (Shanghai, China). In cell

experiments, COM crystals were prepared and weighted, and were then suspended in sterile distilled water by different concentrations (193). Kaempferol or dihydrotestosterone (DHT, Sigma-Aldrich, USA) was dissolved by using dimethyl sulfoxide (DMSO, Sigma-Aldrich, USA) with final 1‰ DMSO concentrations. During cell experiments, DHT (100nM) was treated to HK-2 cell for 12 hours to obtain the overexpression of AR, and kaempferol (50mM) was treated to HK-2 cell for 12 hours to exert effects. Three independent experiments were conducted.

2.3. Measurement of renal function and acute kidney injury

The level of neutrophil gelatinase-associated lipocalin (NGAL), creatinine (Cr), or blood urea nitrogen (BUN) in blood was separately tested by two kits (NGAL: R&D Systems, USA; Cr and BUN: Huili, China;) in line with the manufacturer's instructions.

2.4. Renal histology

Complete cross-sections (2-4 μm) of the kidney at the renal papillae level were made after 24h fixation by 4% paraformaldehyde and paraffin embedding. HE stainings (Wuhan Servicebio, China) were applied to stain sections and crystals in kidney were observed through a polarization microscope (CX31P; Olympus, Japan) with 20× magnification. For evaluating the formation of renal crystals and injury of renal tubular cells, periodic acid Schiff (PAS) kit (Beijing Solarbio science & technology Co., Ltd, China) and Pizzolato staining solution (Shanghai Sinopharm Group, China) were applied to do PAS staining and Pizzolato staining. PAS staining was used to evaluate tubular damage scores by one

dedicated and experienced pathologist. The standard of evaluation was described as follows: 1) 10 visual fields (magnification of 400x) were randomly selected; 2) tubular damage was referred to the presence of tubular casts and necrotic tubules; 3) the scores were based on the percentage of tubular damage: 0-none, 1-less than 10%, 2-10 to 25%, 3-26 to 75%, and 4- over 75%; 4) the final score was calculated as the mean count of the scores of ten visual fields (194). Immunohistochemistry (IHC) staining of F4/80 (1:250, CST, USA), NFκB-p65 (1:800, CST, USA), OPN (1:100, Affinity, USA), CD44 (1:100, Affinity, USA), iNOS (1:500, Affinity, USA), NOX2 (1:100, Affinity, USA), and AR (1:400, CST, USA) was performed. The analysis of IHC results is to set a specific threshold for each detection indicator through ImageJ to determine the proportions of positive staining cells per LPF in the images obtained under the light microscope, and 8 visual fields (magnification of 200×) were randomly selected. Then, in order to make the data less messy and inconsistent, data were further converted into fold changes normalized to the NC group. TUNEL staining was applied based on the manufacturer's instructions of TUNEL BrightGreen Apoptosis Detection Kit A112 (Vazyme, China). Images were acquired by a PathScope™ 4S scanner (DigiPath, USA) or a 3D HISTECH scanner (Pannoramic MIDI, Hungary), and were quantified by ImageJ software (National Institutes of Health, USA).

2.5. Cell viability assay

HK-2 cells were plated in 100 μl medium in each well at a density of 10^4 cells in 96-well plates. After 24 hours of culture, cells were stimulated by various concentrations (0, 50,

100, 200, 400, 800, and 1600 μg/mL) of COM crystals (Sigma-Aldrich, USA) for 12h. What's more, DMSO or kaempferol (0, 1, 5, 10, 20, 40, 80, and 160 μmol/L) was used to stimulate the cells were for 12h. Cell Counting Kit-8 (CCK-8) (MCE, USA) was applied to evaluate the cell viabilities based on manufacturer's directions. The absorbances were determined with a WallacVictor3™ V microplate reader (PerkinElmer, The Netherlands) at 450 nm. 50% inhibitive concentration (IC50) of CaOx crystal or kaempferol to HK-2 cell was calculated. Lactate dehydrogenase (LDH) Assay Kit (Beyotime Biotechnology, Shanghai, China) was applied for the measurement of LDH based on the manufacturer's directions. Annexin V-FITC/PI Apoptosis Detection Kit (R&D Systems, USA) was used for measuring cell deaths. Fluorescence intensity of Annexin V-FITC/PI was evaluated through flow cytometry (BD Biosciences).

2.6. Crystal adhesion assay

When cells grew to 100% in 6-well plates, HK-2 cells were treated with COM crystals and various concentrations of kaempferol for 12 hours. Then phosphate buffer saline (PBS) was used to wash the plate thoroughly for three times to clean up the crystals which were not bound to cells. The quantity of crystals was measured by a microscope. Random images were acquired from 10 visual fields (magnification of 400x) and quantified by ImageJ (195). Data for the experimental groups were normalized to those for the NC groups from three independently repeated experiments.

2.7. Real-time quantitative Polymerase Chain Reaction (RT-qPCR)

After total RNAs were isolated by TRIzol reagent (Invitrogen, USA) in renal tissues and HK-2 cells, total cDNAs were synthesized with the PrimeScript® RT reagent kit (Takara Biotechnology, Japan). Then the ABI Prism 7500 system (Applied Biosystems, USA) was used to perform RT-qPCR based on the manufacturer's directions. The primers (Tsingke, China) are listed in Table 1. The fold changes of gene expressions were calculated using $2^{-\Delta\Delta Ct}$ and normalized to the NC groups as performed previously (196). Three independently repeated experiments were performed on different days.

Table 1. Primers.

	Forward primer (5′-3′)	**Reverse primer (5′-3′)**
Gene (Human)		
AR	CCAGGGACCATGTTTTGCC	CGAAGACGACAAGATGGACAA
IL-1β	ACGCTCCGGGACTCACAGCA	TGAGGCCCAAGGCCACAGGT
IL-6	GCACTGGCAGAAAACAACCT	TCAAACTCCAAAAGACCAGTGA
TNF-α	CCCAGGGACCTCTCTCTAATC	ATGGGCTACAGGCTTGTCACT
IL-10	GACTTTAAGGGTTACCTGGGTTG	TCACATGCGCCTTGATGTCTG
IL-4	ATGGGTCTCACCTCCCAACT	GATGTCTGTTACGGTCAACTCG
ARG1	GTGGAAACTTGCATGGACAAC	AATCCTGGCACATCGGGAATC
OPN	CTCCATTGACTCGAACGACTC	CAGGTCTGCGAAACTTCTTAGAT
CD44	CACAATCCAGGCAACTCCTA	TACTCTGCTGCGTTGTCAT
NOX1	GTTTTACCGCTCCCAGCAGAA	GGATGCCATTCCAGGAGAGAG

NOX2	CCTAAGATAGCGGTTGATGG	GACTTGAGAATGGATGCGAA
NOX3	GAACCCTCGGCTTGGAAAT	TGGCTTACCACCTTGGTAATGA
NOX4	CCCTCACAATGTGTCCAACTGA	GGCAGAATTTCGGAGTCTTGAC
NOX5	AAGAGTCAAAGGTCGTCCAAGG	GCTTTCTTTTCTGGTGCCTGT
DUOX1	TTCACGCAGCTCTGTGTCAA	AGGGACAGATCATATCCTGGCT
DUOX2	ACGCAGCTCTGTGTCAAAGGT	TGATGAACGAGACTCGACAGC
GAPDH	GACCTGACCTGCCGTCTA	AGGAGTGGGTGTCGCTGT
Gene (Mouse)		
AR	AAATGGGACCTTGGATGGAGA	AGAACGAGGTCTGGAGCAAAG
IL-1β	ACTCCTTAGTCCTCGGCCA	CCATCAGAGGCAAGGAGGAA
IL-6	GAGGATACCACTCCCAACAGACC	AAGTGCATCATCGTTGTTCATACA
TNF-α	TGATCCGCGACGTGGAA	ACCGCCTGGAGTTCTGGAA
IL-10	ACTGGCATGAGGATCAGCAG	CTCCTTGATTTCTGGGCCAT
IL-4	ACTTGAGAGAGATCATCGGCATTT	AGCACCTTGGAAGCCCTACAG
ARG1	TGGCTTGCGAGACGTAGAC	GCTCAGGTGAATCGGCCTTTT
GAPDH	GCACAGTCAAGGCCGAGAAT	GCCTTCTCCATGGTGGTGAA

Note: Reproduced from (1) with permission of publisher (Elsevier GmbH).

2.8. Western blot (WB) assay

Proteins were extracted from HK-2 cells or kidney tissues with sonication. Equivalent proteins (30 μg) from each sample were separated on 10% SDS-PAGE (Beyotime Biotechnology, Shanghai, China), and were transferred to nitrocellulose filter membrane.

Blocked by 5% skim milk in TBST (pH 7.5), the membranes were incubated with primary antibodies of MCP1 (1:2000, Affinity, USA), p-NFκB-p65 (1:1000, CST, USA), Caspase-1 (1:200, BOSTER, China), iNOS (1:1500, Affinity, USA), NOX2 (1:1000, Affinity, USA), AR (1:2000, CST, USA), and GAPDH (1:3000, Abcam, USA) overnight at 4°C, and was then incubated with secondary antibodies (1:3000, 7074, CST) for 2h at room temperature. Enhanced chemiluminescence Bio-Rad Clarity Western ECL kit (Beyotime Biotechnology, Shanghai, China) was applied to detect chemiluminescent signal, and scanned by the LAS4000 analyzer (GE Healthcare). ImageJ was applied to analyze band intensities and levels of proteins were normalized by GAPDH.

2.9. Immunofluorescence (IF) assay

We examined the immunoreactivity by using Histofine Simple Stain Kit based on the protocol of manufacturer's directions. Each HK-2 cell slide was fixed for 20 minutes by 4% buffered formalin. The slides were rinsed by PBS and then blocked by goat serum, and primary antibodies NOX2 (1:1000, Abcam, USA) or AR (1:600, CST, USA) were used for the incubation at 4℃ for over 12h. After that, each slide was incubated with Alexa Fluor-conjugated 488- or CY3-secondary antibody (1:400, Thermo Fisher, USA) for 1h at room temperature. Then the slides were rinsed with PBS, and finally were counterstained by the nuclear marker DAPI and wet-mounted. Fluorescence Images were acquired by the fluorescence microscope (Nikon TE2000-U, Japan), and ImageJ was applied to quantify fluorescence intensities.

2.10. Chromatin Immunoprecipitation (ChIP) assay

We carried out ChIP assay with a ChIP kit (Milliporn, USA) based on the manufacturer's directions. Immunoprecipitation was carried out with antibody against AR (1:100, Abcam). We used a specific designed primer pair (forward: 5'-CCTGTATAAGGCACTTACCAT-3'; reverse: 5'-CATTCACCACTCACTCACT-3') to amplify a targeted sequence of the androgen receptor element (ARE) within the promoter region of human NOX2. We applied qPCR with the DNA samples and eventually identified the PCR products using agarose gel electrophoresis.

2.11. Luciferase reporter assay

Luciferase reporter assay was performed with a Dual luciferase assay kit (Promega, USA) based on the manufacturer's directions. DNA fragments within the upstream region of human NOX2 promoters which contain mutant or wild-type ARE-binding site, were separately inserted into the pGL3 basic vector (Promega, USA). After transient transfections of plasmid into HK-2 cells in 24-well plate by using specific treatments and Lipofectamine 3000 (Invitrogen, USA), the luciferase activities were measured by using a Luciferase Reporter Assay System (Promega, USA), normalized to firefly luciferase activities in NC groups.

2.12. Measurement of ROS and H2O2 levels

ROS Assay Kit with DCFH-DA (Nanjing Jiancheng Bioengineering Institute, China) was used for measuring the production of intracellular ROS levels. Fluorescence intensity of DCFH-DA was evaluated via flow cytometry or fluorescence microscope for cell experiments, and by fluorescence microplates for renal tissues. We used a Hydrogen Peroxide Assay Kit (Beyotime Biotechnology, Shanghai, China) to detect H_2O_2 level based on manufacturer's directions. All data were normalized to the NC group.

2.13. Measurement of SOD, MDA, and glutathione (GSH) levels

Total SOD Assay Kit, Lipid Peroxidation MDA Assay Kit and GSH Assay Kit (Beyotime Biotechnology, Shanghai, China) were respectively performed to detect activities of SOD, MDA, and GSH in cell supernatant according to the instructions of reagents manufacturers. The results of the experimental samples were all normalized to the samples in NC group.

2.14. Statistical analysis

All data are presented as means ± standard deviation (SD). GraphPad Prism 6 (GraphPad Software, USA) was performed for statistical analysis. The group comparisons were measured through unpaired t test for two groups and one-way ANOVA for three or more groups. The Bonferroni's multiple comparisons test was used for correction after ordinary one-way ANOVA. *P* values < 0.05 were thought statistically significant.

3. Results

3.1. Effects of kaempferol on renal tubular damage and CaOx crystal deposition in mice

The deposition of CaOx crystal in the male C57BL/6 mouse kidney was satisfactorily achieved by repeated intraperitoneal injections of GA. No deaths caused by the experimental drugs were observed in this study. By the observation of HE staining slices using polarizing microscope it was indicated that fewer crystals (with white staining indicated CaOx crystals) were deposited in the mice kidney after receiving GA combined with the treatment of kaempferol than receiving GA alone, which was consistent with the results of Pizzolato staining (with black staining indicated CaOx crystals). Moreover, higher kaempferol concentrations was given, the fewer crystals were found to be deposited (Figure 1.1 a-c). These results reveal that kaempferol might inhibit CaOx crystal deposition in mice kidneys.

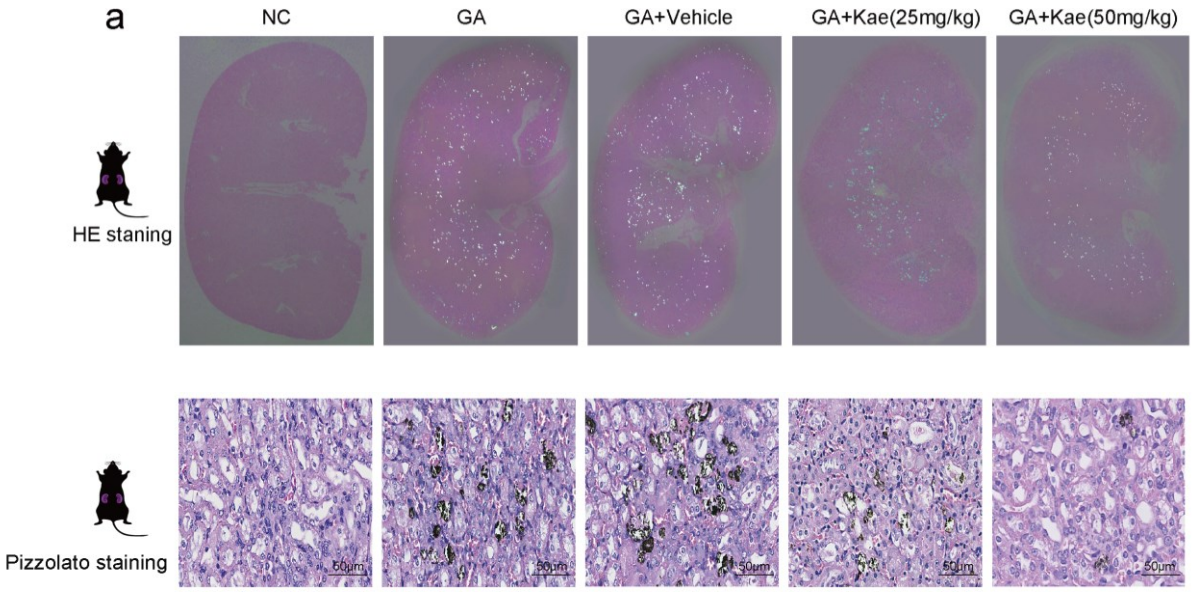

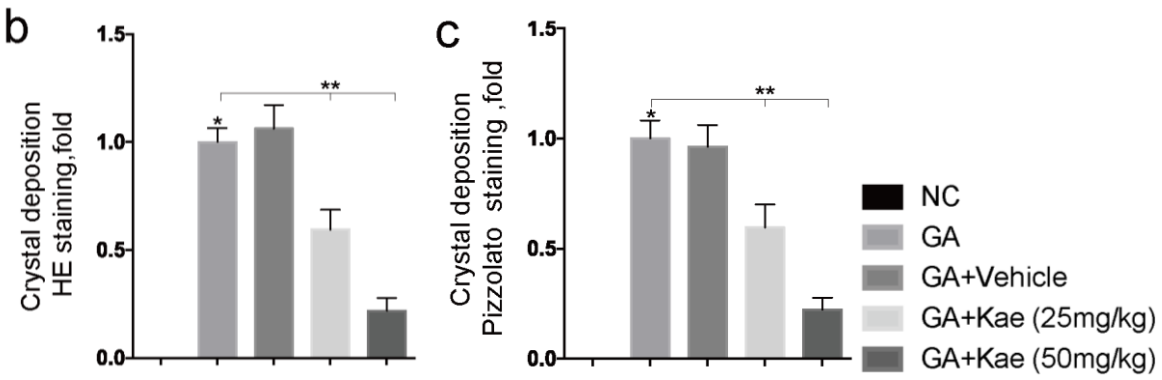

Figure 1.1. Kaempferol inhibited CaOx crystal deposition in mice.

All eligible mice were assigned into 5 groups (n = 8 per group). After a 10-day process, all mice were sacrificed for subsequent measurements. (a) Pathological images of HE staining and Pizzolato stainings of paraffin-embedded sections of kidneys, and (b, c) the corresponding quantitative analyses. Data are the fold changes normalized to GA group and are represented as mean±SD. The group comparisons were measured through unpaired t test for two groups and one-way ANOVA for three groups. $^{*}P < 0.05$ versus NC group; $^{**}P < 0.05$ as GA versus GA+Kae (25 mg/kg) group, GA versus GA+Kae (50mg/kg) group, and GA+Kae (50mg/kg) versus GA+Kae (25mg/kg) group, separately. Reproduced from (1) with permission of publisher (Elsevier GmbH).

Furthermore, PAS staining revealed that CaOx crystals resulted in renal tubular damages including necrotic tubules and tubular casts, while kaempferol could markedly inhibit the structural damage. Based on quantitative scores of the tubular damage, we found that the damage was significantly improved after treatment with kaempferol, and the improvement was more pronounced when higher kaempferol concentrations were given (Figure 1.2 a, c). The same results described above of renal injury could also be identified by TUNEL staining (Figure 1.2 b, d).

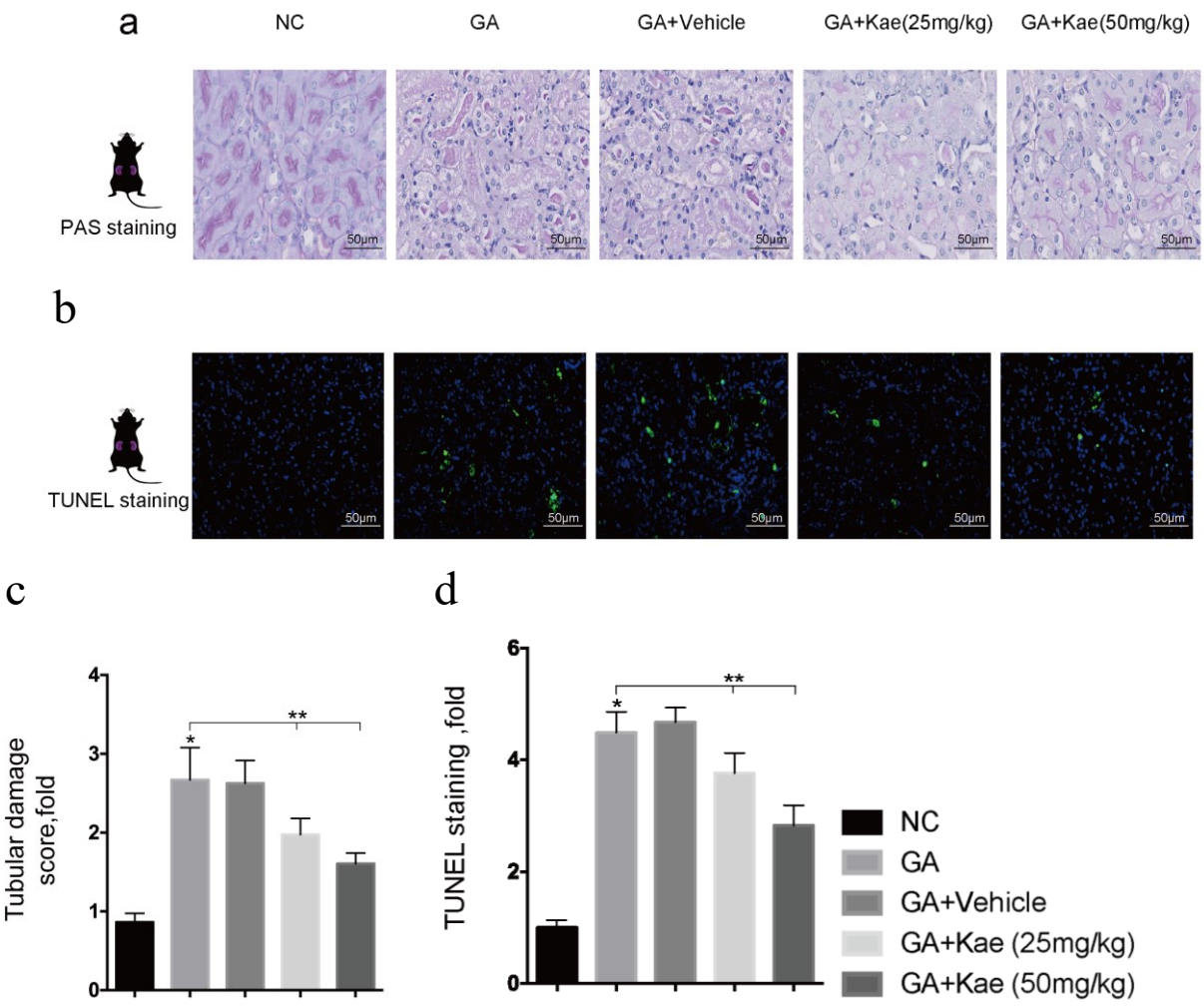

Figure 1.2. Kaempferol suppressed renal tubular injury in mice.

(a, b) Pathological images of PAS staining and TUNEL stainings of paraffin-embedded sections of kidneys, and (c, d) the corresponding quantitative analyses. Data are the fold changes normalized to NC groups and are represented as mean±SD. $^{*}P < 0.05$ versus NC group; $^{**}P < 0.05$ as GA+Kae (25 mg/kg) versus GA group, GA+Kae (50 mg/kg) group versus GA, and GA+Kae (50mg/kg) versus GA+Kae (25mg/kg) group, separately. Reproduced from (1) with permission of publisher (Elsevier GmbH).

By IHC staining, it was revealed that OPN and CD44 expressions were promoted in the GA-treated groups compared with the kaempferol-treated groups. At the same time, the lower expression was associated with the higher kaempferol concentrations (Figure 1.3 a, b,

c, d). This suggested kaempferol might reduce CaOx crystals adhesion to tubular epithelial cells by inhibiting OPN and CD44.

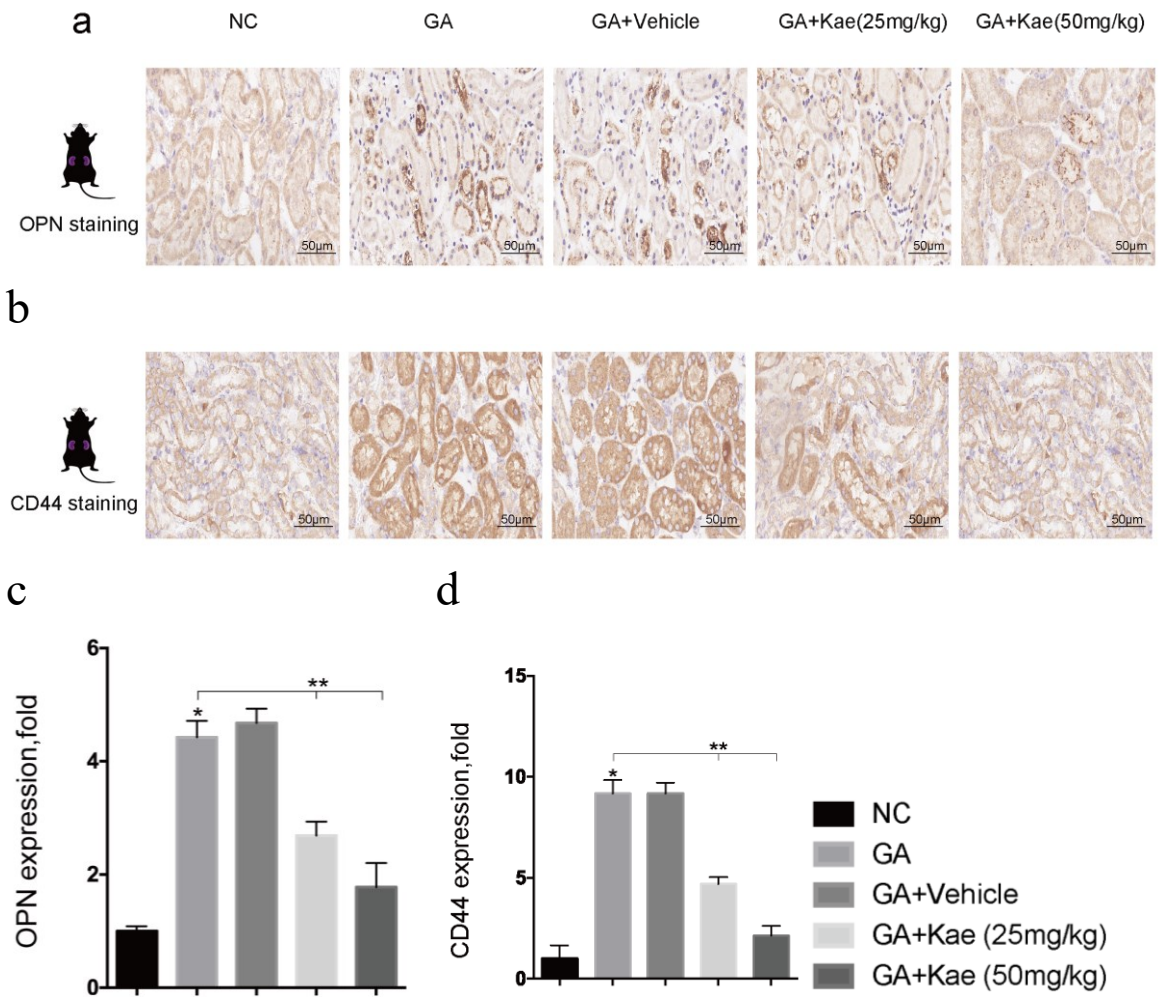

Figure 1.3. Kaempferol inhibited renal crystal adhesion in mice.

(a, b) Pathological images of CD44 and OPN IHC stainings of paraffin-embedded sections of kidneys, and (c, d) the corresponding quantitative analyses. Data are the fold changes normalized to the NC groups and are represented as mean±SD. $^{*}P < 0.05$ versus NC group; $^{**}P < 0.05$ as GA versus GA+Kae (25mg/kg) group, GA versus GA+Kae (50mg/kg) group, and GA+Kae (50mg/kg) versus GA+Kae (25mg/kg) group, separately. Reproduced from (1) with permission of publisher (Elsevier GmbH).

Besides that, serum BUN, Cr and NGAL levels were markedly increased in the GA

groups compared with the NC groups, but the levels were markedly lower in kaempferol-treated groups compared with the GA groups (Figure 1.4 a-c)

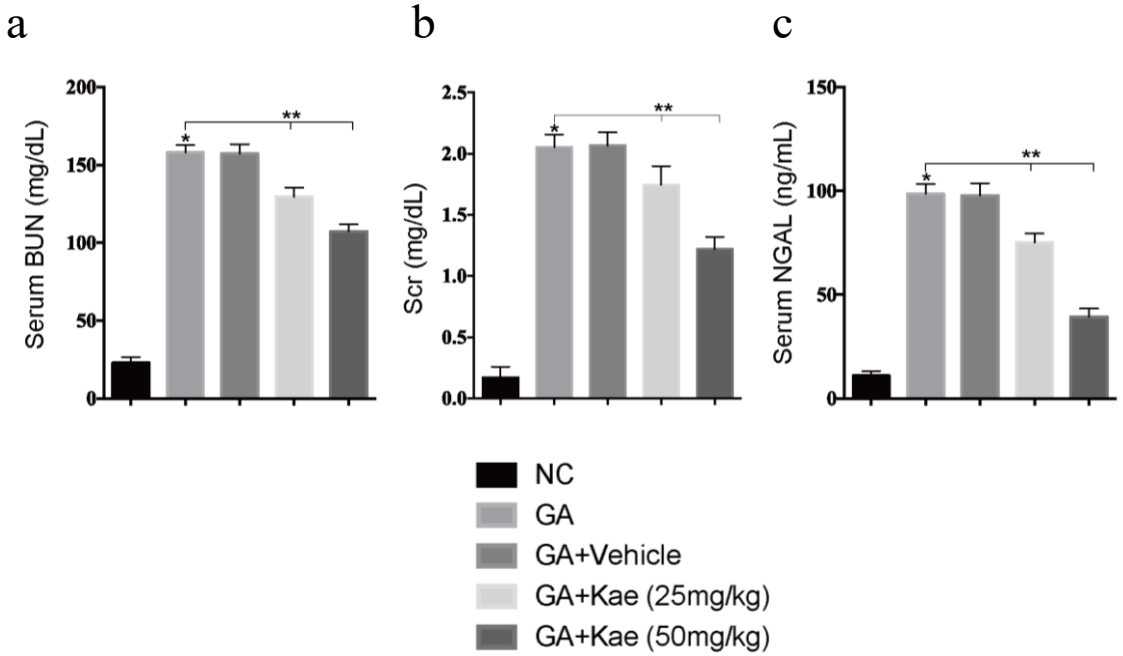

Figure 1.4. Kaempferol inhibited renal dysfunctions and acute kidney injury in mice.

(a-c) Kidney dysfunctions and acute kidney injury were measured by serum levels of NGAL, Cr, and BUN. Data are the quantitative data and are represented as mean±SD. $^{*}P<0.05$ versus NC group; $^{**}P<0.05$ as GA versus GA+Kae (25 mg/kg) group, GA versus GA+Kae (50mg/kg) group, and GA+Kae (50mg/kg) versus GA+Kae (25mg/kg) group, separately. Reproduced from (1) with permission of publisher (Elsevier GmbH).

It was reflected that CaOx promoted renal damage and enhanced CaOx crystal adhesions to tubular epithelial cells. These findings also revealed a potential protective effect of kaempferol treatment in renal injury resulting from CaOx crystal. In summary, it was indicated that kaempferol was able to inhibit renal injury resulted from CaOx crystal and suppress CaOx crystals deposition.

3.2. Effects of kaempferol on cell deaths induced by CaOx crystals, and crystal adhesions to HK-2 cells

We performed a series of experiments to verify whether kaempferol could alleviate COM crystal-induced cell deaths *in vitro*. First, we examined the effect of different concentrations of COM crystals on cell viabilities by using CCK-8 assay (Figure 2.1 a). The IC50 of crystal on HK-2 cell was 437.8μg/mL. Therefore, combined with methods in previously published studies, we chose the concentration of 400 μg/mL COM crystal to process subsequent cell experiments.

Based on the methodology in previous studies, three preliminary concentrations of kaempferol (10, 20 and 40 μM) were selected. By using CCK-8 assay, we found that three concentrations of kaempferol had no significant cytotoxic effect on cell viability compared with the NC group (Figure 2.1 b).

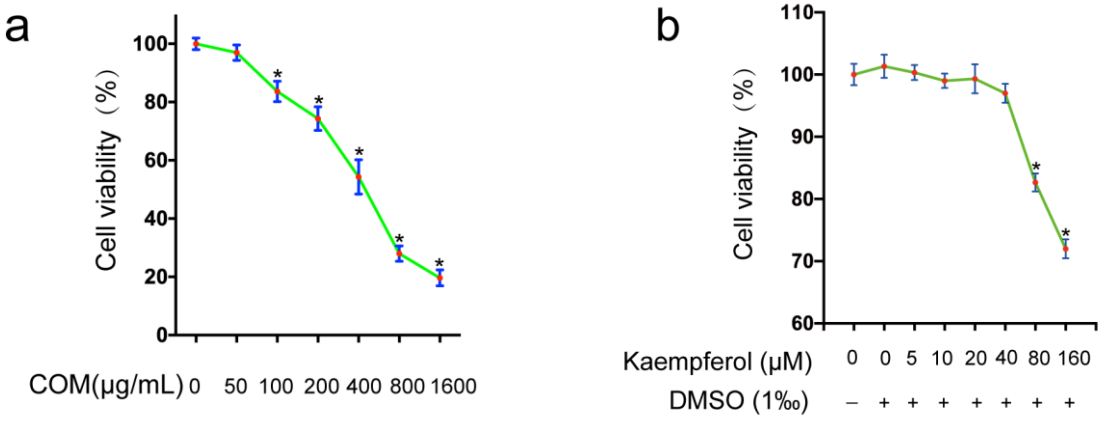

Figure 2.1. Effects of different concentrations of COM crystal and kaempferol on HK-2 cell in vitro. Cell viabilities were detected by using CCK-8 assays. (a) Different concentrations of COM crystal (0, 50, 100, 200, 400, 800, 1600 μg/mL) were treated to HK-2 cell (1×10^5 cells per well) for 12h. (b) DMSO (1‰) or different concentrations of

kaempferol (0, 1, 5, 10, 20, 40, 80, and 160 μmol/L) was treated to HK-2 cell for 12h. Data are the proportions of cell viability and are represented as means ± SD. *P<0.05 versus NC group. Reproduced from (1) with permission of publisher (Elsevier GmbH).

Additionally, it was revealed that COM crystal stimulation generated much more LDH production and cell deaths than NC groups. Cell deaths and LDH release were promoted after simultaneously treated with kaempferol with a concentration-dependent fashion and 40 μM kaempferol had the strongest protective role in HK-2 cell when with exposure to COM crystal (Figure 2.2 c, d).

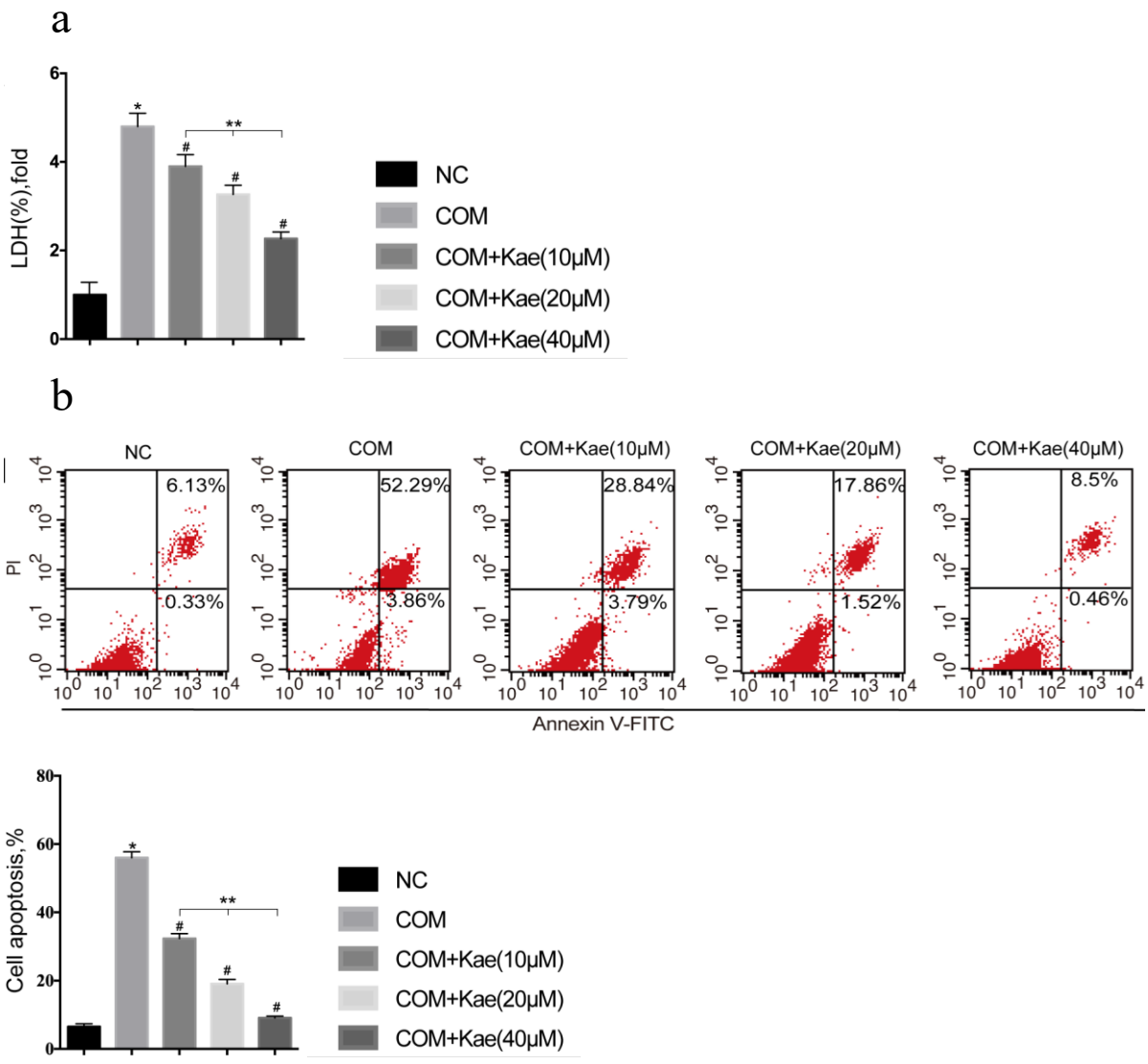

Figure 2.2. Kaempferol inhibited cell deaths resulted from CaOx crystal in HK-2 cell. COM crystal (400μg/mL) and simultaneous kaempferol (10, 20, and 40μM) were applied to HK-2 cell (1×10^5 cells per well) for 12h. (a) Measurement of cellular LDH level. (b) Evaluation of cell deaths by flow cytometry. In a, data are the fold changes normalized to the NC group and in b, data are the proportions of cell apoptosis. Data are represented as means ± SD. *P<0.05 versus NC groups; $^{\#}$ P<0.05 versus COM group; **P<0.05 as pairwise comparisons between COM+Kae (10μM), COM+Kae (20μM), and COM+Kae (40μM). Reproduced from (1) with permission of publisher (Elsevier GmbH).

Moreover, we demonstrated that COM crystal adhesion to HK-2 cells was decreased when treated with kaempferol in a concentration-dependent manner (Figure 2.3 a).

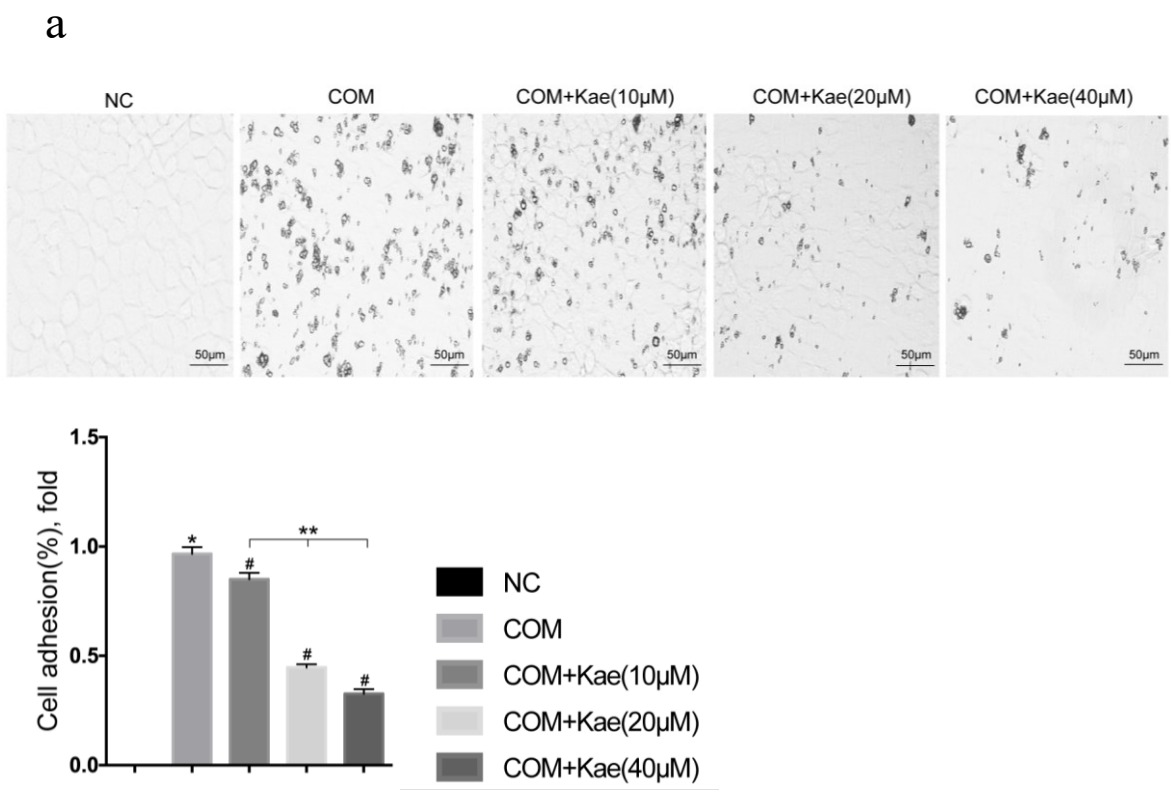

Figure 2.3. Kaempferol inhibited crystal adhesions to HK-2 cell. (a) COM crystal adhesions to HK-2 cells. Data are fold changes normalized to the COM group and are

represented as mean±SD. *P<0.05 versus NC group; # P<0.05 versus COM group; **P<0.05 as pairwise comparisons between COM+Kae (10μM), COM+Kae (20μM), and COM+Kae (40μM). Reproduced from (1) with permission of publisher (Elsevier GmbH).

In addition, WB analysis showed that after the exposure to COM, the expression of caspase-1 was markedly increased compared to NC group. Nevertheless, the treatment with kaempferol was able to suppress the expression of caspase-1 in HK-2 cell (Figure 2.4 a). Thus, caspase-1 might take part in the inhibitive effect of kaempferol on cell deaths resulted from crystal.

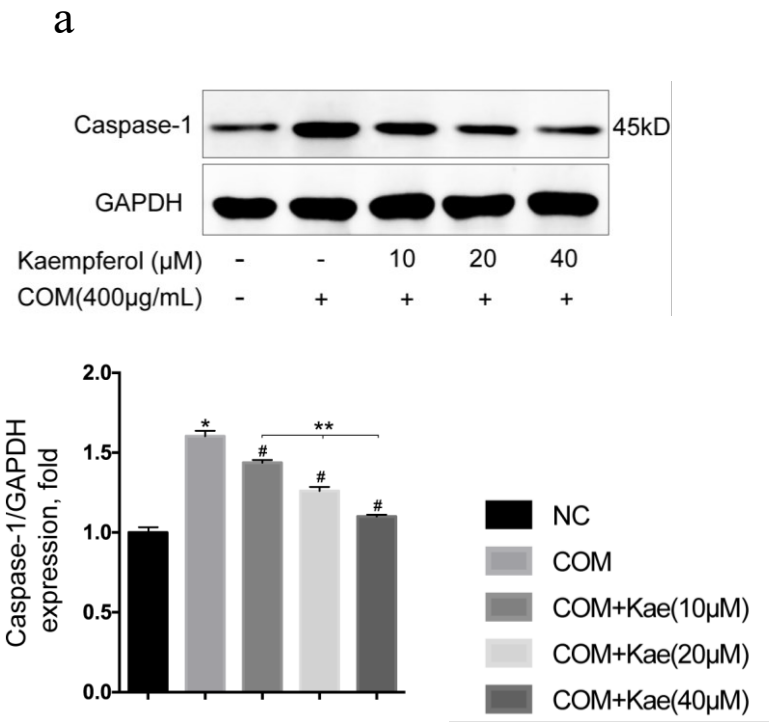

Figure 2.4. Kaempferol inhibited caspase-1 expression in HK-2 cell. (a) Measurement of caspase-1 expression by WB. Data are the fold changes normalized to the NC group and are represented as mean±SD. *P<0.05 versus NC group; # P<0.05 versus COM group; **P<0.05 as pairwise comparisons between COM+Kae (10μM), COM+Kae (20μM), and COM+Kae (40μM). Reproduced from (1) with permission of publisher (Elsevier GmbH).

Therefore, we suggested kaempferol could inhibit cell deaths induced by CaOx crystals, and crystal adhesions to HK-2 cells in a dose-dependent fashion.

3.3. Effects of kaempferol on OS and inflammation led by CaOx crystals in HK-2 cells and in mice

In mice experiments, by IHC assays, it was revealed that expressions of F4/80, NFκB-P65, iNOS and NOX2 in renal tubular epithelial cells were significantly higher while the effects were reversed in the kaempferol-treated groups (Figure 3.1 a-e).

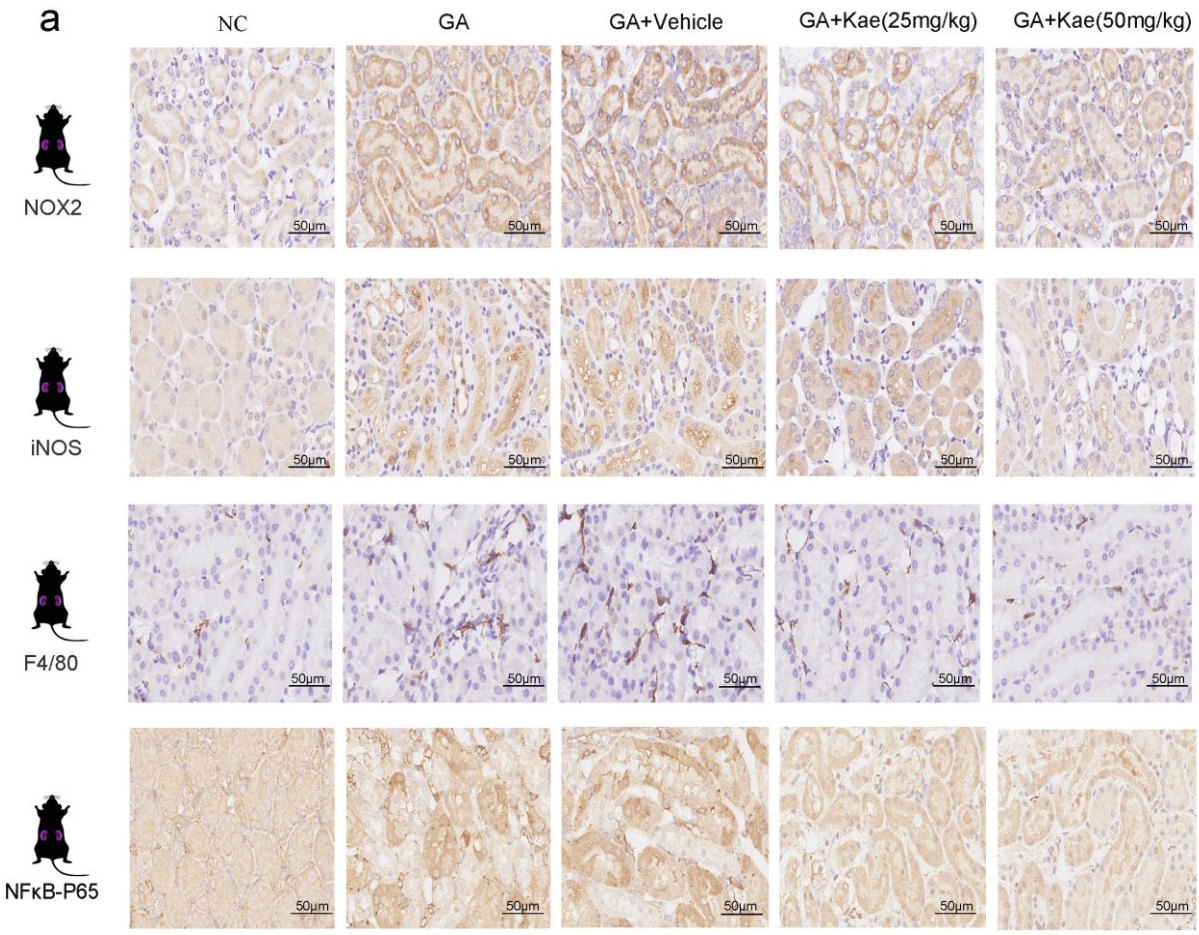

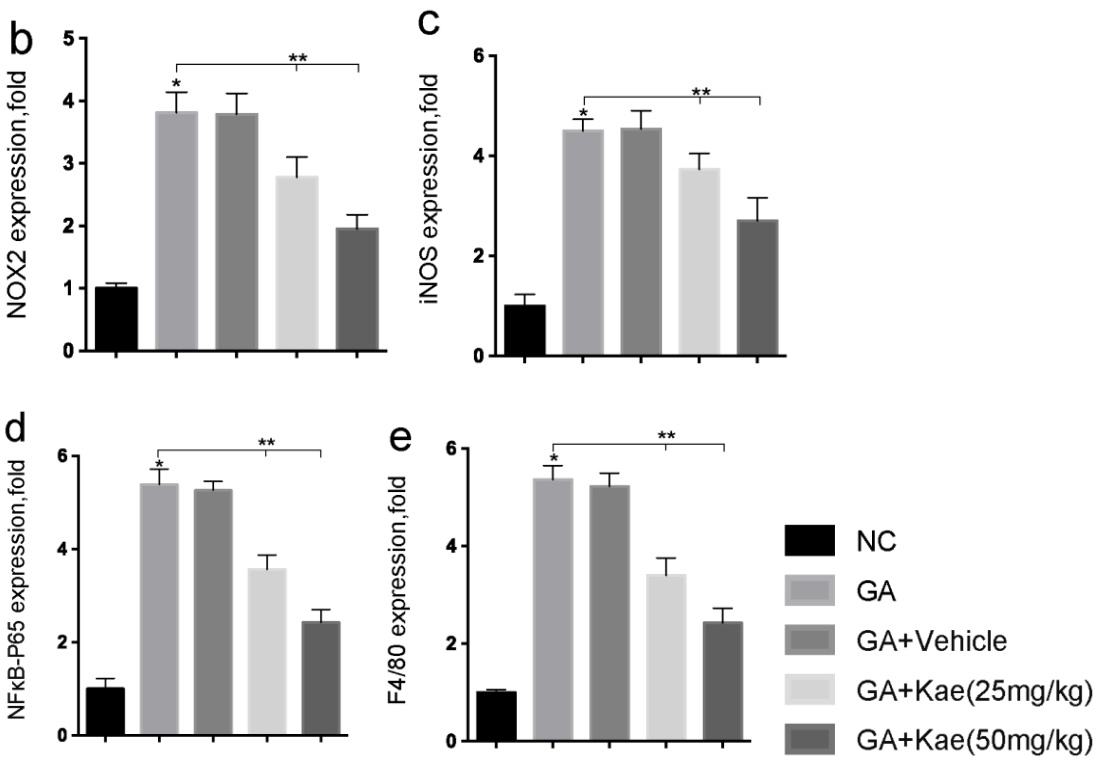

Figure 3.1. Kaempferol suppressed renal OS and inflammation in vivo. (a) IHC staining for F4/80, iNOS, NOX2 and NFκB-p65, and (b-e) the corresponding quantitative analyses. Data are the fold changes normalized to the NC group and are represented as mean±SD. $^{*}P<0.05$ versus NC group; $^{**}P<0.05$ as GA versus GA + Kae (25mg/kg) group, GA versus GA+Kae (50mg/kg) group, and GA+Kae (50mg/kg) versus GA+Kae (25mg/kg) group, respectively. Reproduced from (1) with permission of publisher (Elsevier GmbH).

We revealed that ROS, H_2O_2 and MDA levels in kidney were promoted while SOD and GSH levels were suppressed when treated with GA. The effects were reversed when treated with kaempferol, whereby 50 mg/kg kaempferol showed a much more significant effect than 25 mg/kg (Figure 3.2 a-c).

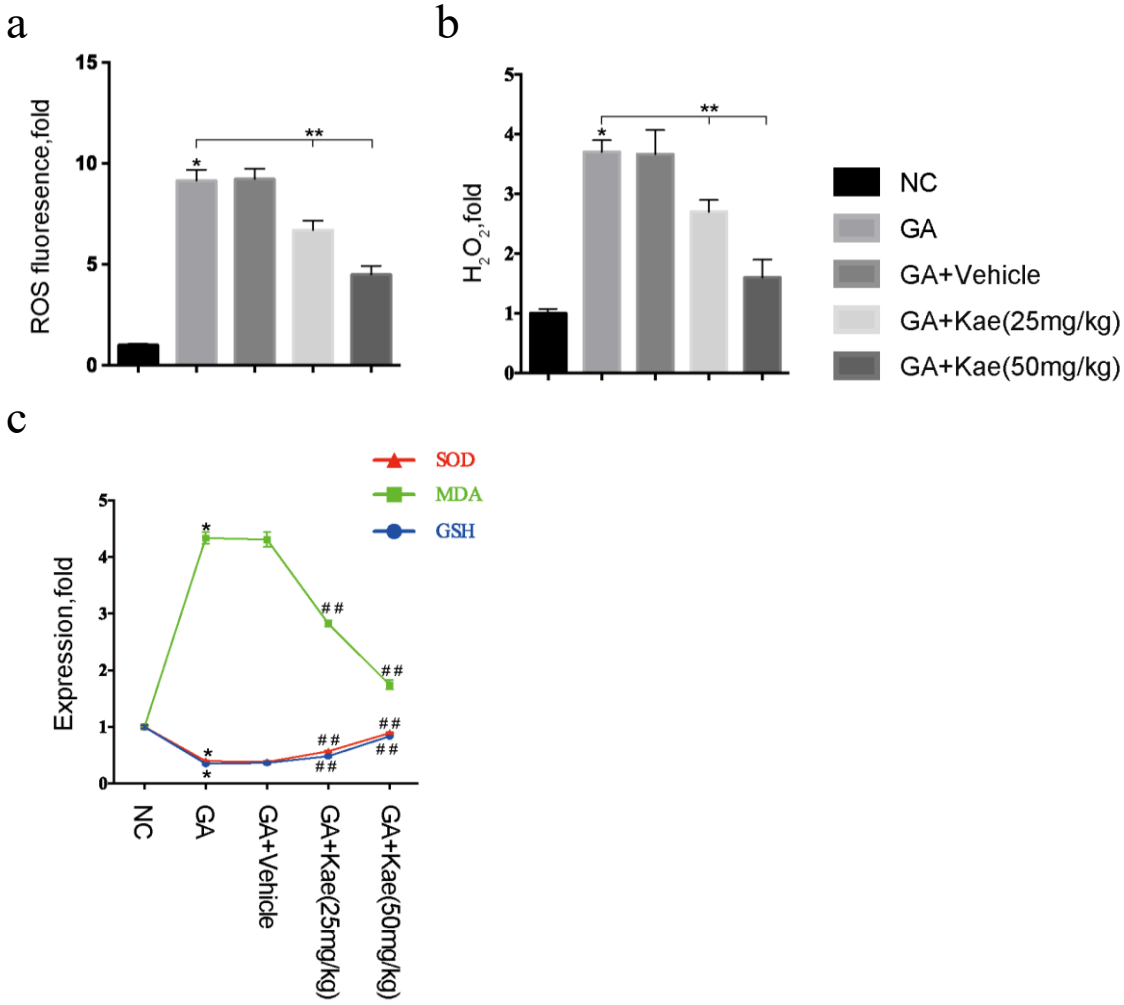

Figure 3.2. Kaempferol suppressed renal OS in vivo. (a) Detections of ROS in kidney by fluorescence microplates with DCFH-DA. (b) H_2O_2 levels. (c) Detections of SOD, MDA and GSH levels in mice kidney. Data are the fold changes normalized to the NC group and are represented as mean±SD. $^{*}P<0.05$ versus NC group; $^{**}P<0.05$ as GA versus GA+Kae (25mg/kg) group, GA versus GA+Kae (50mg/kg) group, and GA+Kae (50mg/kg) versus GA+Kae (25mg/kg) group, respectively. Reproduced from (1) with permission of publisher (Elsevier GmbH).

Moreover, using RT-qPCR assay, we detected that the expressions of TNF-α, IL-6 and IL-1β in kidney were markedly higher, and the expressions of Arg1, IL-4 and IL-10 were markedly lower in the GA group than the NC group. Nevertheless, all the effects were

reversed when treated with kaempferol (Figure 3.3 a-f).

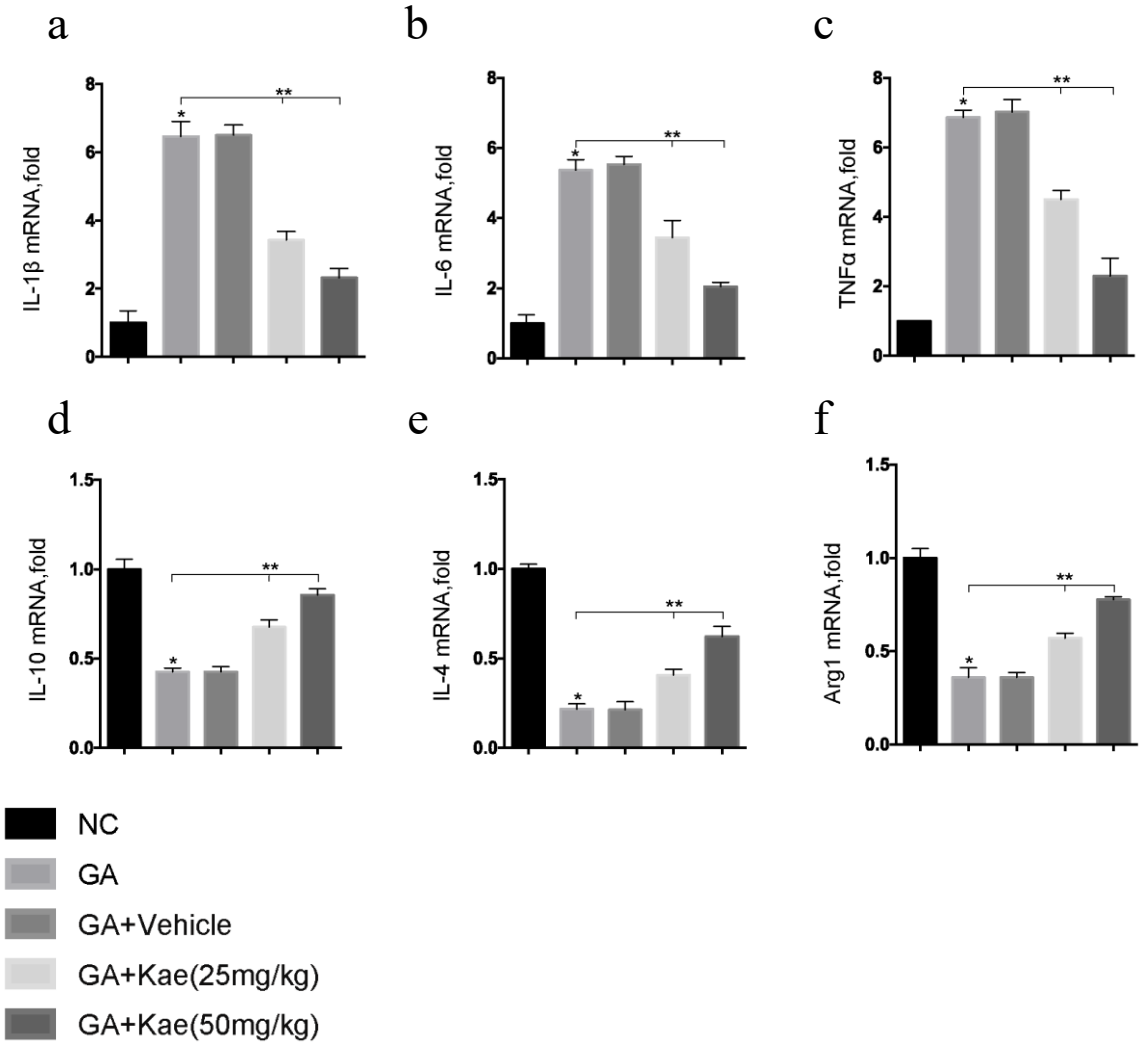

Figure 3.3. Kaempferol suppressed renal inflammation in vivo. (a-f) Measurements of mRNA levels in kidney via RT-qPCR. Data are the fold changes normalized to the NC group and are represented as mean±SD. $^{*}P<0.05$ versus NC group; $^{**}P<0.05$ as GA versus GA + Kae (25mg/kg) group, GA versus GA+Kae (50mg/kg) group, and GA+Kae (25mg/kg) versus GA+Kae (50mg/kg) group, respectively. Reproduced from (1) with permission of publisher (Elsevier GmbH).

Based on all above results, CaOx crystals might aggravate the oxidative damage and inflammation response with macrophage infiltration, which could be inhibited by

kaempferol, whereby 50 mg/kg kaempferol showed the strongest effect.

On the other hand, *in vitro*-experiments determined that the intracellular ROS level in HK-2 cell was increased after exposure to COM crystal, but was decreased when treated with kaempferol in a concertation-dependent fashion (Figure 4.1 a, b).

H_2O_2 and MDA were higher, while SOD and GSH were lower in HK-2 cell when received crystal intervention. This effect was reversible when treated with kaempferol in a dose-dependent fashion (Figure 4.1 c, d).

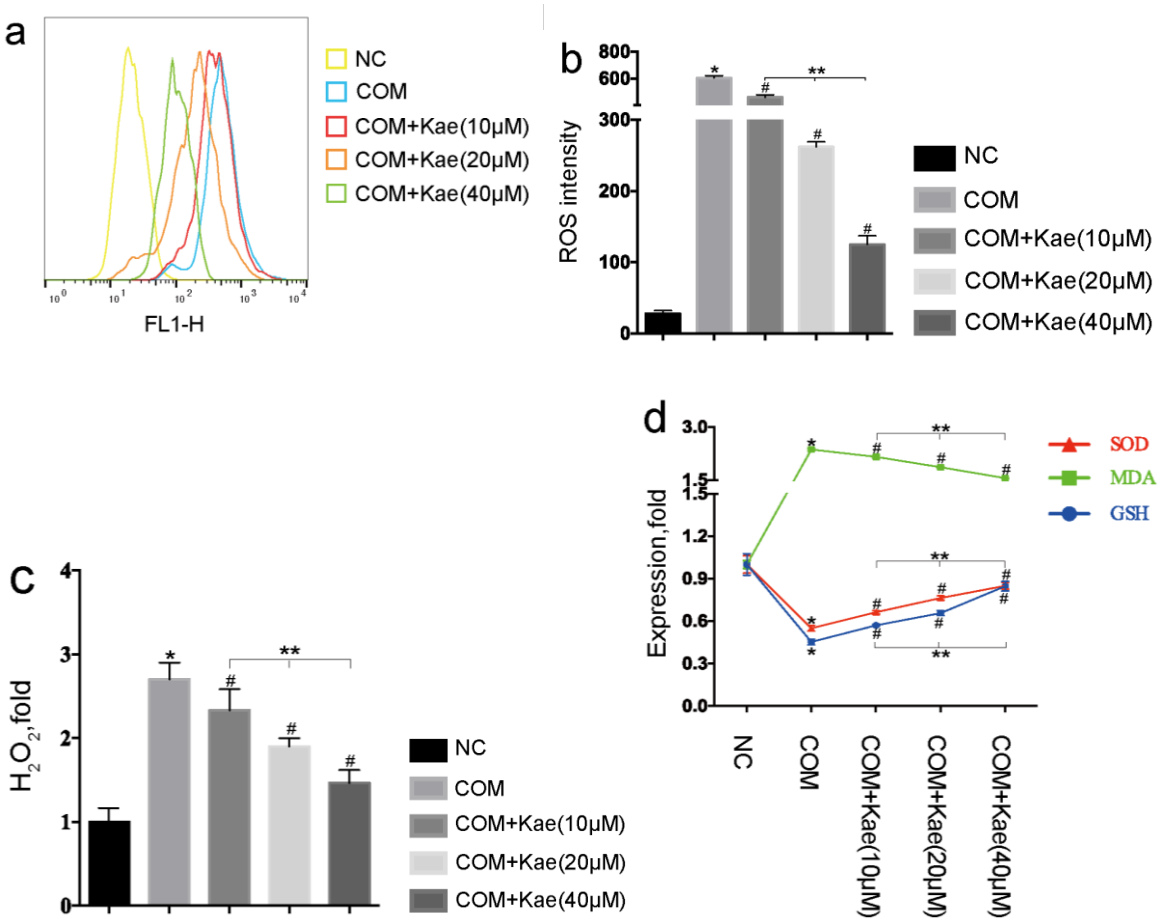

Figure 4.1. Kaempferol suppressed renal OS in vitro. (a-b) Detections of intracellular ROS levels via flow cytometry. (c) H_2O_2 levels. (d) Measurements of SOD, MDA and GSH levels. In a, c and d, data are expressed as the fold changes normalized to the NC

groups, and in b, data are quantitative data. Data are represented as mean±SD. *P<0.05 versus NC group; # P<0.05 versus COM group; **P<0.05 as pairwise comparisons between COM+Kae (10μM), COM+Kae (20μM) and COM+Kae (40μM). Reproduced from (1) with permission of publisher (Elsevier GmbH).

The RT-qPCR assay results demonstrated that enhanced expressions of TNF-α, IL-1β, IL-6, OPN and CD44, and suppressed expressions of Arg1, IL-4 and IL-10 were observed in HK-2 cell after the exposure to COM crystal when compared to the NC group. Again, kaempferol was able to reverse the observed changes in a dose-dependent manner (Figure 4.2 a-h).

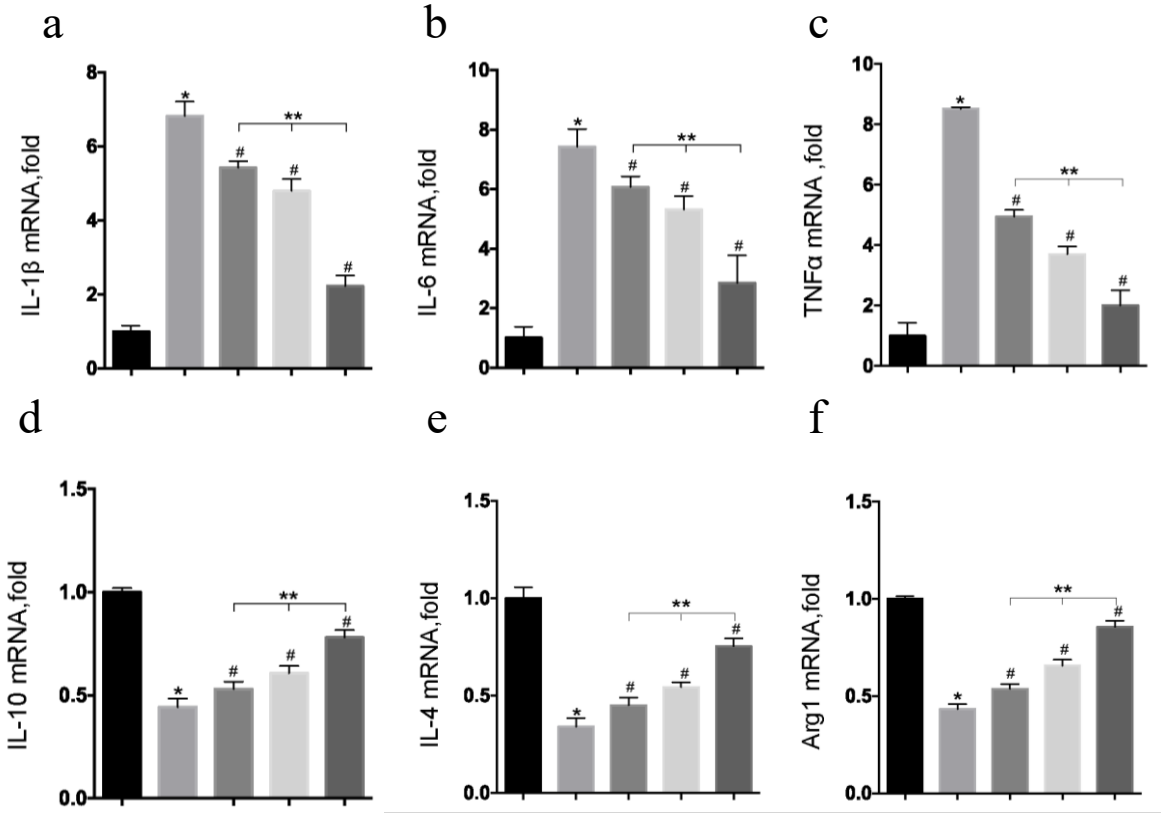

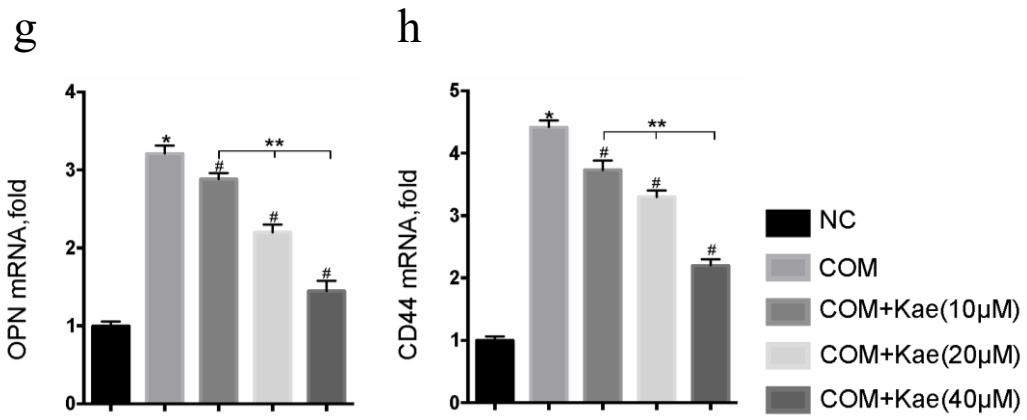

Figure 4.2. Kaempferol suppressed renal inflammation in vitro. (a-h) Measurements of the mRNA levels by RT-qPCR. Data are expressed as the fold changes normalized to the NC groups, and are represented as mean±SD. $^{*}P<0.05$ versus NC group; $^{\#}P<0.05$ versus COM group; $^{**}P<0.05$ as pairwise comparisons between COM+Kae (10μM), COM+Kae (20μM) and COM+Kae (40μM). Reproduced from (1) with permission of publisher (Elsevier GmbH).

Furthermore, we investigated the expressions patterns of NADPH oxidase family in HK-2 cell under different treatments. Consequently, NOX2 was the most significant overexpression when stimulated by COM crystals, while the expression was markedly decreased after the treatment with kaempferol. In summary, the anti-inflammatory and antioxidative stress effect of kaempferol in suppressing the renal injury induced by COM crystals might be mediated through NOX2-involved pathway (Figure 4.3 a).

By using WB analysis, we further found out that the MCP1, p-NFκB-P65 and iNOS expressions in HK-2 cell were markedly decreased in kaempferol-treated groups than COM group. Again, kaempferol reduced the observed increased expressions in a concertation-dependent fashion with the strongest effect of 40μM. Interestingly, we also

found out that the NOX2 expression in HK-2 cell was markedly decreased in kaempferol-treated groups than COM group, whereby 40μM kaempferol reflected the strongest effect (Figure 4.3 b, c).

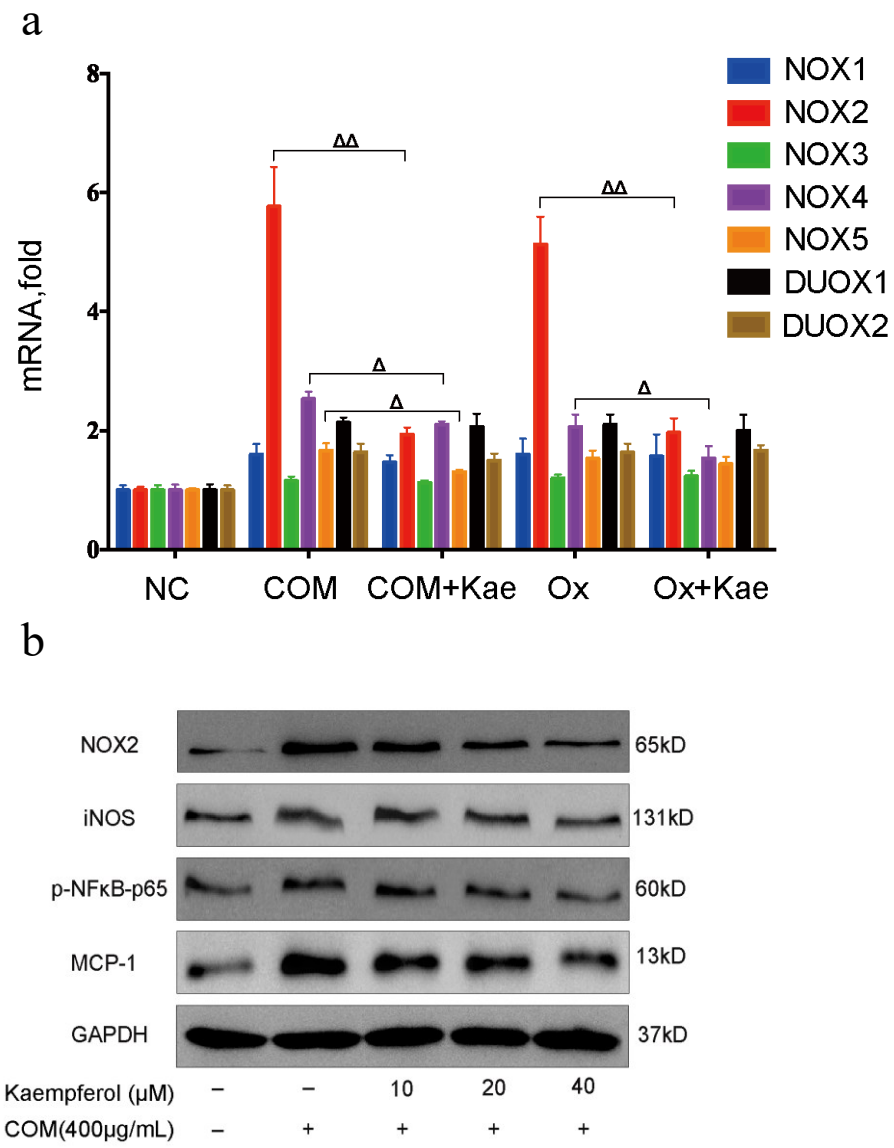

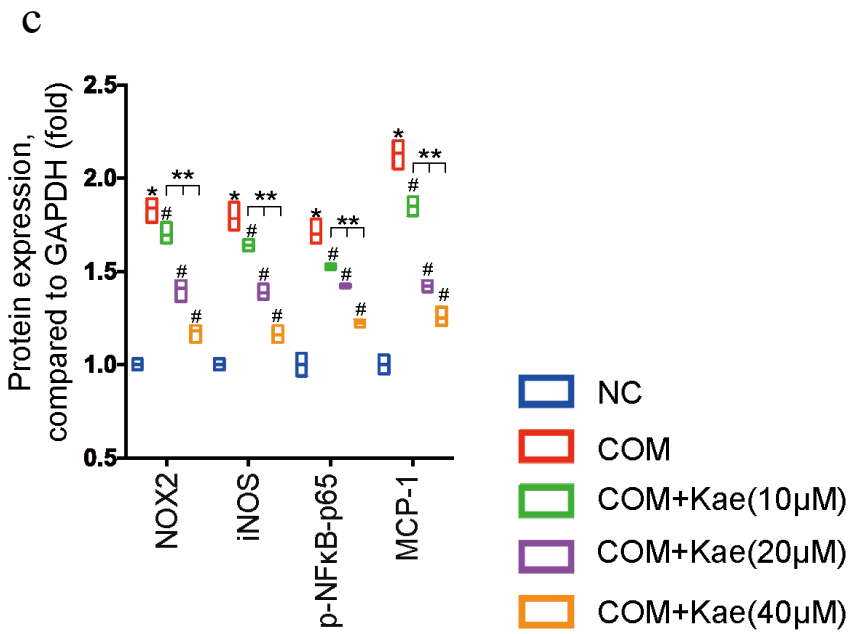

Figure 4.3. Kaempferol might suppress renal OS and inflammation by mediating the expression of NOX2 in vitro. (a) Measurements of the NOX subunits by RT-qRCR after exposed to COM crystal (400μg/mL) or 0.5mM oxalate with or without treatment of kaempferol (40μM) for 12h. (b, c) Measurements of the expressions of genes in HK-2 cell via performing WB. Data are expressed as the fold changes normalized to the NC group, and are represented as means ± SD. $^{\Delta}P<0.05$; $^{\Delta\Delta}P<0.01$; $^{*}P<0.05$ versus NC group; $^{\#}P<0.05$ versus COM group; $^{**}P<0.05$ as pairwise comparisons between COM+Kae (10μM), COM+Kae (20μM) and COM+Kae (40μM). Reproduced from (1) with permission of publisher (Elsevier GmbH).

According to the above results, we believed that kaempferol could inhibit OS and inflammation resulted from CaOx crystals both *in vivo* and *in vitro*.

3.4. Possible mechanisms on how kaempferol inhibited NOX2 expression via mediating AR expression

To detect whether kaempferol might inhibit renal AR expression, we firstly underwent animal experiments, in which an AR-overexpressed model was set up by intramuscular injection of testosterone propionate. The renal AR expression in the murine kidney was increased after receiving testosterone propionate compared to NC group and the vehicle group which was used in the drug dissolution had no significant effect on AR expression. But the kaempferol treatment was able to markedly inhibit the renal AR expressions in a dose-dependent fashion in mice (Figure 5.1 a, b).

Moreover, it was demonstrated that kaempferol reduced renal AR mRNA expression in mice by using RT-qPCR assay (Figure 5.1 c).

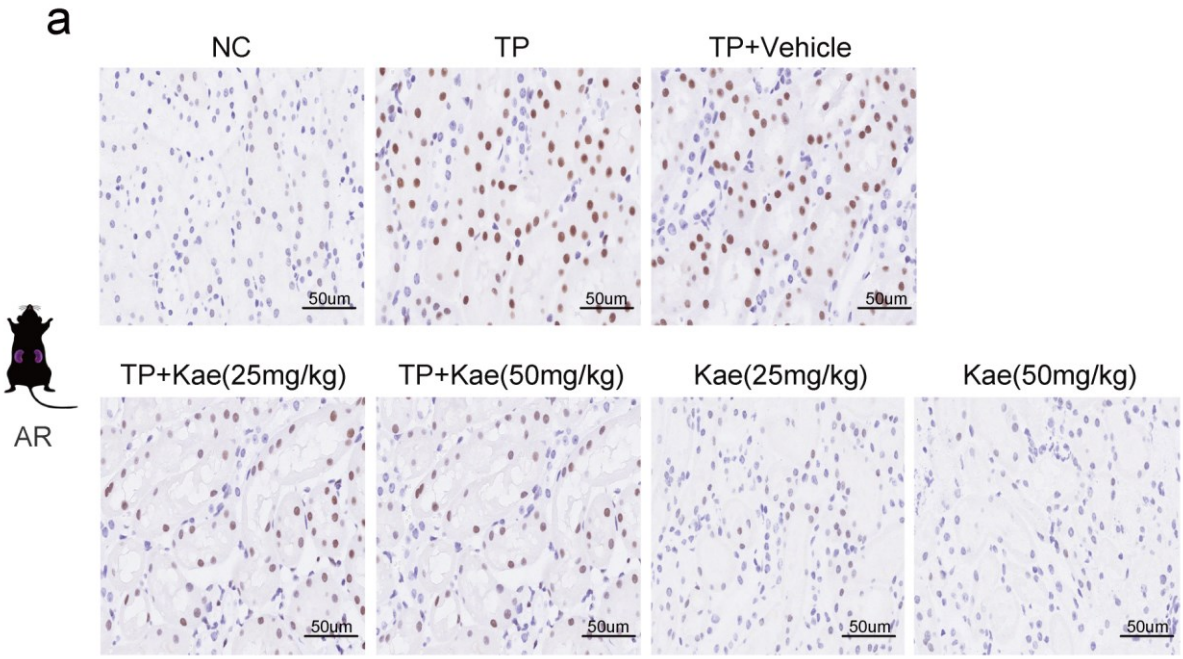

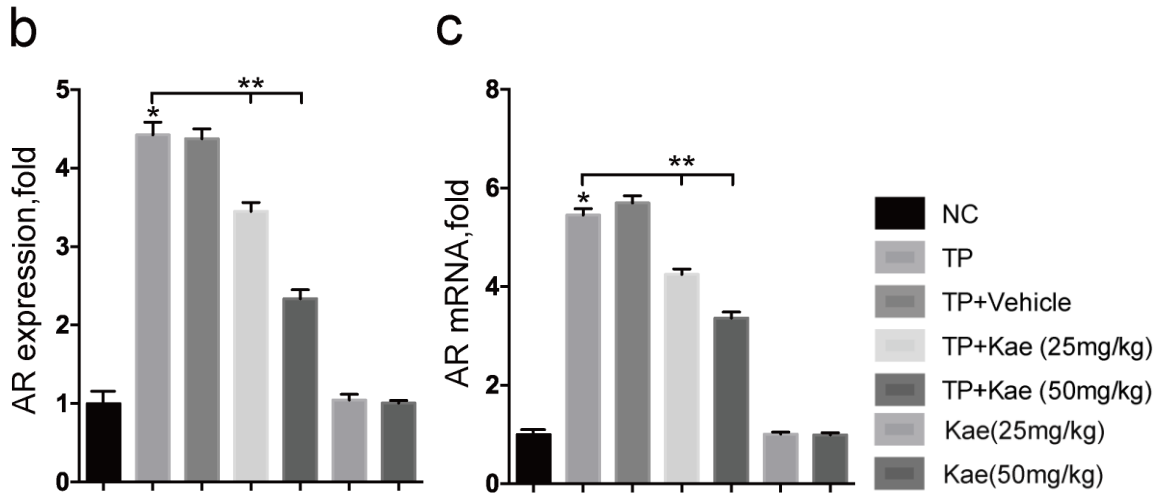

Figure 5.1. Kaempferol inhibited renal AR expression. (a, b) IHC stainings, and (c) RT-qPCR assay were respectively performed to detect the expressions of AR in tubular epithelial cell in male mice (n=8 per group). Data are expressed as the fold changes normalized to NC group, and data are represented as mean±SD. $^{*}P<0.05$; $^{**}P<0.05$ as comparisons by pairs among the three groups. Reproduced from (1) with permission of publisher (Elsevier GmbH).

Consistent with these findings, by assays of WB and RT-qPCR on HK-2 cells, we confirmed that kaempferol was able to decrease the AR expressions resulted from DHT administration in a concentration-dependent manner (Figure 5.2 a-c). It is worth noting that the alone kaempferol treatment did not markedly influence the basal expression level of renal AR.

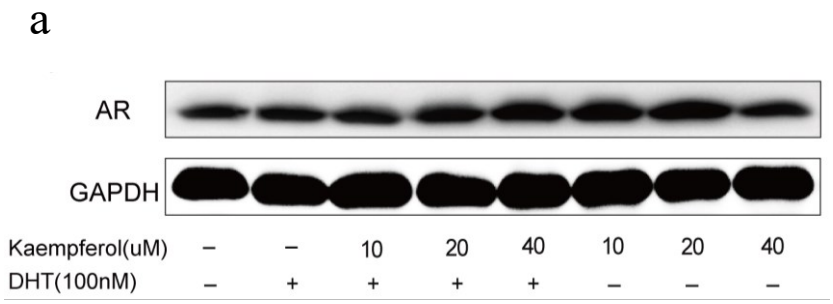

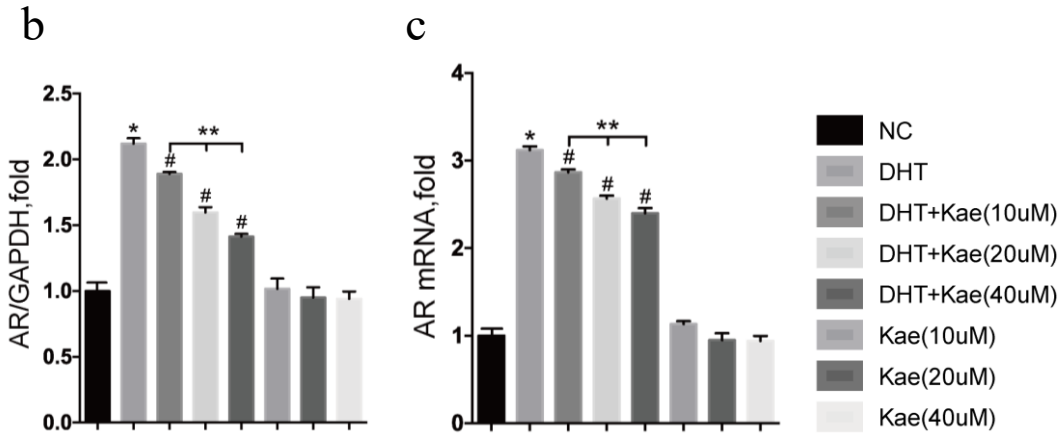

Figure 5.2. Kaempferol inhibited AR expressions in HK-2 cell. (a, b) WB, and (c) RT-qPCR assay were conducted to measure the expressions of AR in HK-2 cell. Data are expressed as the fold changes normalized to NC group, and data are represented as mean±SD. $^{*}P<0.05$; $^{\#}p<0.05$ versus DHT group; $^{***}P<0.05$ as comparisons by pairs between the three groups. Reproduced from (1) with permission of publisher (Elsevier GmbH).

Taken these data together, in AR-overexpression model, we found that kaempferol played a crucial positive role in inhibiting the AR expressions in tubular epithelial cells. Again, the higher the concentration, the stronger anti-AR ability of kaempferol could be observed.

Immunofluorescence results indicated that the expressions of AR and NOX2 were instantaneously significantly higher after treated with COM and DHT, while they were markedly lower after treated with kaempferol (Figure 5.3 a, b).

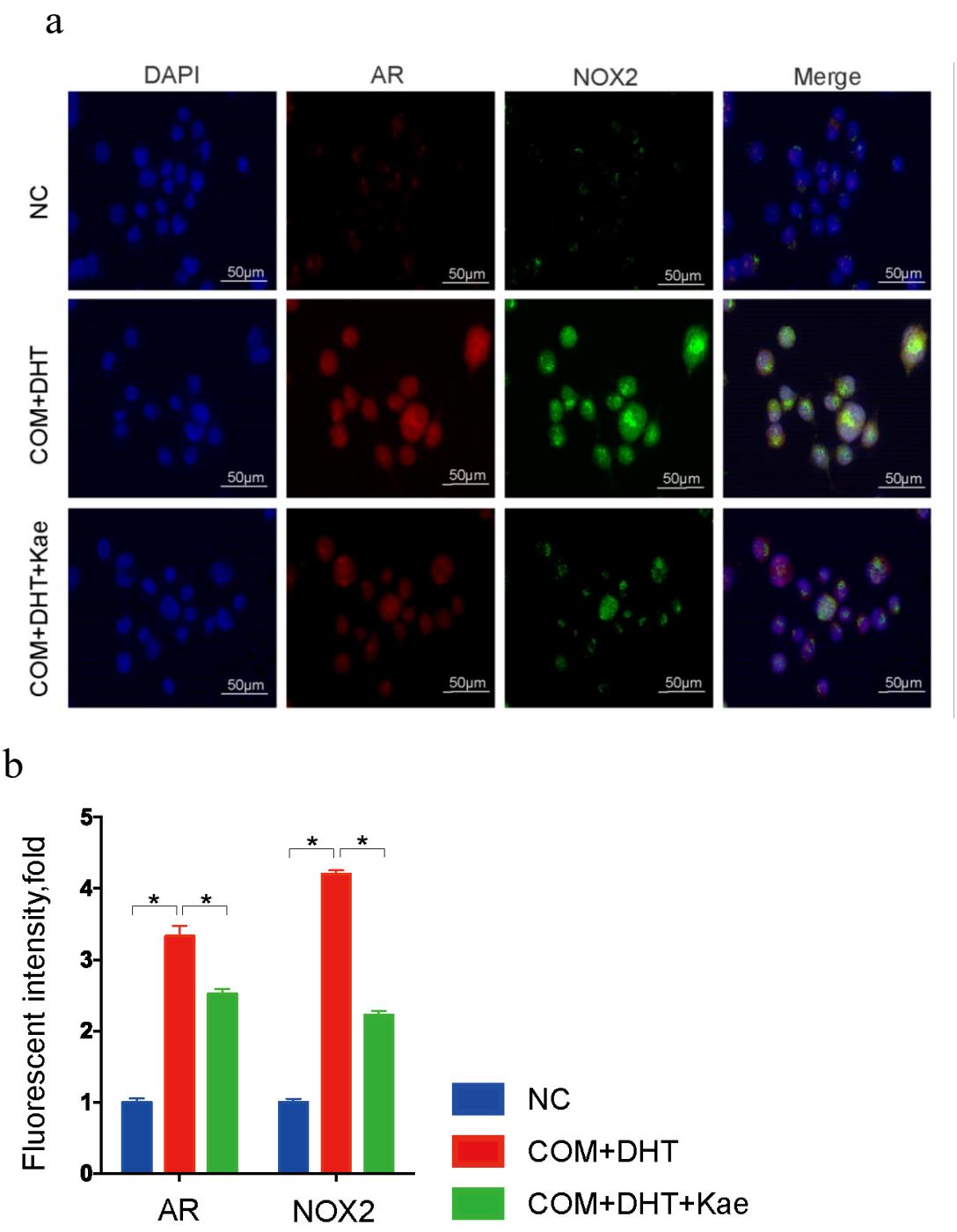

Figure 5.3. Kaempferol suppressed NOX2 and AR expressions with the same trend. (a, b) The expressions of NOX2 (green) and AR (red) in HK-2 cells were detected by IF. Data are expressed as the fold changes normalized to NC group, and data are represented as means ± SD. $^{*}P<0.05$. Reproduced from (1) with permission of publisher (Elsevier GmbH).

For exploring whether the AR might enhance NOX2 upregulation by a transcriptional mechanism, within the 2000bp of the upstream region of promoter of NOX2, one possible ARE was selected by performing the JASPAR database. ChIP assays were performed on HK-2 cells, and finally we found out that AR was able to bind to the ARE which was at -1822bp to -1808 bp in the upstream region of the transcriptional start site of NOX2 (Figure 5.4a).

Moreover, the luciferase reporter assay was performed on HK-2 cell, and the results suggested that only the luciferase expression of wild-type NOX2 promoter construct was markedly decreased after treated with kaempferol compared to COM+DHT group while no significant change was found with the mutated-type NOX2 promoter construct (Figure 5.4 b, c).

a

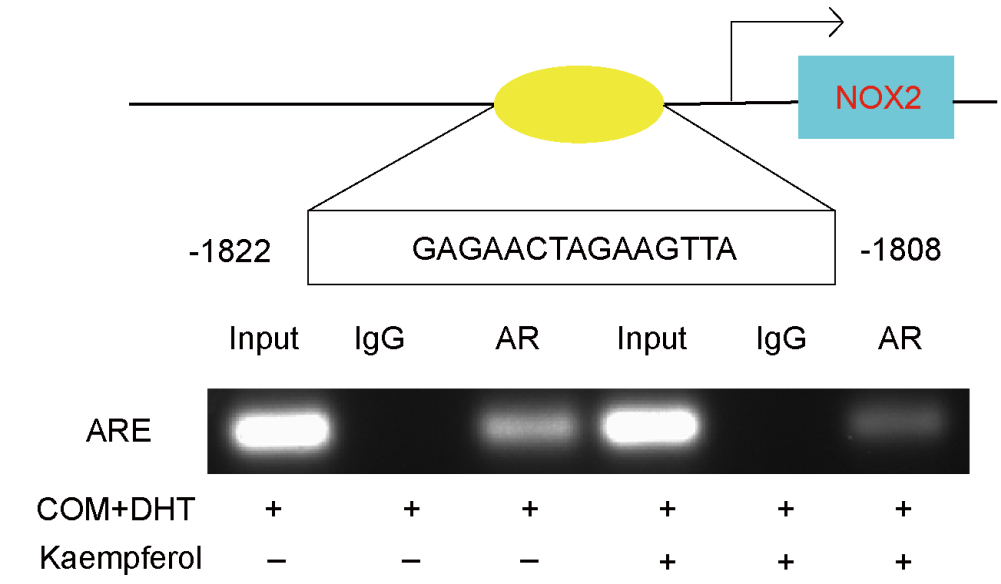

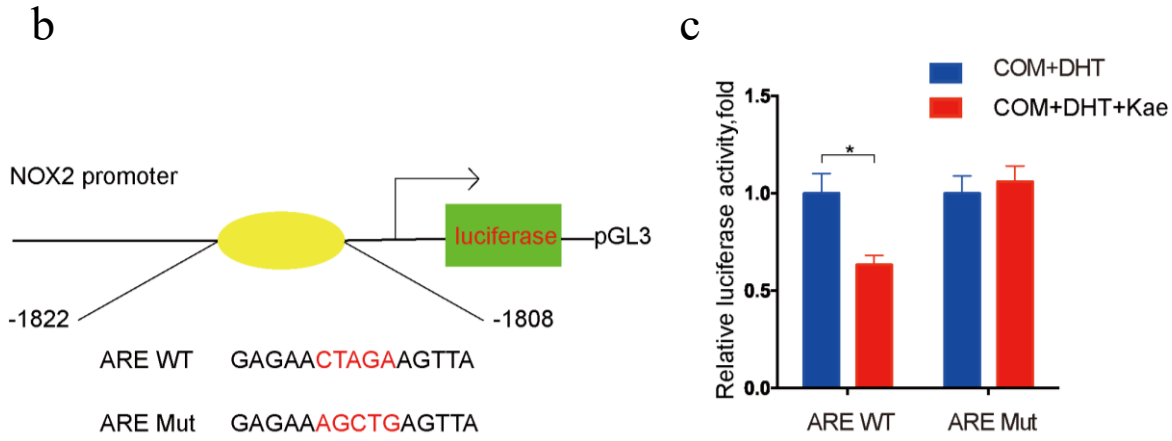

Figure 5.4. AR could enhance NOX2 expression at the transcriptional level by binding to the promoter region of NOX2. (a) CHIP assays were conducted in lysates of HK-2 cells. ARE enrichment was confirmed via qPCR. (b, c) Luciferase reporter assays. Data are expressed as the fold changes normalized to the control group, and data are represented as means ± SD. $^{*}P<0.05$. Reproduced from (1) with permission of publisher (Elsevier GmbH).

In summary, the above results of the *in vitro*-experiments demonstrate that AR contributes to NOX2 up-regulation, and kaempferol could inhibit NOX2 expression at the transcriptional level via decreasing AR expression.

3.5. Kaempferol ameliorates CaOx crystal deposition, tubular injury, and OS and inflammation induced by CaOx crystals by regulating the AR/NOX2 pathway in murine kidneys

The results of HE, Pizzolato, PAS, TUNEL and IHC staining examination of murine kidneys showed that crystal deposition, tubular injury, and CD44 and OPN expression levels were markedly promoted in the GA+TP group compared with the GA group. On the

other hand, the added kaempferol treatment was able to reverse the above effects, whereby 50 mg/kg kaempferol had a better suppressive role than 25 mg/kg kaempferol (Figure 6.1 a-g).

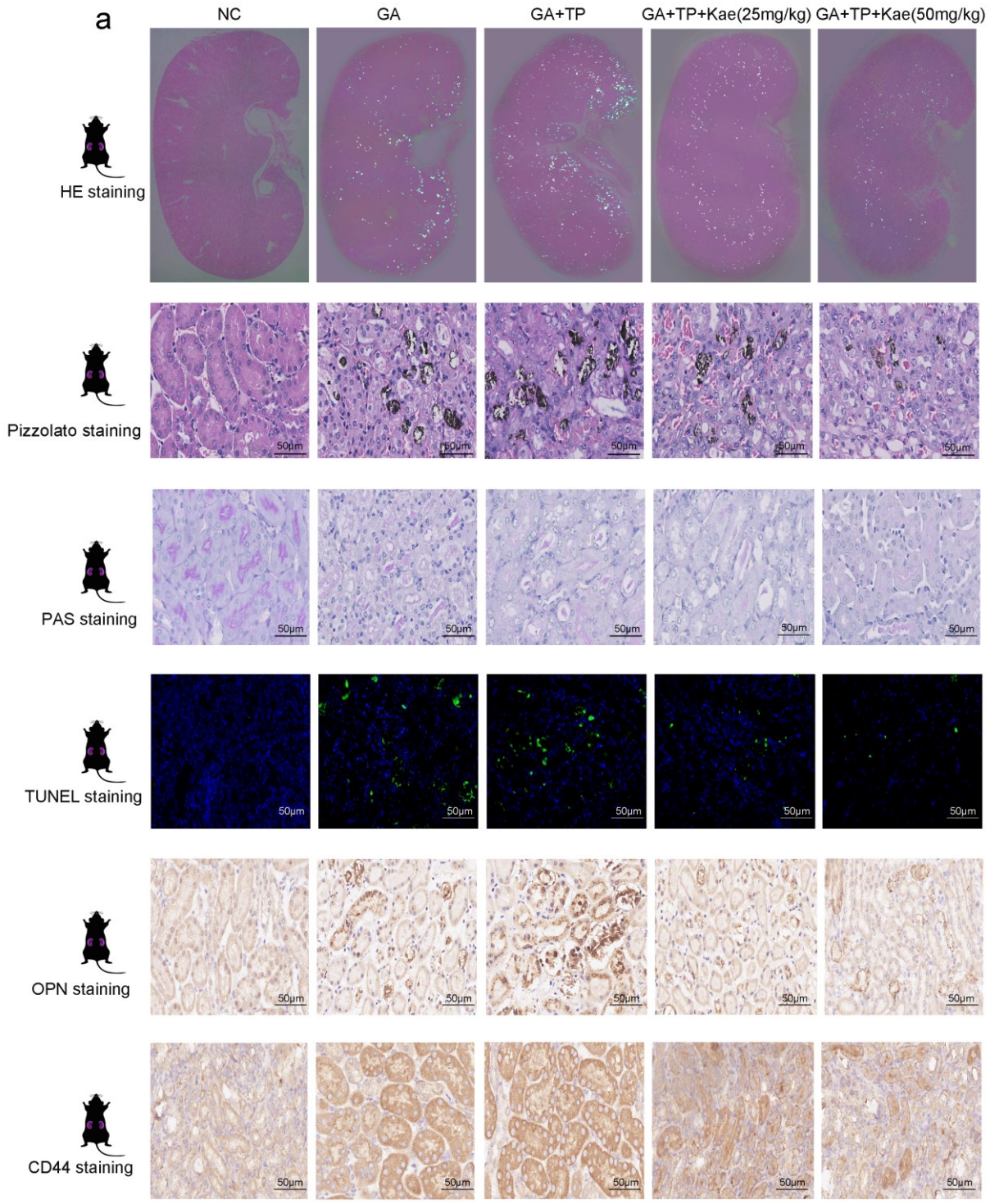

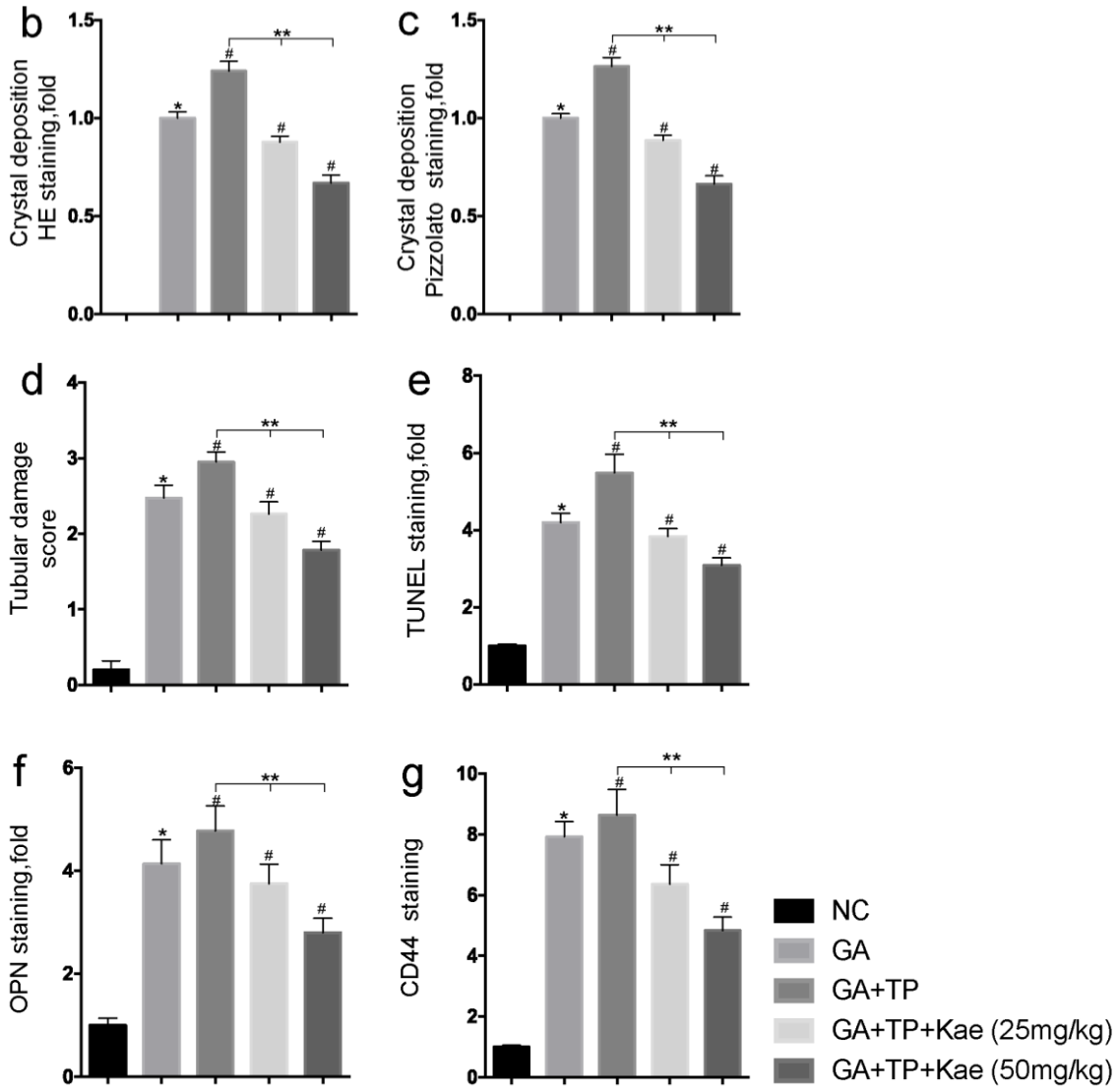

Figure 6.1. Kaempferol ameliorated CaOx crystal deposition and tubular injury by regulating the AR/NOX2 pathways in mice kidney. Mice were assigned into 5 groups (n=8 per group). Then mice were sacrificed after 10 days administration for later experiments. (a) Images of tissue stainings, and (b-g) the quantitative analyses of HE stainings, Pizzolato stainings, PAS stainings, TUNEL stainings, and IHC stainings of OPN and CD44. Data are expressed as fold changes of the experimental groups with normalization to NC groups, and were represented as mean±SD. $^{*}P<0.05$ versus NC group; $^{\#}P<0.05$ versus GA group; $^{**}P<0.05$ as comparisons by pairs between three groups.

Reproduced from (1) with permission of publisher (Elsevier GmbH).

Moreover, serum BUN, Cr, and NGAL levels were markedly enhanced in the GA+TP group compared with GA group, while the levels were markedly suppressed in the kaempferol-treated group than in the GA group or GA+TP group (Figure 6.2 a-c).

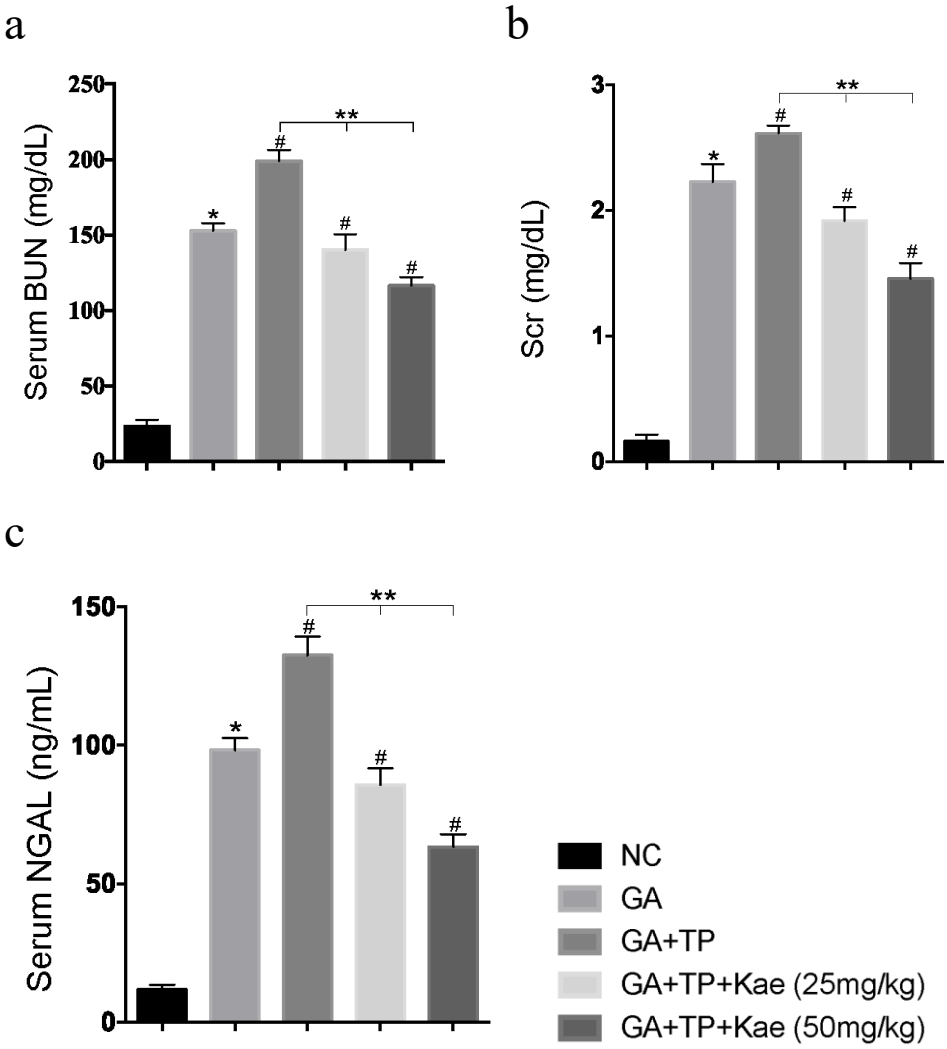

Figure 6.2. Kaempferol ameliorated acute kidney injury by regulating the AR/NOX2 pathways in mice. (a-c) Serum levels of NGAL, BUN and Cr were detected. Data are expressed as fold changes of the experimental groups with normalization to the NC group, and were represented as mean±SD. $^{*}P<0.05$ versus NC group; $^{\#}P<0.05$ versus GA group; $^{**}P<0.05$ as comparisons by pairs between three groups. Reproduced from (1) with

permission of publisher (Elsevier GmbH).

Additionally, these results indicated that the expression of AR, NOX2, iNOS, NFκB-p65, or F4/80 in mice tubular cells was markedly increased in GA+TP group compared with GA group. But, kaempferol treatment was able to reverse the effect (Figure 7.1 a-f).

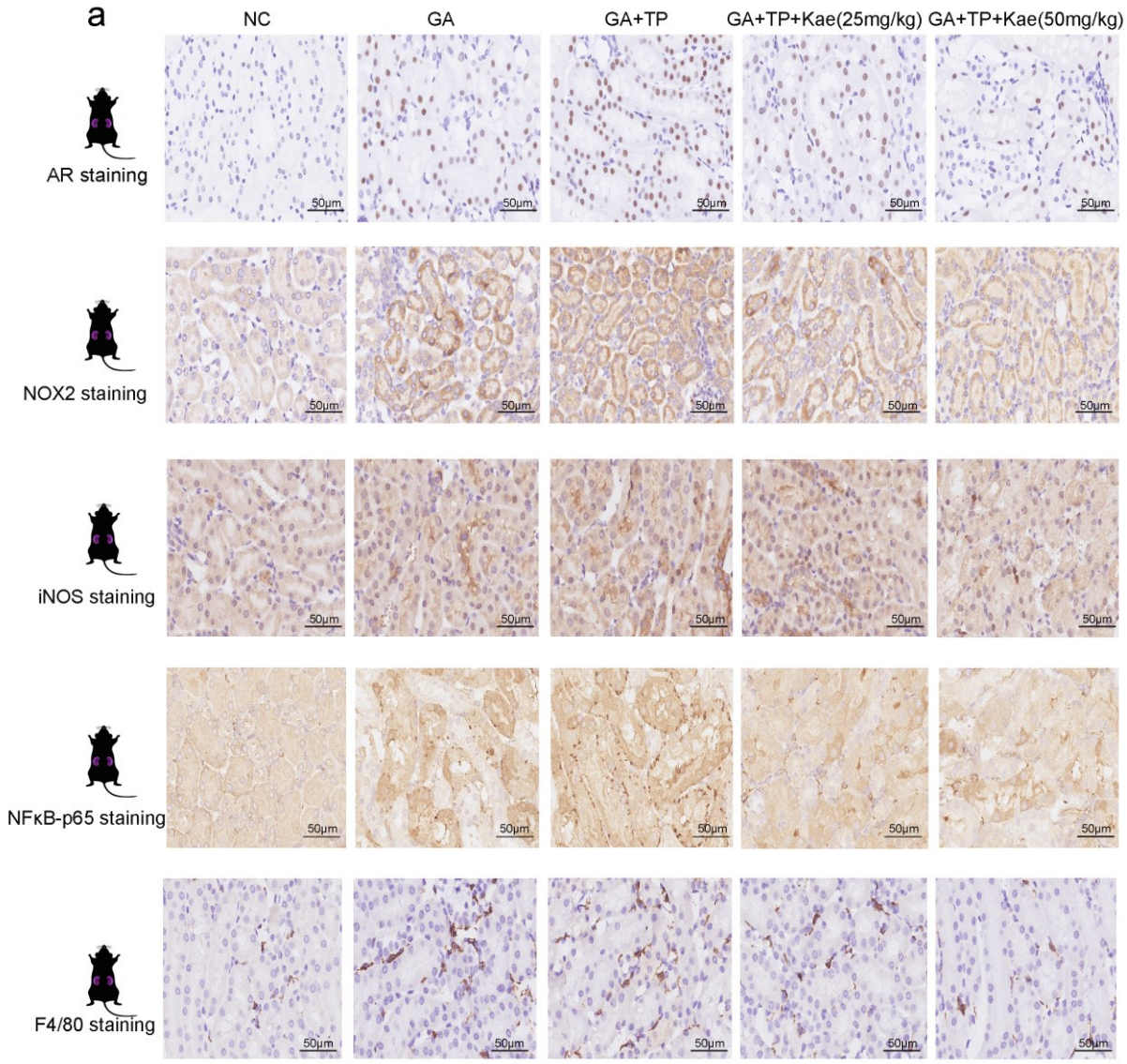

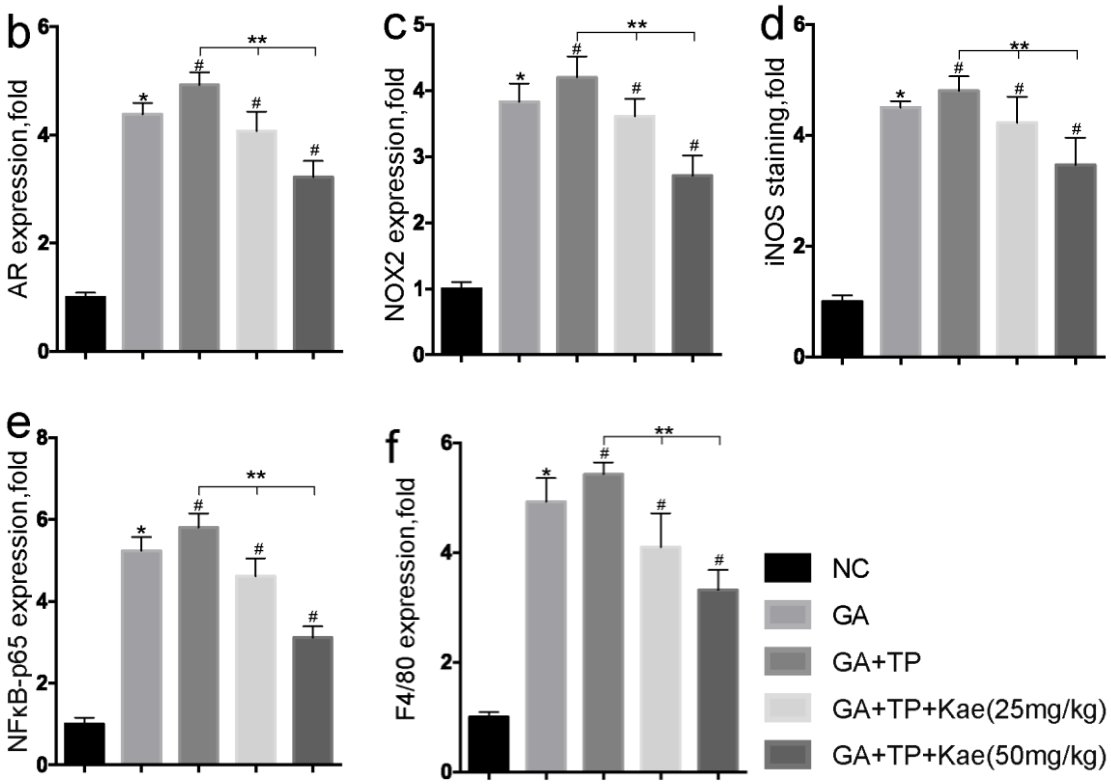

Figure 7.1. Kaempferol inhibited renal OS and inflammation induced by CaOx crystals by downregulating AR/NOX2 pathway in mice. (a) Images of IHC staining, and (b-f) quantitative analyses of IHC staining of AR, NOX2, iNOS, NFκB-p65, and F4/80. Data are fold changes of experimental groups with normalization to NC groups, and were represented as mean±SD. $^{*}P<0.05$ versus NC group; $^{\#}P<0.05$ versus GA group; $^{**}P<0.05$ as comparisons by pairs between three groups. Reproduced from (1) with permission of publisher (Elsevier GmbH).

Moreover, ROS, H_2O_2 and MDA levels in murine kidney were markedly higher, while SOD and GSH were markedly lower in GA and TP group compared with GA treatment group, while these changes were reversed with kaempferol treatment, whereby 50mg/kg kaempferol had a much more significant effect than 25mg/kg dose (Figure 7.2 a-c).

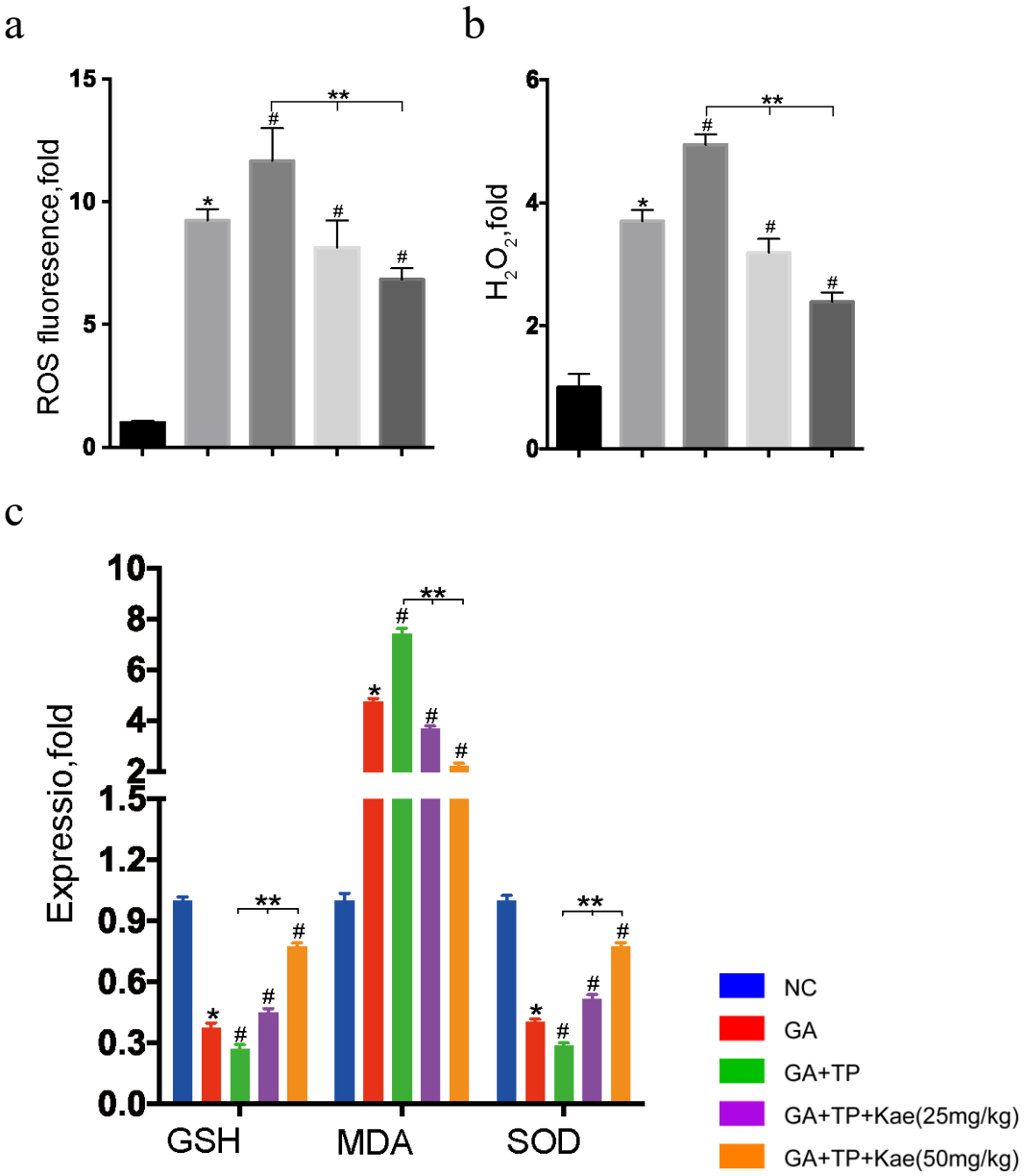

Figure 7.2. Kaempferol inhibited renal OS induced by CaOx crystals by downregulating AR/NOX2 pathway in mice. (a) ROS levels in kidney were measured with fluorescence microplates. (b) Measurement of H_2O_2 levels. (c) Measurements of GSH, SOD, and MDA levels. Data are fold changes of experimental groups with normalization to NC groups, and were represented as mean±SD. $^{*}P<0.05$ versus NC group; $^{\#}P<0.05$ versus GA group; $^{**}P<0.05$ as comparisons by pairs between three groups. Reproduced from (1) with permission of publisher (Elsevier GmbH).

In the next step, we used RT-qPCR to confirm that TNF-α, IL-6 and IL-1β levels in kidney tissues were markedly higher, and the Arg1, IL-4, IL-10 levels were markedly suppressed in GA+TP group than in GA group. But these above effects could be reversed in kaempferol-treated group (Figure 7.3 a-fj-o).

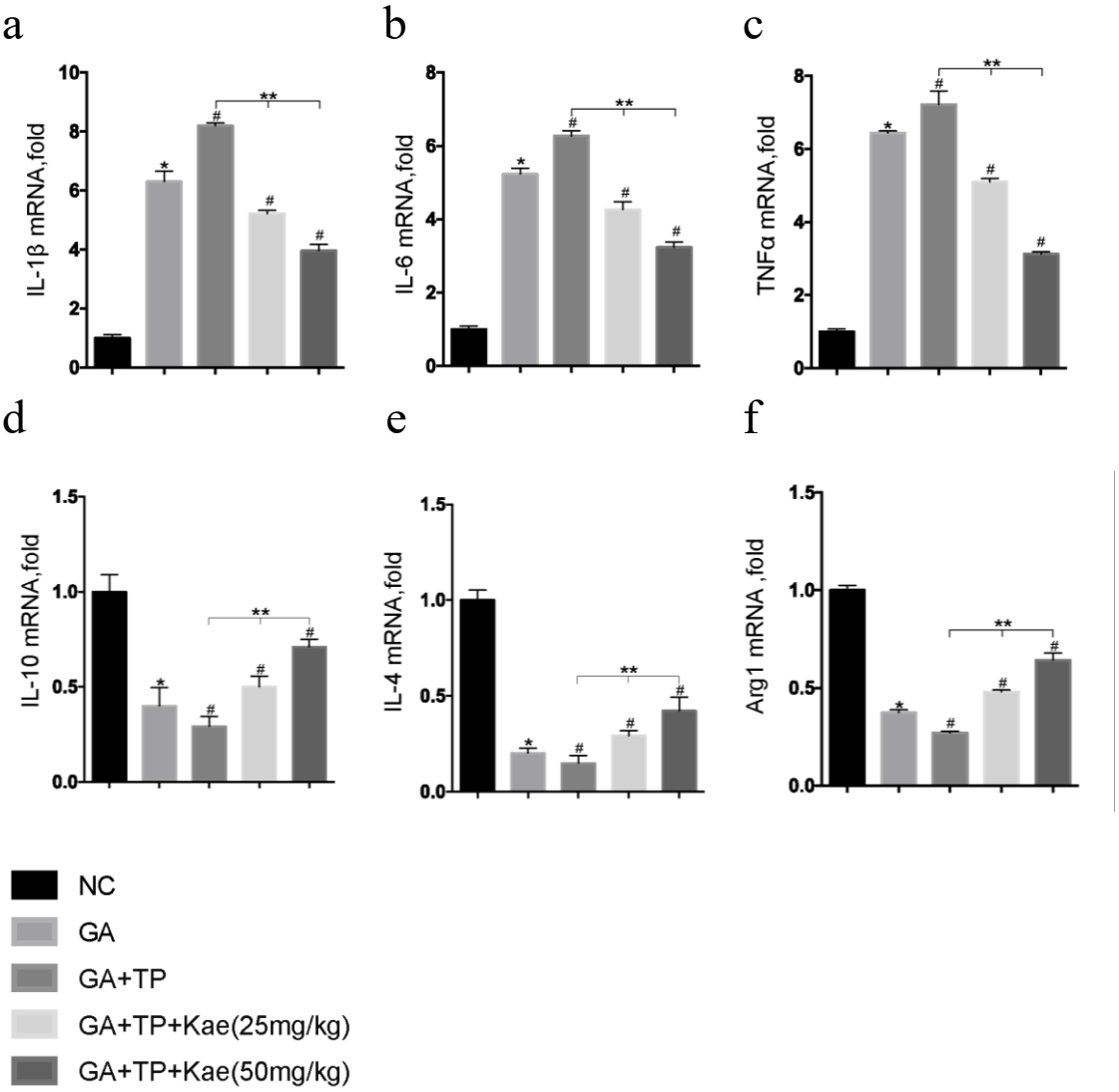

Figure 7.3. Kaempferol inhibited renal inflammation induced by CaOx crystals by downregulating AR/NOX2 pathway in mice. (a-f) Measurement of mRNA level of Arg1, IL-4, IL-10, TNF-α, IL-1β, or IL-6 via RT-qPCR. Data are fold changes of experimental groups with normalization to NC group, and were represented as mean±SD. $^{*}P<0.05$

versus NC group; #P<0.05 versus GA group; **P<0.05 as comparisons by pairs between three groups. Reproduced from (1) with permission of publisher (Elsevier GmbH).

Based on these above experimental results, it was indicated that the AR might be able to further aggravate CaOx crystal-induced inflammatory and oxidative damage in renal tubules by increasing the expression of NOX2, which subsequently promoted the CaOx crystal deposition on renal tubular cells. The inflammation response might be aroused by the secretion of inflammatory factors and the infiltration of macrophages mediated by NFκB pathway. Nevertheless, kaempferol could effectively alleviate these worsened changes by regulating the AR/NOX2 pathways.

3.6. Kaempferol suppressed cell injury, crystal-cell adhesion, OS, and inflammation induced by CaOx crystals by downregulating AR/NOX2 pathway in HK-2 cells

First, we found that the crystal adhesion was increased after the exposure to both COM and DHT compared with only COM. At the same time, crystal adhesion was markedly lower after treated with kaempferol (10 μM and 40 μM) (Figure 8.1 a).

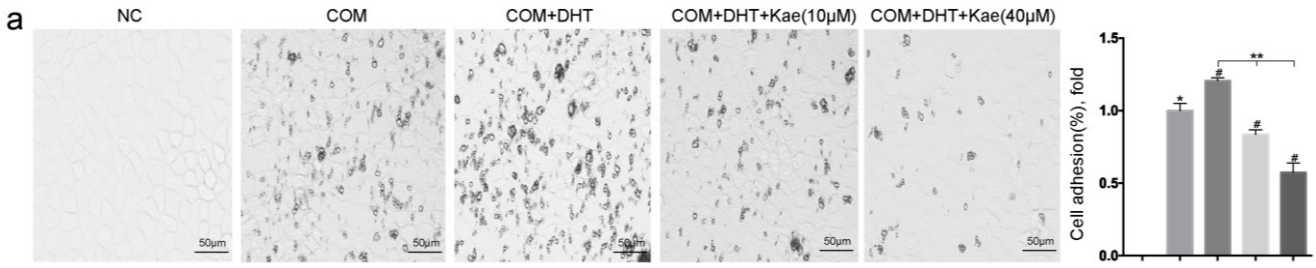

Figure 8.1. Kaempferol suppressed crystal-cell adhesion to HK-2 cells by downregulating AR/NOX2 pathway. (a) Measurement of COM crystals adhesion to HK-2

cell. Data are fold changes normalized to NC group, and are represented as mean±SD. *P<0.05 versus NC group; # P<0.05 versus COM group; **P<0.05 as pairwise comparisons of three groups. Reproduced from (1) with permission of publisher (Elsevier GmbH).

Afterwards, we were able to confirm that cell death, levels of ROS and H_2O_2 in HK-2 cell after both two administrations, the overexpression of AR after DHT treatment and exposure to COM crystal, were significantly higher than after only the exposure to COM crystals without AR overexpression, indicating that the AR promoted to COM crystal-induced OS in HK-2 cell; but with added kaempferol treatment, the oxidative injury decreased and 40 μM kaempferol showed a better improvement (Figure 8.2 a-c).

Also, we found that MDA level was increased, however the level of SOD or GSH was decreased after exposure to both DHT and COM crystals in HK-cells when compared with the group exposed to COM crystals alone without an AR-overexpression. But, with added kaempferol treatment, the above changes were reversed (Figure 8.2 d).

a

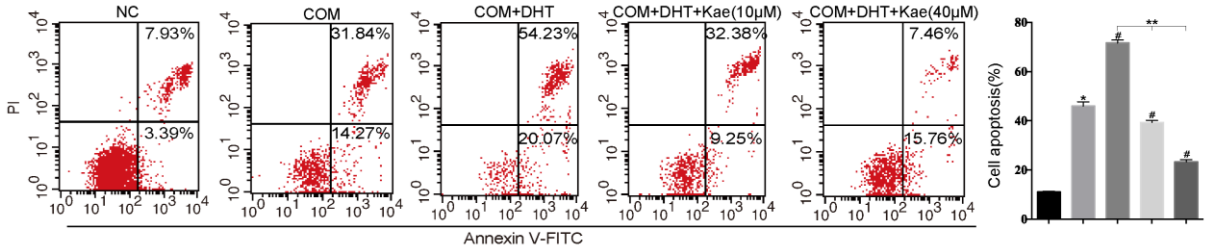

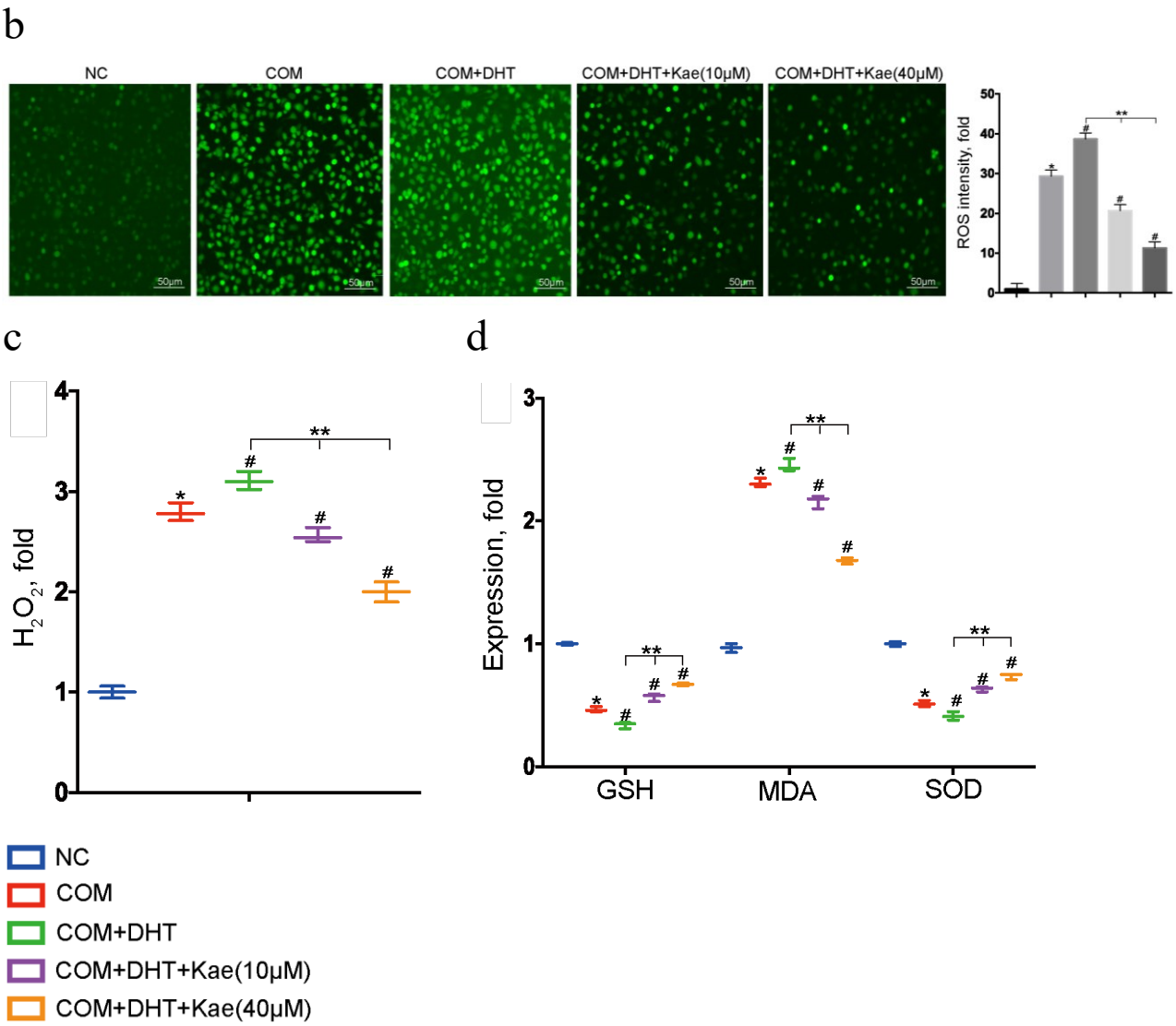

Figure 8.2. Kaempferol suppressed cell death and OS induced by CaOx crystals by downregulating AR/NOX2 pathway in HK-2 cell. (a) Measurement of apoptosis of HK-2 cells via flow cytometry. (b) Measurement of intracellular ROS level by fluorescence microscope. (c) Measurement of H_2O_2 level. (d) Measurement of levels of MDA, SOD and GSH. In a, data are quantitative data, and in b, c and d, data are the fold changes normalized to NC group. Data are represented as mean±SD. $^{*}P<0.05$ versus NC group; $^{\#}P<0.05$ versus COM group; $^{**}P<0.05$ as pairwise comparisons of three groups. Reproduced from (1) with permission of publisher (Elsevier GmbH).

Moreover, these RT-qPCR results indicated that CD44, OPN, IL-1β, IL-6 and TNF-α expressions were markedly increased, however IL-4, IL-10, and Arg1 expressions were markedly decreased in DHT+COM group compared with COM group. Finally, in the DHT + COM + kaempferol group, the above changes were reversed by kaempferol treatment (Figure 8.3 a-h).

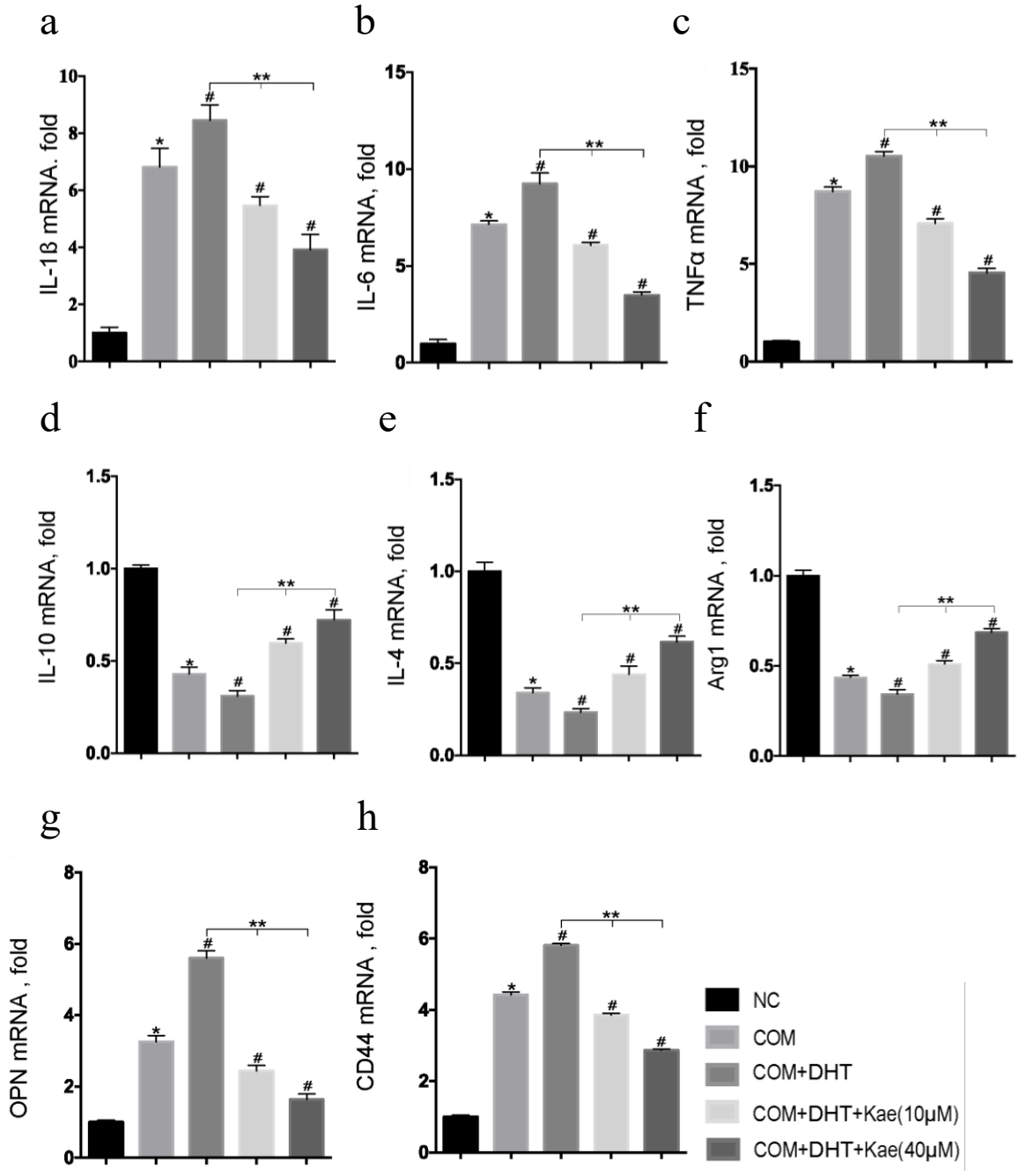

Figure 8.3. Kaempferol suppressed inflammation induced by CaOx crystals by

downregulating AR/NOX2 pathway in HK-2 cells. (a-h) Measurement of IL-10, IL-4, Arg1, IL-1β, IL-6, TNF-α, CD44 and OPN mRNA levels via RT-qPCR. Data are fold changes normalized to NC group, and are represented as mean±SD. $^{*}P<0.05$ versus NC group; $^{\#}P<0.05$ versus COM group; $^{**}P<0.05$ as pairwise comparisons of three groups. Reproduced from (1) with permission of publisher (Elsevier GmbH).

It was proved that secretions of inflammatory cytokines, as well as adhesion molecules could be promoted by crystal damage and AR overexpression, but it could be curbed by the treatment with kaempferol.

Finally, using WB assays, we discovered that the expressions of AR, NOX2, iNOS, p-NFκB-p65, Caspase-1 and MCP-1 were markedly promoted after treatment of COM and DHT than only COM. But, with synchronous kaempferol treatment, the above changes were reversed (Figure 8.4 a, b).

a

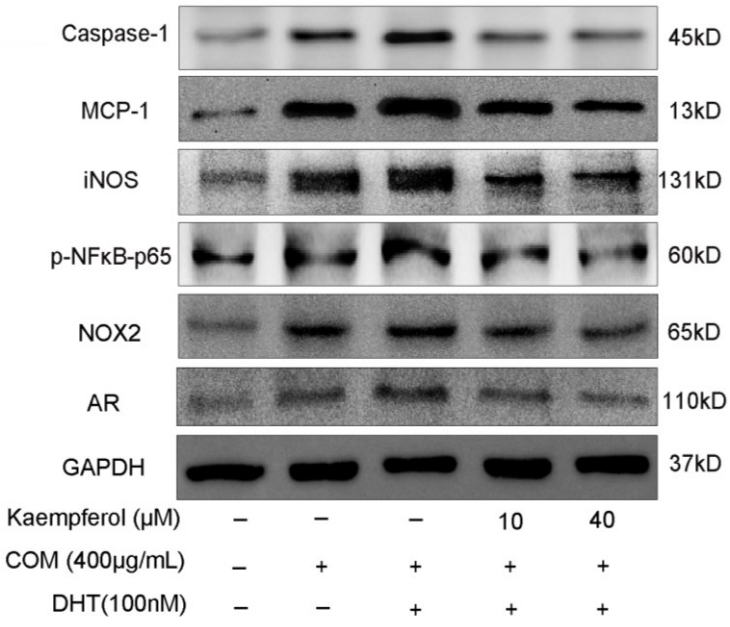

b

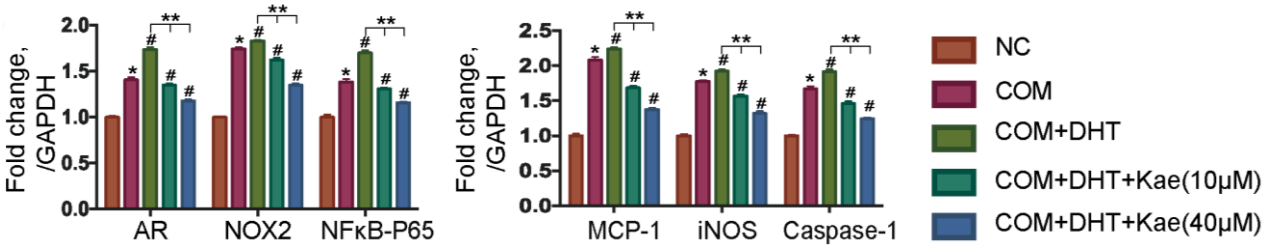

Figure 8.4. Kaempferol suppressed OS and inflammation induced by CaOx crystals by downregulating AR expression in HK-2 cell. (a, b) Measurement of AR, NOX2, p-NFκB-p65, iNOS, MCP-1 and Caspase-1 expressions via WB. Data are fold changes normalized to NC group, and are represented as mean±SD of three independent experiments. *P<0.05 versus NC group; $^{\#}$P<0.05 versus COM group; **P<0.05 as pairwise comparisons of these three groups. Reproduced from (1) with permission of publisher (Elsevier GmbH).

In summary, it was demonstrated that reduction of ROS, down-regulation of NFκB signal pathway and adhesion molecules, were involved in the antioxidative stress and anti-inflammatory role of kaempferol mediated by AR/NOX2 signal pathway, which might effectively suppress crystal-induced cellular injury and crystal adhesions to renal tubular epithelial cells.

4. Discussion

Nowadays, CaOx urolithiasis is considered as a chronic renal disease which over time can lead to heavy medical disorders throughout the rest of the patient's life (197). Growing incidence, heavy medical cost, various complications of surgery, as well as high recurrence rate have been continuously noticed by urology doctors despite the markedly developed minimally invasive procedures of surgery, like flexible ureteroscopy, percutaneous nephrolithotomy (PCNL) and extracorporeal shock wave lithotripsy (ESWL) (198). Therefore, potentially effective medicine therapy for preventing CaOx urolithiasis is strongly needed, demanding further ongoing researches to find effective and safe medicines.

CaOx crystals formation involves many essential steps, including nucleation, crystal growth, aggregation, and retention (15, 199). Any existing unfavorable influencing factors may as well result in the promotion of urolithiasis. There are a few anti-urolithiasis drugs, which have been applied to promote the dissolution of cystine and uric acid kidney stones based on the unique pharmacological properties to increase urine PH (49, 200). Unfortunately, so far, no efficacious drugs can dissolve CaOx stones in a direct way. Therefore, several research groups have attempted to find potentially available drugs that may prevent the deposition and formation of CaOx stones.

Several common and similar characteristics between atherosclerosis and urolithiasis were found due to the common calcification components OPN, calcium and phosphate acid (201). The highest prevalence of these two diseases are found in postmenopausal females,

and elderly and middle-aged males (202-205), in which cytokines and macrophage are closely involved (206). Because of the high incidence of kidney stones in developed countries and regions, western eating habits are considered to be the primary cause (207). It has been reported that excess intake of cholesterol could cause urinary stones, and OPN expression in tubular cell was promoted in a rat model on a 3% cholesterol diet (208). EPA, a medicine for treating atherosclerosis, was reported to decrease OPN expression and suppress stone formations in rats and humans (209, 210). Moreover, excess cholesterol intake could promote the binding of cholesterol to intestinal bile acid, which increased the release of oxalic acid and subsequently increased the absorption in the gut, leading to increased urinary excretion of oxalic acid (211, 212). Abnormal lipid metabolism of KSF was found in clinical practice with increased serum cholesterol levels (213, 214). Aortic wall calcification wall detected by computed tomography was found in approximately 40% stone disease patients compared with a 5% in healthy population (215). EPA is an efficient treatment for preventing hyperlipidemia and atherosclerosis, so EPA may be one potential therapeutic option to prevent renal CaOx stone formation in clinical practice.

Adipocytes can secret adipocytokines, which plays a crucial role in metabolic syndrome (216, 217). A previous study revealed that the expression of adiponectin was reduced in tubular cells in renal stone mice model while the expression of OPN was elevated, resulting in kidney stone formation (218). The renal expression of OPN was significantly elevated, and renal stone formation was observed in leptin-deficient mice model; at the same time, adiponectin was found to suppress renal stone formation in the model (218). Because adiponectin can prevent atherosclerosis, adiponectin may be another potential

preventive treatment option for urolithiasis (216). Therefore, anti-obesity drugs may also have potential preventive efficiency for treating kidney stones.

Pioglitazone is a PPARγ agonist, and is usually used as a treatment for mellitus diabetes by improving insulin sensitivity, and it owns antioxidative stress and anti-inflammatory effects. A previous epidemiological study revealed that serum insulin level and insulin resistance were correlated with kidney stone disease in female patients (219). One study demonstrated pioglitazone could suppress CaOx crystal deposition via anti-inflammatory effect, antioxidative stress effect and renal tubular cell protection in mice model, and renal stones were significantly fewer and smaller with pioglitazone treatment compared with the control group while MCP-1 expression was markedly reduced and SOD level was markedly increased with pioglitazone treatment (220). Chen et al. revealed that pioglitazone decreased renal inflammatory injury and CaOx crystal formation via inhibiting the polarization of M1 macrophages through a PPARγ-miR-23-IRF1/Pknox1 pathway (221). Therefore, the results suggested PPARγ agonists could inhibit stone formation via suppressing renal OS, inflammation, and injury of tubular cells, and could be a potential therapeutic option to treat renal stone patients.

Furthermore, more and more plant extracts have been studied for possible effects to prevent kidney stones (222, 223). Drugs consisting of compound from natural fruits and plants, would be the most satisfied therapy choice (56). Recently, traditional medicine and herbal for preventing and treating various diseases have been found (224). Medicinal plants have been applied worldwide for the inhibition of recurrence and progress of renal stone disease for thousands of years (225). Well-designed preclinical and/or clinicalstudies

have evaluated many plants and phytochemical constituents for the effects to treat and prevent urolithiasis, especially whether they are favorable suppressors of the formation and development of different types of stones (226-229). Their antioxidative stress effects are considered the main reason for suppressing kidney stone. Phyto-phenols in diet have more than eight thousand structural variants, and are the most abundant antioxidants in daily diet (230, 231). Various bioflavonoids such as hyperoside and quercetin are most common in fruits and vegetables, and exhibit good antioxidative stress, anti-inflammatory, hypo-uricemic and diuretic properties for inhibiting the deposition of CaOx crystals and renal tubular cell injury (232-234).

Several works have found that NFκB, TLR4, and MAPK signal pathways played important roles in the therapeutic processes of kaempferol (235, 236). Kaempferol is one of the most common flavonoids in plentiful fruits and vegetables with potent antioxidant, anti-inflammatory, anti-apoptotic effects (188, 189). Moreover, kaempferol could mediate the expressions of sex hormone receptors of progesterone and estrogen, which further exerted antitumor activity in various malignant diseases (190-192). Several studies have demonstrated the anti-stone formation effects of several dietary plants of which kaempferol is an important constituent (237-240).

Renal tubular cell injury is known to take an important part in cell-crystal interactions. Cell injuries induced by disadvantaged stimulations could result in anomalous changes of cell membrane, subsequently promoting crystal adhesion and sedimentation on cell surface to promote the stone formation (41). In the development of CaOx urolithiasis, both physical and chemical damages of CaOx crystal or high concentration of oxalate will result

in cell injury by the activation of cellular OS and inflammation responses. In turn, after the cells are subjected to apoptosis or necrosis, OS and inflammation can be promoted by excretive macromolecules that exacerbate the pathological processes and cellular degradations (14). Moreover, adhesive molecules such as CD44 and OPN were upregulated, contributing to crystal deposition and adhesion on renal tubules.

However, the precise mechanism of kaempferol on CaOx urolithiasis is still unknown now. This work is the first to comprehensively explore the anti-lithiasis efficacy of kaempferol rather than complex extracts from dietary plants. In our study, we aimed to demonstrate the possible effects of kaempferol, and its mechanisms at the molecular level in the pathological processes of urolithiasis in vivo and in vitro. We revealed that kaempferol, a natural flavonoid, played a significant role in inhibiting renal OS, inflammation, tubular epithelium cell damage induced by CaOx crystals, and CaOx crystals deposition and formation by downregulating the AR/NOX2 signal. AR/NOX2/ROS and AR/NOX2/NFκB signals were emphasized in the protective sense of kaempferol against renal OS and inflammatory injury, and crystal deposition. Kaempferol might serve as a target of AR on the renal tubular epithelium cells, and a promising drug for treating and preventing CaOx urolithiasis.

In our study, by observing staining slices using polarizing microscope and Pizzolato staining, we demonstrated the inhibiting effects of kaempferol on CaOx crystals formation and deposition in murine kidneys. The PAS and TUNEL staining results indicated that kaempferol had suppressive effects on tubular injury induced by CaOx crystals in mice model. By IHC staining, we found that expressions of adhesion promoters OPN and CD44

expression were inhibited by kaempferol, leading to decreased CaOx crystal adhesions to the tubular epithelial cells. Renal function results indicated that the levels of serum NGAL, Cr and BUN were markedly lower in the kaempferol-treated groups, which reflected a potential protective role of kaempferol on renal damage induced by CaOx crystals. In summary, we suggested that kaempferol was able to suppress renal injury induced by CaOx crystals and CaOx crystal deposition.

Moreover, by using CCK-8 assay, we found that different concentrations of kaempferol (10, 20 and 40 μM) had no significant cytotoxic effect on cell viability. LDH release and cell death were decreased with added kaempferol treatment. The crystal adhesion assay showed that the COM crystal adhesions to HK-2 cell could be suppressed with kaempferol treatment in a dose-dependent manner. The WB results indicated that kaempferol treatment was able to reduce the caspase-1 expression in HK-2 cell, which suggested caspase-1 was involved in the inhibitive effect of kaempferol in cell deaths induced by crystals. Hence, we believe that kaempferol could suppress cell deaths induced by crystals and crystal adhesions to HK-2 cells in a dose-dependent fashion.

Using IHC assays or WB analysis, we found that F4/80, NFκB-P65, iNOS and NOX2 expressions in renal tubule epithelial cells were decreased with kaempferol treatment. Results of a series of assays showed that the levels of ROS, H_2O_2 and MDA in kidney were markedly lower while SOD and GSH were markedly higher after kaempferol treatment *in vivo* and *in vitro*. The RT-qPCR assay results indicated that the expressions of TNF-α, IL-1β and IL-6 were markedly lower, and the expressions of Arg1, IL-4 and IL-10 were markedly higher with kaempferol treatment *in vitro* and *in vivo*.

Interestingly, we discovered that NOX2 expression in HK-2 cell was significantly decreased with kaempferol treatment. Furthermore, we investigated the change patterns of the expressions of NADPH oxidase family in HK-2 cells under different conditions, and found that NOX2 was most significantly over-expressed when stimulated by COM crystals, but under-expressed with kaempferol treatment. The above findings indicated that kaempferol was able to suppress OS and inflammation induced by CaOx crystals by downregulating the NOX2-involved pathway.

We revealed that kaempferol was able to suppress renal OS and inflammation. With kaempferol treatment, the NOX2 expression was decreased, inhibiting the level of ROS. Kaempferol was able to upregulate the expressions of antioxidant enzymes like SOD and GSH. Kaempferol was able to suppress OS by increased antioxidants. Moreover, CaOx crystal-induced proinflammatory cytokines were downregulated, while anti-inflammatory cytokines were upregulated with kaempferol treatment. Kaempferol could reduce renal inflammation, which could be ascribed to the weak expression of NFκB. Furthermore, decreased infiltration of macrophages played a crucial role in anti-inflammatory effects of kaempferol. It was identified in previous works that deposition of CaOx crystal could be regulated by macrophage infiltration and polarizations of M1 and M2 macrophages, in which M1 macrophages led to crystal boost, whereas M2 macrophages favored the elimination of crystals (110, 221). Dominguez-Gutierrez et al. have revealed that CaOx crystals could induce M1 macrophage polarization and stimulate inflammatory response in monocytes through LPS-mediated mechanism (114). And several studies have demonstrated that the increased M2 macrophage polarization could inhibit the

inflammatory responses, resulting in the prevention of cascade which led to CaOx nucleation (150, 241, 242).

Based on the above results, we thought that kaempferol might play an anti-AR role in renal tubular epithelial cells with the following considerations. Increasing evidence indicate that AR pathways are related to renal CaOx crystal formation. Regulating renal AR receptors might have an important influence in mediating formation of CaOx crystals (243). On the other hand, kaempferol, as a common flavonoid, is likely to exert a function on the AR receptor. Dietary flavonoids are structurally similar to estrogen, and can be applied as estrogen substitutes for the prevention of postmenopausal symptoms and other estrogen-related diseases (244). Kaempferol was discovered to represent a selective estrogen-related receptor modulator, which had both estrogenic, as well as anti-estrogenic activity (245). Other researchers also have found out that kaempferol inhibited the AR expression in Lymph Node Carcinoma of the Prostate (LNCaP) cells, which might represent a potential treatment choice for treating prostate cancer (246).

To reveal the possible mechanisms of kaempferol on AR and NOX2, we firstly performed a series of experiments in an AR-overexpressed mouse model. RT-qPCR and IHC results revealed that the renal AR expression in the murine kidneys was increased after receiving TP but was decreased with additional kaempferol treatments in a concentration-dependent manner. WB and RT-qPCR results confirmed that kaempferol could reduce the DHT-induced increased expression of AR in HK-2 cells in a dose-dependent fashion. Kaempferol did not markedly influence the basal renal AR expression level. Immunofluorescence results indicated that NOX2 and AR expressions

were increased after treated with COM and DHT, but decreased with the added kaempferol treatment. To explore the possible relationship between AR and NOX2, using the JASPAR database, we select a potential ARE within the 2000bp of the upstream region of NOX2 promoter. Results of ChIP assay in HK-2 cell revealed that AR was able to bind to this ARE (-1822 to -1808 bp) at the transcriptional start site of NOX2, which was confirmed by results of luciferase reporter assay. The above results demonstrate that AR could upregulate the NOX2 expression at transcriptional level, and kaempferol might inhibit the NOX2 expression by downregulating the AR expression.

In mouse model, the HE, Pizzolato, PAS, TUNEL and IHC staining results of mice kidneys revealed that deposition of CaOx crystals, tubular injury, and expressions of CD44 and OPN were significantly promoted in GA+TP group but the effect was significantly suppressed by additional kaempferol treatment. Serum BUN, Cr, NGAL levels, and renal F4/80, NFκB-p65, iNOS, AR, and NOX2 expressions were significantly increased with GA+TP treatment, but were significantly decreased with kaempferol treatment. Renal ROS, H2O2 and MDA levels were markedly lower, but SOD and GSH levels were markedly higher in the kaempferol treatment group compared with the GA+TP group. RT-qPCR results confirmed that kaempferol treatment could reverse the increased TNF-α, IL-6 and IL-1β levels, and the decreased IL-4, IL-10 and Arg1 levels in kidney tissues with the GA+TP treatment. Taken together, AR could promote CaOx crystal-induced inflammatory and OS damage in kidney by upregulating the NOX2 expression, resulting in increased renal CaOx crystal deposition. Renal inflammation may be promoted by the secreted inflammatory factors and the M1 macrophage infiltration regulated by NFκB signal

pathway. Kaempferol could ameliorate deposition of CaOx crystals, tubular injury, and OS and inflammation induced by CaOx crystals by the regulation of the AR/NOX2 signal pathways.

In cell culture experiments, we firstly confirmed that exposure to COM crystals did not influence AR expression, and kaempferol could decrease the increased crystal adhesion, cell deaths, ROS and H2O2 levels after exposed to both DHT and COM crystals. Also, the MDA level was increased, while the SOD and GSH levels were decreased after exposed to both DHT and COM crystals in HK-cells, and the additional kaempferol treatment reversed these changes, indicating that the AR could promote COM crystal-induced OS injury in HK-2 cell. Subsequently, the RT-qPCR results revealed that the TNF-α, IL-6, IL-1β, CD44 and OPN expressions were markedly increased, while the Arg1, IL-4 and IL-10 expressions were markedly decreased with DHT and COM crystals compared with COM group, and the kaempferol treatment reversed these changes, indicating that the secretion of inflammatory cytokines and adhesion molecules could be upregulated by crystal exposure and AR overexpression, but downregulated by the kaempferol treatment. Finally, the WB assay results indicated that MCP-1, Caspase-1, iNOS, p-NFκB-p65, AR and NOX2 expressions were increased with COM and DHT than only COM, and kaempferol reversed these changes. Taken together, it was proved that the downregulations of ROS, NFκB, adhesion molecules and M1 macrophage polarization, were involved in the antioxidative stress and anti-inflammatory effects of kaempferol mediated by AR/NOX2 signal pathways, which might effectively suppress cell injury, OS and inflammation induced by CaOx crystal, and inhibit crystal adhesions to tubular cells.

The different effects of sex hormone in the regulation of NOX expression were demonstrated in previous studies. Estrogen receptor β could suppress OS stimulated by oxalate in HK-2 cell, and inhibit NOX2 by binding to the EREs on the 5′ promoter of NOX2 at the transcriptional level in this process (153). AR could transcriptionally upregulate NOX4 expression in HK-2 cells (147).

Through this mechanism, kaempferol could decease the formation, development, and deposition of CaOx crystals, and inhibit renal cellular injury, crystal adhesion, OS and inflammatory response induced by CaOx crystals, in which the AR/NOX2/ROS and AR/NOX2/NFκB signal pathways were involved. Kaempferol might become a potential option for treating urolithiasis patients and preventing kidney stones among individuals with latent risks of developing urolithiasis.

There are three main limitations of our study: (1) by achieving high urinary oxalate concentrations, the male mice model could not comprehensively simulate the formation and growth processes of kidney CaOx urolithiasis; (2) the high intake doses of kaempferol (25mg/kg, 50mg/kg) in the mice model were not comparable to the daily intake of humans; (3) effects of kaempferol may be gentle and indirect, which can influence the effects by other latent factors and mechanisms.

The effects of kaempferol on formation of CaOx crystals, and the preventive and therapeutic effects for clinical practice on CaOx urolithiasis need further confirmations by more and further well-designed and comprehensive experiments, and well-designed clinical studies in the future. And further clinical and preclinical researches of dietary plants, medicinal plants and phytonutrients should try to study all aspects of urolithiasis,

especially the antioxidant and anti-inflammatory effects, to reveal the comprehensive efficacy, safety, and cellular and molecular mechanisms for preventing and treating kidney stones. This will provide more knowledge including the side effects, pharmacological efficacy, and underlying mechanisms of the medical and dietary plants to urologists to make beneficial recommendations of daily diet for urolithiasis patients. Also, as for the immunotherapy for stone disease, future therapeutic studies for kidney stone may also target the regulation of macrophage polarizations and the capability of macrophages to phagocytose and digest CaOx crystals to reduce the occurrence of kidney stones.

To conclude, we suggest that kaempferol plays an important role in suppressing the renal formation and deposition of CaOx crystals by reducing OS, inflammation, crystal adhesion, and tubular epithelium cell injury via the downregulation of AR/NOX2 signal pathways. Therefore, we believe that Kaempferol may be a potential therapeutic option for the prevention and treatment for CaOx urolithiasis in the future.

Bibliography

1. Yuan P, Sun X, Liu X, Hutterer G, Pummer K, Hager B, et al. Kaempferol alleviates calcium oxalate crystal-induced renal injury and crystal deposition via regulation of the AR/NOX2 signaling pathway. Phytomedicine. 2021;86:153555.
2. Morgan MS, Pearle MS. Medical management of renal stones. Bmj. 2016;352:i52.
3. Romero V, Akpinar H, Assimos DG. Kidney stones: a global picture of prevalence, incidence, and associated risk factors. Rev Urol. 2010;12(2-3):e86-96.
4. Raheem OA, Khandwala YS, Sur RL, Ghani KR, Denstedt JD. Burden of Urolithiasis: Trends in Prevalence, Treatments, and Costs. Eur Urol Focus. 2017;3(1):18-26.
5. Zeng G, Mai Z, Xia S, Wang Z, Zhang K, Wang L, et al. Prevalence of kidney stones in China: an ultrasonography based cross-sectional study. BJU Int. 2017;120(1):109-16.
6. Ziemba JB, Matlaga BR. Epidemiology and economics of nephrolithiasis. Investig Clin Urol. 2017;58(5):299-306.
7. Eisner BH, Goldfarb DS. A nomogram for the prediction of kidney stone recurrence. J Am Soc Nephrol. 2014;25(12):2685-7.
8. Brikowski TH, Lotan Y, Pearle MS. Climate-related increase in the prevalence of urolithiasis in the United States. Proc Natl Acad Sci U S A. 2008;105(28):9841-6.
9. Abeywickarama B, Ralapanawa U, Chandrajith R. Geoenvironmental factors related to high incidence of human urinary calculi (kidney stones) in Central Highlands of Sri Lanka. Environ Geochem Health. 2016;38(5):1203-14.
10. Wang Z, Zhang JW, Zhang Y, Zhang SP, Hu QY, Liang H. Analyses of long non-coding RNA and mRNA profiling using RNA sequencing in calcium oxalate monohydrate-stimulated renal tubular epithelial cells. Urolithiasis. 2019;47(3):225-34.
11. Parmar MS. Kidney stones. Bmj. 2004;328(7453):1420-4.
12. Evan AP. Physiopathology and etiology of stone formation in the kidney and the urinary tract. Pediatr Nephrol. 2010;25(5):831-41.
13. Ye Z, Zeng G, Yang H, Li J, Tang K, Wang G, et al. The status and characteristics of urinary stone composition in China. BJU Int. 2020;125(6):801-9.
14. Aggarwal KP, Narula S, Kakkar M, Tandon C. Nephrolithiasis: molecular mechanism of renal stone formation and the critical role played by modulators. Biomed Res Int. 2013;2013:292953.

15. Khan SR, Pearle MS, Robertson WG, Gambaro G, Canales BK, Doizi S, et al. Kidney stones. Nat Rev Dis Primers. 2016;2:16008.
16. Sun X, Shen L, Cong X, Zhu H, He L, Lu J. Infrared spectroscopic analysis of 5,248 urinary stones from Chinese patients presenting with the first stone episode. Urol Res. 2011;39(5):339-43.
17. Pak CY, Sakhaee K, Moe O, Preminger GM, Poindexter JR, Peterson RD, et al. Biochemical profile of stone-forming patients with diabetes mellitus. Urology. 2003;61(3):523-7.
18. Obligado SH, Goldfarb DS. The association of nephrolithiasis with hypertension and obesity: a review. Am J Hypertens. 2008;21(3):257-64.
19. Johri N, Cooper B, Robertson W, Choong S, Rickards D, Unwin R. An update and practical guide to renal stone management. Nephron Clin Pract. 2010;116(3):c159-71.
20. Devarajan A. Cross-talk between renal lithogenesis and atherosclerosis: an unveiled link between kidney stone formation and cardiovascular diseases. Clin Sci (Lond). 2018;132(6):615-26.
21. Carbone A, Al Salhi Y, Tasca A, Palleschi G, Fuschi A, De Nunzio C, et al. Obesity and kidney stone disease: a systematic review. Minerva Urol Nefrol. 2018;70(4):393-400.
22. Kohjimoto Y, Sasaki Y, Iguchi M, Matsumura N, Inagaki T, Hara I. Association of metabolic syndrome traits and severity of kidney stones: results from a nationwide survey on urolithiasis in Japan. Am J Kidney Dis. 2013;61(6):923-9.
23. Taguchi K, Okada A, Hamamoto S, Iwatsuki S, Naiki T, Ando R, et al. Proinflammatory and Metabolic Changes Facilitate Renal Crystal Deposition in an Obese Mouse Model of Metabolic Syndrome. J Urol. 2015;194(6):1787-96.
24. Strazzullo P, Barba G, Vuotto P, Farinaro E, Siani A, Nunziata V, et al. Past history of nephrolithiasis and incidence of hypertension in men: a reappraisal based on the results of the Olivetti Prospective Heart Study. Nephrol Dial Transplant. 2001;16(11):2232-5.
25. Keddis MT, Rule AD. Nephrolithiasis and loss of kidney function. Curr Opin Nephrol Hypertens. 2013;22(4):390-6.
26. Dhondup T, Kittanamongkolchai W, Vaughan LE, Mehta RA, Chhina JK, Enders FT, et al. Risk of ESRD and Mortality in Kidney and Bladder Stone Formers. Am J Kidney Dis. 2018;72(6):790-7.
27. Voss S, Hesse A, Zimmermann DJ, Sauerbruch T, von Unruh GE. Intestinal oxalate

absorption is higher in idiopathic calcium oxalate stone formers than in healthy controls: measurements with the [(13)C2]oxalate absorption test. J Urol. 2006;175(5):1711-5.
28. Ha YS, Tchey DU, Kang HW, Kim YJ, Yun SJ, Lee SC, et al. Phosphaturia as a promising predictor of recurrent stone formation in patients with urolithiasis. Korean J Urol. 2010;51(1):54-9.
29. Dean C, Kanellos J, Pham H, Gomes M, Oates A, Grover P, et al. Effects of inter-alpha-inhibitor and several of its derivatives on calcium oxalate crystallization in vitro. Clin Sci (Lond). 2000;98(4):471-80.
30. Khan SR, Byer KJ, Thamilselvan S, Hackett RL, McCormack WT, Benson NA, et al. Crystal-cell interaction and apoptosis in oxalate-associated injury of renal epithelial cells. J Am Soc Nephrol. 1999;10 Suppl 14:S457-63.
31. Fong-Ngern K, Vinaiphat A, Thongboonkerd V. Microvillar injury in renal tubular epithelial cells induced by calcium oxalate crystal and the protective role of epigallocatechin-3-gallate. Faseb j. 2017;31(1):120-31.
32. Sun XY, Ouyang JM, Gan QZ, Liu AJ. Renal Epithelial Cell Injury Induced by Calcium Oxalate Monohydrate Depends on their Structural Features: Size, Surface, and Crystalline Structure. J Biomed Nanotechnol. 2016;12(11):2001-14.
33. Rodgers AL. Physicochemical mechanisms of stone formation. Urolithiasis. 2017;45(1):27-32.
34. Daudon M, Frochot V, Bazin D, Jungers P. Drug-Induced Kidney Stones and Crystalline Nephropathy: Pathophysiology, Prevention and Treatment. Drugs. 2018;78(2):163-201.
35. Thongboonkerd V. Proteomics of Crystal-Cell Interactions: A Model for Kidney Stone Research. Cells. 2019;8(9).
36. Wang Z, Li MX, Xu CZ, Zhang Y, Deng Q, Sun R, et al. Comprehensive study of altered proteomic landscape in proximal renal tubular epithelial cells in response to calcium oxalate monohydrate crystals. BMC Urol. 2020;20(1):136.
37. Kumar V, Farell G, Deganello S, Lieske JC. Annexin II is present on renal epithelial cells and binds calcium oxalate monohydrate crystals. J Am Soc Nephrol. 2003;14(2):289-97.
38. Fong-Ngern K, Sueksakit K, Thongboonkerd V. Surface heat shock protein 90 serves as a potential receptor for calcium oxalate crystal on apical membrane of renal tubular

epithelial cells. J Biol Inorg Chem. 2016;21(4):463-74.
39. Wiener SV, Ho SP, Stoller ML. Beginnings of nephrolithiasis: insights into the past, present and future of Randall's plaque formation research. Curr Opin Nephrol Hypertens. 2018;27(4):236-42.
40. Anan G, Yoneyama T, Noro D, Tobisawa Y, Hatakeyama S, Sutoh Yoneyama M, et al. The Impact of Glycosylation of Osteopontin on Urinary Stone Formation. Int J Mol Sci. 2019;21(1).
41. Sheng X, Ward MD, Wesson JA. Crystal surface adhesion explains the pathological activity of calcium oxalate hydrates in kidney stone formation. J Am Soc Nephrol. 2005;16(7):1904-8.
42. Ketha H, Singh RJ, Grebe SK, Bergstralh EJ, Rule AD, Lieske JC, et al. Altered Calcium and Vitamin D Homeostasis in First-Time Calcium Kidney Stone-Formers. PLoS One. 2015;10(9):e0137350.
43. Vezzoli G, Macrina L, Magni G, Arcidiacono T. Calcium-sensing receptor: evidence and hypothesis for its role in nephrolithiasis. Urolithiasis. 2019;47(1):23-33.
44. Farell G, Huang E, Kim SY, Horstkorte R, Lieske JC. Modulation of proliferating renal epithelial cell affinity for calcium oxalate monohydrate crystals. J Am Soc Nephrol. 2004;15(12):3052-62.
45. Gao J, Xue JF, Xu M, Gui BS, Wang FX, Ouyang JM. Nanouric acid or nanocalcium phosphate as central nidus to induce calcium oxalate stone formation: a high-resolution transmission electron microscopy study on urinary nanocrystallites. Int J Nanomedicine. 2014;9:4399-409.
46. Ratkalkar VN, Kleinman JG. Mechanisms of Stone Formation. Clin Rev Bone Miner Metab. 2011;9(3-4):187-97.
47. Moe OW, Abate N, Sakhaee K. Pathophysiology of uric acid nephrolithiasis. Endocrinol Metab Clin North Am. 2002;31(4):895-914.
48. Shekarriz B, Stoller ML. Uric acid nephrolithiasis: current concepts and controversies. J Urol. 2002;168(4 Pt 1):1307-14.
49. Farmanesh S, Chung J, Sosa RD, Kwak JH, Karande P, Rimer JD. Natural promoters of calcium oxalate monohydrate crystallization. J Am Chem Soc. 2014;136(36):12648-57.
50. Worcester EM. Urinary calcium oxalate crystal growth inhibitors. J Am Soc Nephrol. 1994;5(5 Suppl 1):S46-53.

51. Schepers MS, van der Boom BG, Romijn JC, Schröder FH, Verkoelen CF. Urinary crystallization inhibitors do not prevent crystal binding. J Urol. 2002;167(4):1844-7.
52. Hess B, Jordi S, Zipperle L, Ettinger E, Giovanoli R. Citrate determines calcium oxalate crystallization kinetics and crystal morphology-studies in the presence of Tamm-Horsfall protein of a healthy subject and a severely recurrent calcium stone former. Nephrol Dial Transplant. 2000;15(3):366-74.
53. Khan SR, Kok DJ. Modulators of urinary stone formation. Front Biosci. 2004;9:1450-82.
54. Siener R. Dietary Treatment of Metabolic Acidosis in Chronic Kidney Disease. Nutrients. 2018;10(4).
55. Cicerello E, Ciaccia M, Cova G, Mangano M. The impact of potassium citrate therapy in the natural course of Medullary Sponge Kidney with associated nephrolithiasis. Arch Ital Urol Androl. 2019;91(2).
56. Chung J, Granja I, Taylor MG, Mpourmpakis G, Asplin JR, Rimer JD. Molecular modifiers reveal a mechanism of pathological crystal growth inhibition. Nature. 2016;536(7617):446-50.
57. Kim D, Rimer JD, Asplin JR. Hydroxycitrate: a potential new therapy for calcium urolithiasis. Urolithiasis. 2019;47(4):311-20.
58. Grases F, Rodriguez A, Costa-Bauza A. Efficacy of Mixtures of Magnesium, Citrate and Phytate as Calcium Oxalate Crystallization Inhibitors in Urine. J Urol. 2015;194(3):812-9.
59. Ryall RL, Harnett RM, Marshall VR. The effect of urine, pyrophosphate, citrate, magnesium and glycosaminoglycans on the growth and aggregation of calcium oxalate crystals in vitro. Clin Chim Acta. 1981;112(3):349-56.
60. Robertson WG. Do "inhibitors of crystallisation" play any role in the prevention of kidney stones? A critique. Urolithiasis. 2017;45(1):43-56.
61. Randall A. THE ORIGIN AND GROWTH OF RENAL CALCULI. Ann Surg. 1937;105(6):1009-27.
62. Wiener SV, Chen L, Shimotake AR, Kang M, Stoller ML, Ho SP. Novel insights into renal mineralization and stone formation through advanced imaging modalities. Connect Tissue Res. 2018;59(sup1):102-10.
63. Daudon M, Bazin D, Letavernier E. Randall's plaque as the origin of calcium oxalate

kidney stones. Urolithiasis. 2015;43 Suppl 1:5-11.
64. Khan SR, Canales BK, Dominguez-Gutierrez PR. Randall's plaque and calcium oxalate stone formation: role for immunity and inflammation. Nat Rev Nephrol. 2021;17(6):417-33.
65. Chung HJ. The role of Randall plaques on kidney stone formation. Transl Androl Urol. 2014;3(3):251-4.
66. Winfree S, Weiler C, Bledsoe SB, Gardner T, Sommer AJ, Evan AP, et al. Multimodal imaging reveals a unique autofluorescence signature of Randall's plaque. Urolithiasis. 2021;49(2):123-35.
67. Bouderlique E, Tang E, Perez J, Coudert A, Bazin D, Verpont MC, et al. Vitamin D and Calcium Supplementation Accelerates Randall's Plaque Formation in a Murine Model. Am J Pathol. 2019;189(11):2171-80.
68. Zhu Z, Cui Y, Huang F, Zeng H, Xia W, Zeng F, et al. Long non-coding RNA H19 promotes osteogenic differentiation of renal interstitial fibroblasts through Wnt-β-catenin pathway. Mol Cell Biochem. 2020;470(1-2):145-55.
69. Zhu Z, Huang F, Xia W, Zeng H, Gao M, Li Y, et al. Osteogenic Differentiation of Renal Interstitial Fibroblasts Promoted by lncRNA MALAT1 May Partially Contribute to Randall's Plaque Formation. Front Cell Dev Biol. 2020;8:596363.
70. Liu H, Ye T, Yang X, Liu J, Jiang K, Lu H, et al. H19 promote calcium oxalate nephrocalcinosis-induced renal tubular epithelial cell injury via a ceRNA pathway. EBioMedicine. 2019;50:366-78.
71. Whiteside SA, Razvi H, Dave S, Reid G, Burton JP. The microbiome of the urinary tract--a role beyond infection. Nat Rev Urol. 2015;12(2):81-90.
72. Bichler KH, Eipper E, Naber K, Braun V, Zimmermann R, Lahme S. Urinary infection stones. Int J Antimicrob Agents. 2002;19(6):488-98.
73. Espinosa-Ortiz EJ, Eisner BH, Lange D, Gerlach R. Current insights into the mechanisms and management of infection stones. Nat Rev Urol. 2019;16(1):35-53.
74. Marien T, Miller NL. Treatment of the Infected Stone. Urol Clin North Am. 2015;42(4):459-72.
75. Flannigan R, Choy WH, Chew B, Lange D. Renal struvite stones--pathogenesis, microbiology, and management strategies. Nat Rev Urol. 2014;11(6):333-41.
76. de Cógáin MR, Lieske JC, Vrtiska TJ, Tosh PK, Krambeck AE. Secondarily infected

nonstruvite urolithiasis: a prospective evaluation. Urology. 2014;84(6):1295-300.
77. Martel J, Peng HH, Young D, Wu CY, Young JD. Of nanobacteria, nanoparticles, biofilms and their role in health and disease: facts, fancy and future. Nanomedicine (Lond). 2014;9(4):483-99.
78. Mehta M, Goldfarb DS, Nazzal L. The role of the microbiome in kidney stone formation. Int J Surg. 2016;36(Pt D):607-12.
79. Wu J, Tao Z, Deng Y, Liu Q, Liu Y, Guan X, et al. Calcifying nanoparticles induce cytotoxicity mediated by ROS-JNK signaling pathways. Urolithiasis. 2019;47(2):125-35.
80. Ansari H, Akhavan Sepahi A, Akhavan Sepahi M. Different Approaches to Detect "Nanobacteria" in Patients with Kidney Stones: an Infectious Cause or a Subset of Life? Urol J. 2017;14(5):5001-7.
81. Kajander EO, Ciftcioglu N, Aho K, Garcia-Cuerpo E. Characteristics of nanobacteria and their possible role in stone formation. Urol Res. 2003;31(2):47-54.
82. Ciftçioglu N, Björklund M, Kuorikoski K, Bergström K, Kajander EO. Nanobacteria: an infectious cause for kidney stone formation. Kidney Int. 1999;56(5):1893-8.
83. Kajander EO, Ciftçioglu N. Nanobacteria: an alternative mechanism for pathogenic intra- and extracellular calcification and stone formation. Proc Natl Acad Sci U S A. 1998;95(14):8274-9.
84. Khullar M, Sharma SK, Singh SK, Bajwa P, Shiekh FA, Relan V, et al. Morphological and immunological characteristics of nanobacteria from human renal stones of a north Indian population. Urol Res. 2004;32(3):190-5.
85. Shiekh FA, Khullar M, Singh SK. Lithogenesis: induction of renal calcifications by nanobacteria. Urol Res. 2006;34(1):53-7.
86. Abrol N, Panda A, Kekre NS, Devasia A. Nanobacteria in the pathogenesis of urolithiasis: Myth or reality? Indian J Urol. 2015;31(1):3-7.
87. Hong X, Wang X, Wang T, Yu C, Li H. Role of nanobacteria in the pathogenesis of kidney stone formation. Am J Transl Res. 2016;8(7):3227-34.
88. Sadaf H, Raza SI, Hassan SW. Role of gut microbiota against calcium oxalate. Microb Pathog. 2017;109:287-91.
89. Ticinesi A, Milani C, Guerra A, Allegri F, Lauretani F, Nouvenne A, et al. Understanding the gut-kidney axis in nephrolithiasis: an analysis of the gut microbiota composition and functionality of stone formers. Gut. 2018;67(12):2097-106.

90. Ticinesi A, Nouvenne A, Chiussi G, Castaldo G, Guerra A, Meschi T. Calcium Oxalate Nephrolithiasis and Gut Microbiota: Not just a Gut-Kidney Axis. A Nutritional Perspective. Nutrients. 2020;12(2).
91. Stern JM, Moazami S, Qiu Y, Kurland I, Chen Z, Agalliu I, et al. Evidence for a distinct gut microbiome in kidney stone formers compared to non-stone formers. Urolithiasis. 2016;44(5):399-407.
92. Worcester EM, Fellner SK, Nakagawa Y, Coe FL. Effect of renal transplantation on serum oxalate and urinary oxalate excretion. Nephron. 1994;67(4):414-8.
93. Hatch M, Freel RW, Vaziri ND. Mechanisms of oxalate absorption and secretion across the rabbit distal colon. Pflugers Arch. 1994;426(1-2):101-9.
94. Peck AB, Canales BK, Nguyen CQ. Oxalate-degrading microorganisms or oxalate-degrading enzymes: which is the future therapy for enzymatic dissolution of calcium-oxalate uroliths in recurrent stone disease? Urolithiasis. 2016;44(1):45-50.
95. Knight J, Deora R, Assimos DG, Holmes RP. The genetic composition of Oxalobacter formigenes and its relationship to colonization and calcium oxalate stone disease. Urolithiasis. 2013;41(3):187-96.
96. Batagello CA, Monga M, Miller AW. Calcium Oxalate Urolithiasis: A Case of Missing Microbes? J Endourol. 2018;32(11):995-1005.
97. Falony G. Beyond Oxalobacter: the gut microbiota and kidney stone formation. Gut. 2018;67(12):2078-9.
98. Cornelius JG, Peck AB. Colonization of the neonatal rat intestinal tract from environmental exposure to the anaerobic bacterium Oxalobacter formigenes. J Med Microbiol. 2004;53(Pt 3):249-54.
99. Ticinesi A, Nouvenne A, Meschi T. Gut microbiome and kidney stone disease: not just an Oxalobacter story. Kidney Int. 2019;96(1):25-7.
100. Curhan GC, Willett WC, Rimm EB, Stampfer MJ. A prospective study of dietary calcium and other nutrients and the risk of symptomatic kidney stones. N Engl J Med. 1993;328(12):833-8.
101. Curhan GC, Willett WC, Speizer FE, Spiegelman D, Stampfer MJ. Comparison of dietary calcium with supplemental calcium and other nutrients as factors affecting the risk for kidney stones in women. Ann Intern Med. 1997;126(7):497-504.
102. Prezioso D, Strazzullo P, Lotti T, Bianchi G, Borghi L, Caione P, et al. Dietary

treatment of urinary risk factors for renal stone formation. A review of CLU Working Group. Arch Ital Urol Androl. 2015;87(2):105-20.

103. Gambaro G, Croppi E, Coe F, Lingeman J, Moe O, Worcester E, et al. Metabolic diagnosis and medical prevention of calcium nephrolithiasis and its systemic manifestations: a consensus statement. J Nephrol. 2016;29(6):715-34.

104. Miller AW, Dearing D. The metabolic and ecological interactions of oxalate-degrading bacteria in the Mammalian gut. Pathogens. 2013;2(4):636-52.

105. Nikolic-Paterson DJ, Wang S, Lan HY. Macrophages promote renal fibrosis through direct and indirect mechanisms. Kidney Int Suppl (2011). 2014;4(1):34-8.

106. Okada A, Yasui T, Fujii Y, Niimi K, Hamamoto S, Hirose M, et al. Renal macrophage migration and crystal phagocytosis via inflammatory-related gene expression during kidney stone formation and elimination in mice: Detection by association analysis of stone-related gene expression and microstructural observation. J Bone Miner Res. 2010;25(12):2701-11.

107. Singhto N, Kanlaya R, Nilnumkhum A, Thongboonkerd V. Roles of Macrophage Exosomes in Immune Response to Calcium Oxalate Monohydrate Crystals. Front Immunol. 2018;9:316.

108. Singhto N, Thongboonkerd V. Exosomes derived from calcium oxalate-exposed macrophages enhance IL-8 production from renal cells, neutrophil migration and crystal invasion through extracellular matrix. J Proteomics. 2018;185:64-76.

109. Tamura M, Aizawa R, Hori M, Ozaki H. Progressive renal dysfunction and macrophage infiltration in interstitial fibrosis in an adenine-induced tubulointerstitial nephritis mouse model. Histochem Cell Biol. 2009;131(4):483-90.

110. Kusmartsev S, Dominguez-Gutierrez PR, Canales BK, Bird VG, Vieweg J, Khan SR. Calcium Oxalate Stone Fragment and Crystal Phagocytosis by Human Macrophages. J Urol. 2016;195(4 Pt 1):1143-51.

111. Sintiprungrat K, Singhto N, Thongboonkerd V. Characterization of calcium oxalate crystal-induced changes in the secretome of U937 human monocytes. Mol Biosyst. 2016;12(3):879-89.

112. Vervaet BA, Verhulst A, Dauwe SE, De Broe ME, D'Haese PC. An active renal crystal clearance mechanism in rat and man. Kidney Int. 2009;75(1):41-51.

113. Okada A, Yasui T, Hamamoto S, Hirose M, Kubota Y, Itoh Y, et al. Genome-wide

analysis of genes related to kidney stone formation and elimination in the calcium oxalate nephrolithiasis model mouse: detection of stone-preventive factors and involvement of macrophage activity. J Bone Miner Res. 2009;24(5):908-24.

114.Dominguez-Gutierrez PR, Kusmartsev S, Canales BK, Khan SR. Calcium Oxalate Differentiates Human Monocytes Into Inflammatory M1 Macrophages. Front Immunol. 2018;9:1863.

115.Taguchi K, Okada A, Hamamoto S, Unno R, Moritoki Y, Ando R, et al. M1/M2-macrophage phenotypes regulate renal calcium oxalate crystal development. Sci Rep. 2016;6:35167.

116.Dominguez-Gutierrez PR, Kwenda EP, Khan SR, Canales BK. Immunotherapy for stone disease. Curr Opin Urol. 2020;30(2):183-9.

117.Gambaro G, D'Angelo A, Fabris A, Tosetto E, Anglani F, Lupo A. Crystals, Randall's plaques and renal stones: do bone and atherosclerosis teach us something? J Nephrol. 2004;17(6):774-7.

118.Reiner AP, Kahn A, Eisner BH, Pletcher MJ, Sadetsky N, Williams OD, et al. Kidney stones and subclinical atherosclerosis in young adults: the CARDIA study. J Urol. 2011;185(3):920-5.

119.Bagga HS, Chi T, Miller J, Stoller ML. New insights into the pathogenesis of renal calculi. Urol Clin North Am. 2013;40(1):1-12.

120. Fabris A, Ferraro PM, Comellato G, Caletti C, Fantin F, Zaza G, et al. The relationship between calcium kidney stones, arterial stiffness and bone density: unraveling the stone-bone-vessel liaison. J Nephrol. 2015;28(5):549-55.

121. Taylor ER, Stoller ML. Vascular theory of the formation of Randall plaques. Urolithiasis. 2015;43 Suppl 1:41-5.

122. Shanahan CM. Mechanisms of vascular calcification in renal disease. Clin Nephrol. 2005;63(2):146-57.

123. Moe SM, Chen NX. Mechanisms of vascular calcification in chronic kidney disease. J Am Soc Nephrol. 2008;19(2):213-6.

124. Shanahan CM, Crouthamel MH, Kapustin A, Giachelli CM. Arterial calcification in chronic kidney disease: key roles for calcium and phosphate. Circ Res. 2011;109(6):697-711.

125. Kapustin AN, Davies JD, Reynolds JL, McNair R, Jones GT, Sidibe A, et al.

Calcium regulates key components of vascular smooth muscle cell-derived matrix vesicles to enhance mineralization. Circ Res. 2011;109(1):e1-12.

126. Shroff RC, Shanahan CM. The vascular biology of calcification. Semin Dial. 2007;20(2):103-9.

127. Byon CH, Javed A, Dai Q, Kappes JC, Clemens TL, Darley-Usmar VM, et al. Oxidative stress induces vascular calcification through modulation of the osteogenic transcription factor Runx2 by AKT signaling. J Biol Chem. 2008;283(22):15319-27.

128. Tada Y, Yano S, Yamaguchi T, Okazaki K, Ogawa N, Morita M, et al. Advanced glycation end products-induced vascular calcification is mediated by oxidative stress: functional roles of NAD(P)H-oxidase. Horm Metab Res. 2013;45(4):267-72.

129. Murshed M, McKee MD. Molecular determinants of extracellular matrix mineralization in bone and blood vessels. Curr Opin Nephrol Hypertens. 2010;19(4):359-65.

130. Mezzabotta F, Cristofaro R, Ceol M, Del Prete D, Priante G, Familiari A, et al. Spontaneous calcification process in primary renal cells from a medullary sponge kidney patient harbouring a GDNF mutation. J Cell Mol Med. 2015;19(4):889-902.

131. Jia Z, Wang S, Tang J, He D, Cui L, Liu Z, et al. Does crystal deposition in genetic hypercalciuric rat kidney tissue share similarities with bone formation? Urology. 2014;83(2):509.e7-14.

132. Kageyama S, Ohtawara Y, Fujita K, Watanabe T, Ushiyama T, Suzuki K, et al. Microlith formation in vitro by Madin Darby canine kidney (MDCK) cells. Int J Urol. 1996;3(1):23-6.

133. Naito Y, Ohtawara Y, Kageyama S, Nakano M, Ichiyama A, Fujita M, et al. Morphological analysis of renal cell culture models of calcium phosphate stone formation. Urol Res. 1997;25(1):59-65.

134. Aihara K, Byer KJ, Khan SR. Calcium phosphate-induced renal epithelial injury and stone formation: involvement of reactive oxygen species. Kidney Int. 2003;64(4):1283-91.

135. Joshi S, Saylor BT, Wang W, Peck AB, Khan SR. Apocynin-treatment reverses hyperoxaluria induced changes in NADPH oxidase system expression in rat kidneys: a transcriptional study. PLoS One. 2012;7(10):e47738.

136. Khan SR, Khan A, Byer KJ. Temporal changes in the expression of mRNA of

NADPH oxidase subunits in renal epithelial cells exposed to oxalate or calcium oxalate crystals. Nephrol Dial Transplant. 2011;26(6):1778-85.

137. Thamilselvan S, Byer KJ, Hackett RL, Khan SR. Free radical scavengers, catalase and superoxide dismutase provide protection from oxalate-associated injury to LLC-PK1 and MDCK cells. J Urol. 2000;164(1):224-9.

138. Thamilselvan S, Hackett RL, Khan SR. Lipid peroxidation in ethylene glycol induced hyperoxaluria and calcium oxalate nephrolithiasis. J Urol. 1997;157(3):1059-63.

139. Zuo J, Khan A, Glenton PA, Khan SR. Effect of NADPH oxidase inhibition on the expression of kidney injury molecule and calcium oxalate crystal deposition in hydroxy-L-proline-induced hyperoxaluria in the male Sprague-Dawley rats. Nephrol Dial Transplant. 2011;26(6):1785-96.

140. Joshi S, Clapp WL, Wang W, Khan SR. Osteogenic changes in kidneys of hyperoxaluric rats. Biochim Biophys Acta. 2015;1852(9):2000-12.

141. Khan SR, Canales BK. Unified theory on the pathogenesis of Randall's plaques and plugs. Urolithiasis. 2015;43 Suppl 1(0 1):109-23.

142. Fan J, Chandhoke PS, Grampsas SA. Role of sex hormones in experimental calcium oxalate nephrolithiasis. J Am Soc Nephrol. 1999;10 Suppl 14:S376-80.

143. Li JY, Zhou T, Gao X, Xu C, Sun Y, Peng Y, et al. Testosterone and androgen receptor in human nephrolithiasis. J Urol. 2010;184(6):2360-3.

144. Gupta K, Gill GS, Mahajan R. Possible role of elevated serum testosterone in pathogenesis of renal stone formation. Int J Appl Basic Med Res. 2016;6(4):241-4.

145. Fuster DG, Morard GA, Schneider L, Mattmann C, Lüthi D, Vogt B, et al. Association of urinary sex steroid hormones with urinary calcium, oxalate and citrate excretion in kidney stone formers. Nephrol Dial Transplant. 2022;37(2):335-48.

146. Yoshihara H, Yamaguchi S, Yachiku S. Effect of sex hormones on oxalate-synthesizing enzymes in male and female rat livers. J Urol. 1999;161(2):668-73.

147. Liang L, Li L, Tian J, Lee SO, Dang Q, Huang CK, et al. Androgen receptor enhances kidney stone-CaOx crystal formation via modulation of oxalate biosynthesis & oxidative stress. Mol Endocrinol. 2014;28(8):1291-303.

148. Peng Y, Fang Z, Liu M, Wang Z, Li L, Ming S, et al. Testosterone induces renal tubular epithelial cell death through the HIF-1α/BNIP3 pathway. J Transl Med. 2019;17(1):62.

149. Changtong C, Peerapen P, Khamchun S, Fong-Ngern K, Chutipongtanate S, Thongboonkerd V. In vitro evidence of the promoting effect of testosterone in kidney stone disease: A proteomics approach and functional validation. J Proteomics. 2016;144:11-22.
150. Zhu W, Zhao Z, Chou F, Zuo L, Liu T, Yeh S, et al. Loss of the androgen receptor suppresses intrarenal calcium oxalate crystals deposition via altering macrophage recruitment/M2 polarization with change of the miR-185-5p/CSF-1 signals. Cell Death Dis. 2019;10(4):275.
151. Sueksakit K, Thongboonkerd V. Protective effects of finasteride against testosterone-induced calcium oxalate crystallization and crystal-cell adhesion. J Biol Inorg Chem. 2019;24(7):973-83.
152. Peerapen P, Thongboonkerd V. Protective Cellular Mechanism of Estrogen Against Kidney Stone Formation: A Proteomics Approach and Functional Validation. Proteomics. 2019;19(19):e1900095.
153. Zhu W, Zhao Z, Chou FJ, Zuo L, Liu T, Bushinsky D, et al. The Protective Roles of Estrogen Receptor β in Renal Calcium Oxalate Crystal Formation via Reducing the Liver Oxalate Biosynthesis and Renal Oxidative Stress-Mediated Cell Injury. Oxid Med Cell Longev. 2019;2019:5305014.
154. Hu H, Zhou H, Xu D. A review of the effects and molecular mechanisms of dimethylcurcumin (ASC-J9) on androgen receptor-related diseases. Chem Biol Drug Des. 2021;97(4):821-35.
155. Tian H, Chou FJ, Tian J, Zhang Y, You B, Huang CP, et al. ASC-J9® suppresses prostate cancer cell proliferation and invasion via altering the ATF3-PTK2 signaling. J Exp Clin Cancer Res. 2021;40(1):3.
156. Loughlin KR. The clinical applications of five-alpha reductase inhibitors. Can J Urol. 2021;28(2):10584-8.
157. Andy G, John M, Mirna S, Rachita D, Michael K, Maja K, et al. Controversies in the treatment of androgenetic alopecia: The history of finasteride. Dermatol Ther. 2019;32(2):e12647.
158. Khan SR. Reactive oxygen species as the molecular modulators of calcium oxalate kidney stone formation: evidence from clinical and experimental investigations. J Urol. 2013;189(3):803-11.
159. Hirose M, Yasui T, Okada A, Hamamoto S, Shimizu H, Itoh Y, et al. Renal tubular

epithelial cell injury and oxidative stress induce calcium oxalate crystal formation in mouse kidney. Int J Urol. 2010;17(1):83-92.

160. Kohri K, Nomura S, Kitamura Y, Nagata T, Yoshioka K, Iguchi M, et al. Structure and expression of the mRNA encoding urinary stone protein (osteopontin). J Biol Chem. 1993;268(20):15180-4.

161. Okada A, Nomura S, Saeki Y, Higashibata Y, Hamamoto S, Hirose M, et al. Morphological conversion of calcium oxalate crystals into stones is regulated by osteopontin in mouse kidney. J Bone Miner Res. 2008;23(10):1629-37.

162. Hirose M, Tozawa K, Okada A, Hamamoto S, Higashibata Y, Gao B, et al. Role of osteopontin in early phase of renal crystal formation: immunohistochemical and microstructural comparisons with osteopontin knock-out mice. Urol Res. 2012;40(2):121-9.

163. Asselman M, Verhulst A, De Broe ME, Verkoelen CF. Calcium oxalate crystal adherence to hyaluronan-, osteopontin-, and CD44-expressing injured/regenerating tubular epithelial cells in rat kidneys. J Am Soc Nephrol. 2003;14(12):3155-66.

164. Kohjimoto Y, Kennington L, Scheid CR, Honeyman TW. Role of phospholipase A2 in the cytotoxic effects of oxalate in cultured renal epithelial cells. Kidney Int. 1999;56(4):1432-41.

165. Itoh Y, Yasui T, Okada A, Tozawa K, Hayashi Y, Kohri K. Preventive effects of green tea on renal stone formation and the role of oxidative stress in nephrolithiasis. J Urol. 2005;173(1):271-5.

166. Itoh Y, Yasui T, Okada A, Tozawa K, Hayashi Y, Kohri K. Examination of the anti-oxidative effect in renal tubular cells and apoptosis by oxidative stress. Urol Res. 2005;33(4):261-6.

167. Khan SR. Crystal-induced inflammation of the kidneys: results from human studies, animal models, and tissue-culture studies. Clin Exp Nephrol. 2004;8(2):75-88.

168. Umekawa T, Byer K, Uemura H, Khan SR. Diphenyleneiodium (DPI) reduces oxalate ion- and calcium oxalate monohydrate and brushite crystal-induced upregulation of MCP-1 in NRK 52E cells. Nephrol Dial Transplant. 2005;20(5):870-8.

169. Delvecchio FC, Brizuela RM, Khan SR, Byer K, Li Z, Zhong P, et al. Citrate and vitamin E blunt the shock wave-induced free radical surge in an in vitro cell culture model. Urol Res. 2005;33(6):448-52.

170. Khan SR. Hyperoxaluria-induced oxidative stress and antioxidants for renal protection. Urol Res. 2005;33(5):349-57.
171. Umekawa T, Hatanaka Y, Kurita T, Khan SR. Effect of angiotensin II receptor blockage on osteopontin expression and calcium oxalate crystal deposition in rat kidneys. J Am Soc Nephrol. 2004;15(3):635-44.
172. McKee MD, Nanci A, Khan SR. Ultrastructural immunodetection of osteopontin and osteocalcin as major matrix components of renal calculi. J Bone Miner Res. 1995;10(12):1913-29.
173. Niimi K, Yasui T, Hirose M, Hamamoto S, Itoh Y, Okada A, et al. Mitochondrial permeability transition pore opening induces the initial process of renal calcium crystallization. Free Radic Biol Med. 2012;52(7):1207-17.
174. Cao LC, Honeyman TW, Cooney R, Kennington L, Scheid CR, Jonassen JA. Mitochondrial dysfunction is a primary event in renal cell oxalate toxicity. Kidney Int. 2004;66(5):1890-900.
175. Niimi K, Yasui T, Okada A, Hirose Y, Kubota Y, Umemoto Y, et al. Novel effect of the inhibitor of mitochondrial cyclophilin D activation, N-methyl-4-isoleucine cyclosporin, on renal calcium crystallization. Int J Urol. 2014;21(7):707-13.
176. Taguchi K, Okada A, Kitamura H, Yasui T, Naiki T, Hamamoto S, et al. Colony-stimulating factor-1 signaling suppresses renal crystal formation. J Am Soc Nephrol. 2014;25(8):1680-97.
177. Khan SR. Reactive oxygen species, inflammation and calcium oxalate nephrolithiasis. Transl Androl Urol. 2014;3(3):256-76.
178. Taguchi K, Hamamoto S, Okada A, Unno R, Kamisawa H, Naiki T, et al. Genome-Wide Gene Expression Profiling of Randall's Plaques in Calcium Oxalate Stone Formers. J Am Soc Nephrol. 2017;28(1):333-47.
179. Magnani F, Mattevi A. Structure and mechanisms of ROS generation by NADPH oxidases. Curr Opin Struct Biol. 2019;59:91-7.
180. Brandes RP, Weissmann N, Schröder K. Nox family NADPH oxidases: Molecular mechanisms of activation. Free Radic Biol Med. 2014;76:208-26.
181. You YH, Okada S, Ly S, Jandeleit-Dahm K, Barit D, Namikoshi T, et al. Role of Nox2 in diabetic kidney disease. Am J Physiol Renal Physiol. 2013;304(7):F840-8.
182. Sedeek M, Nasrallah R, Touyz RM, Hébert RL. NADPH oxidases, reactive

oxygen species, and the kidney: friend and foe. J Am Soc Nephrol. 2013;24(10):1512-8.

183. Kraaij MD, Koekkoek KM, Gelderman KA, van Kooten C. The NOX2-mediated ROS producing capacity of recipient cells is associated with reduced T cell infiltrate in an experimental model of chronic renal allograft inflammation. Transpl Immunol. 2014;30(2-3):65-70.

184. Matsumoto T, Sakari M, Okada M, Yokoyama A, Takahashi S, Kouzmenko A, et al. The androgen receptor in health and disease. Annu Rev Physiol. 2013;75:201-24.

185. Yoshioka I, Tsujihata M, Momohara C, Akanae W, Nonomura N, Okuyama A. Effect of sex hormones on crystal formation in a stone-forming rat model. Urology. 2010;75(4):907-13.

186. Fang Z, Peng Y, Li L, Liu M, Wang Z, Ming S, et al. The molecular mechanisms of androgen receptor in nephrolithiasis. Gene. 2017;616:16-21.

187. Besenhofer LM, Cain MC, Dunning C, McMartin KE. Aluminum citrate prevents renal injury from calcium oxalate crystal deposition. J Am Soc Nephrol. 2012;23(12):2024-33.

188. Choung WJ, Hwang SH, Ko DS, Kim SB, Kim SH, Jeon SH, et al. Enzymatic Synthesis of a Novel Kaempferol-3-O-β-d-glucopyranosyl-(1→4)-O-α-d-glucopyranoside Using Cyclodextrin Glucanotransferase and Its Inhibitory Effects on Aldose Reductase, Inflammation, and Oxidative Stress. J Agric Food Chem. 2017;65(13):2760-7.

189. Tsai MS, Wang YH, Lai YY, Tsou HK, Liou GG, Ko JL, et al. Kaempferol protects against propacetamol-induced acute liver injury through CYP2E1 inactivation, UGT1A1 activation, and attenuation of oxidative stress, inflammation and apoptosis in mice. Toxicol Lett. 2018;290:97-109.

190. Wang J, Fang F, Huang Z, Wang Y, Wong C. Kaempferol is an estrogen-related receptor alpha and gamma inverse agonist. FEBS Lett. 2009;583(4):643-7.

191. Toh MF, Mendonca E, Eddie SL, Endsley MP, Lantvit DD, Petukhov PA, et al. Kaempferol Exhibits Progestogenic Effects in Ovariectomized Rats. J Steroids Horm Sci. 2014;5(3):136.

192. Breinholt V, Hossaini A, Svendsen GW, Brouwer C, Nielsen E. Estrogenic activity of flavonoids in mice. The importance of estrogen receptor distribution, metabolism and bioavailability. Food Chem Toxicol. 2000;38(7):555-64.

193. Thongboonkerd V, Semangoen T, Chutipongtanate S. Factors determining types

and morphologies of calcium oxalate crystals: molar concentrations, buffering, pH, stirring and temperature. Clin Chim Acta. 2006;367(1-2):120-31.

194. Mulay SR, Kulkarni OP, Rupanagudi KV, Migliorini A, Darisipudi MN, Vilaysane A, et al. Calcium oxalate crystals induce renal inflammation by NLRP3-mediated IL-1β secretion. J Clin Invest. 2013;123(1):236-46.

195. Vinaiphat A, Aluksanasuwan S, Manissorn J, Sutthimethakorn S, Thongboonkerd V. Response of renal tubular cells to differential types and doses of calcium oxalate crystals: Integrative proteome network analysis and functional investigations. Proteomics. 2017;17(15-16).

196. Ribeiro J, Malta M, Galaghar A, Silva F, Afonso LP, Medeiros R, et al. P53 deregulation in Epstein-Barr virus-associated gastric cancer. Cancer Lett. 2017;404:37-43.

197. Zisman AL, Evan AP, Coe FL, Worcester EM. Do kidney stone formers have a kidney disease? Kidney Int. 2015;88(6):1240-9.

198. Donaldson JF, Lardas M, Scrimgeour D, Stewart F, MacLennan S, Lam TB, et al. Systematic review and meta-analysis of the clinical effectiveness of shock wave lithotripsy, retrograde intrarenal surgery, and percutaneous nephrolithotomy for lower-pole renal stones. Eur Urol. 2015;67(4):612-6.

199. Farmanesh S, Ramamoorthy S, Chung J, Asplin JR, Karande P, Rimer JD. Specificity of growth inhibitors and their cooperative effects in calcium oxalate monohydrate crystallization. J Am Chem Soc. 2014;136(1):367-76.

200. Taguchi K, Yasui T, Milliner DS, Hoppe B, Chi T. Genetic Risk Factors for Idiopathic Urolithiasis: A Systematic Review of the Literature and Causal Network Analysis. Eur Urol Focus. 2017;3(1):72-81.

201. Scatena M, Liaw L, Giachelli CM. Osteopontin: a multifunctional molecule regulating chronic inflammation and vascular disease. Arterioscler Thromb Vasc Biol. 2007;27(11):2302-9.

202. Heller HJ, Sakhaee K, Moe OW, Pak CY. Etiological role of estrogen status in renal stone formation. J Urol. 2002;168(5):1923-7.

203. Johnson RC, Leopold JA, Loscalzo J. Vascular calcification: pathobiological mechanisms and clinical implications. Circ Res. 2006;99(10):1044-59.

204. Nordin BE, Need AG, Morris HA, Horowitz M, Robertson WG. Evidence for a renal calcium leak in postmenopausal women. J Clin Endocrinol Metab. 1991;72(2):401-7.

205. Osako MK, Nakagami H, Koibuchi N, Shimizu H, Nakagami F, Koriyama H, et al. Estrogen inhibits vascular calcification via vascular RANKL system: common mechanism of osteoporosis and vascular calcification. Circ Res. 2010;107(4):466-75.

206. Kohri K, Yasui T, Okada A, Hirose M, Hamamoto S, Fujii Y, et al. Biomolecular mechanism of urinary stone formation involving osteopontin. Urol Res. 2012;40(6):623-37.

207. Yasui T, Iguchi M, Suzuki S, Kohri K. Prevalence and epidemiological characteristics of urolithiasis in Japan: national trends between 1965 and 2005. Urology. 2008;71(2):209-13.

208. Itoh Y, Yoshimura M, Niimi K, Usami M, Hamamoto S, Kobayashi T, et al. The role of long-term loading of cholesterol in renal crystal formation. Arch Ital Urol Androl. 2011;83(1):23-5.

209. Buck AC, Davies RL, Harrison T. The protective role of eicosapentaenoic acid [EPA] in the pathogenesis of nephrolithiasis. J Urol. 1991;146(1):188-94.

210. Yasui T, Suzuki S, Itoh Y, Tozawa K, Tokudome S, Kohri K. Eicosapentaenoic acid has a preventive effect on the recurrence of nephrolithiasis. Urol Int. 2008;81(2):135-8.

211.Schmiedl A, Schwille PO, Bonucci E, Erben RG, Grayczyk A, Sharma V. Nephrocalcinosis and hyperlipidemia in rats fed a cholesterol- and fat-rich diet: association with hyperoxaluria, altered kidney and bone minerals, and renal tissue phospholipid-calcium interaction. Urol Res. 2000;28(6):404-15.

212. Khan SR, Glenton PA, Backov R, Talham DR. Presence of lipids in urine, crystals and stones: implications for the formation of kidney stones. Kidney Int. 2002;62(6):2062-72.

213. Taylor EN, Stampfer MJ, Curhan GC. Obesity, weight gain, and the risk of kidney stones. Jama. 2005;293(4):455-62.

214. Taylor EN, Stampfer MJ, Curhan GC. Diabetes mellitus and the risk of nephrolithiasis. Kidney Int. 2005;68(3):1230-5.

215. Yasui T, Itoh Y, Bing G, Okada A, Tozawa K, Kohri K. Aortic calcification in urolithiasis patients. Scand J Urol Nephrol. 2007;41(5):419-21.

216. Matsuda M, Shimomura I, Sata M, Arita Y, Nishida M, Maeda N, et al. Role of adiponectin in preventing vascular stenosis. The missing link of adipo-vascular axis. J Biol

Chem. 2002;277(40):37487-91.
217. Kadowaki T, Yamauchi T, Kubota N, Hara K, Ueki K, Tobe K. Adiponectin and adiponectin receptors in insulin resistance, diabetes, and the metabolic syndrome. J Clin Invest. 2006;116(7):1784-92.
218. Fujii Y, Okada A, Yasui T, Niimi K, Hamamoto S, Hirose M, et al. Effect of adiponectin on kidney crystal formation in metabolic syndrome model mice via inhibition of inflammation and apoptosis. PLoS One. 2013;8(4):e61343.
219. Ando R, Suzuki S, Nagaya T, Yamada T, Okada A, Yasui T, et al. Impact of insulin resistance, insulin and adiponectin on kidney stones in the Japanese population. Int J Urol. 2011;18(2):131-8.
220. Taguchi K, Okada A, Yasui T, Kobayashi T, Ando R, Tozawa K, et al. Pioglitazone, a peroxisome proliferator activated receptor γ agonist, decreases renal crystal deposition, oxidative stress and inflammation in hyperoxaluric rats. J Urol. 2012;188(3):1002-11.
221. Chen Z, Yuan P, Sun X, Tang K, Liu H, Han S, et al. Pioglitazone decreased renal calcium oxalate crystal formation by suppressing M1 macrophage polarization via the PPAR-γ-miR-23 axis. Am J Physiol Renal Physiol. 2019;317(1):F137-f51.
222. Grases F, Prieto RM, Fernandez-Cabot RA, Costa-Bauzá A, Tur F, Torres JJ. Effects of polyphenols from grape seeds on renal lithiasis. Oxid Med Cell Longev. 2015;2015:813737.
223. Prabhu VV, Sathyamurthy D, Ramasamy A, Das S, Anuradha M, Pachiappan S. Evaluation of protective effects of diosmin (a citrus flavonoid) in chemical-induced urolithiasis in experimental rats. Pharm Biol. 2016;54(9):1513-21.
224. Farzaei MH, Abdollahi M, Rahimi R. Role of dietary polyphenols in the management of peptic ulcer. World J Gastroenterol. 2015;21(21):6499-517.
225. Gürocak S, Küpeli B. Consumption of historical and current phytotherapeutic agents for urolithiasis: a critical review. J Urol. 2006;176(2):450-5.
226. Byahatti VV, Pai KV, D'Souza MG. Effect of Phenolic Compounds from Bergenia ciliata (Haw.) Sternb.leaves on Experimental kidney stones. Anc Sci Life. 2010;30(1):14-7.
227. Joshi VS, Parekh BB, Joshi MJ, Vaidya AD. Inhibition of the growth of urinary calcium hydrogen phosphate dihydrate crystals with aqueous extracts of Tribulus terrestris and Bergenia ligulata. Urol Res. 2005;33(2):80-6.
228. Lien EJ, Lien LL, Wang R, Wang J. Phytochemical analysis of medicinal plants

with kidney protective activities. Chin J Integr Med. 2012;18(10):790-800.

229. Saha S, Verma RJ. Inhibition of calcium oxalate crystallisation in vitro by an extract of Bergenia ciliata. Arab J Urol. 2013;11(2):187-92.

230. Amengual-Cladera E, Nadal-Casellas A, Gómez-Pérez Y, Gomila I, Prieto RM, Proenza AM, et al. Phytotherapy in a rat model of hyperoxaluria: the antioxidant effects of quercetin involve serum paraoxonase 1 activation. Exp Biol Med (Maywood). 2011;236(10):1133-8.

231. Luca SV, Macovei I, Bujor A, Miron A, Skalicka-Woźniak K, Aprotosoaie AC, et al. Bioactivity of dietary polyphenols: The role of metabolites. Crit Rev Food Sci Nutr. 2020;60(4):626-59.

232. Park HK, Jeong BC, Sung MK, Park MY, Choi EY, Kim BS, et al. Reduction of oxidative stress in cultured renal tubular cells and preventive effects on renal stone formation by the bioflavonoid quercetin. J Urol. 2008;179(4):1620-6.

233. Ghodasara J, Pawar A, Deshmukh C, Kuchekar B. Inhibitory effect of rutin and curcumin on experimentally-induced calcium oxalate urolithiasis in rats. Pharmacognosy Res. 2010;2(6):388-92.

234. Zhu W, Xu YF, Feng Y, Peng B, Che JP, Liu M, et al. Prophylactic effects of quercetin and hyperoside in a calcium oxalate stone forming rat model. Urolithiasis. 2014;42(6):519-26.

235. Zhong X, Zhang L, Li Y, Li P, Li J, Cheng G. Kaempferol alleviates ox-LDL-induced apoptosis by up-regulation of miR-26a-5p via inhibiting TLR4/NF-κB pathway in human endothelial cells. Biomed Pharmacother. 2018;108:1783-9.

236. Sun Z, Li Q, Hou R, Sun H, Tang Q, Wang H, et al. Kaempferol-3-O-glucorhamnoside inhibits inflammatory responses via MAPK and NF-κB pathways in vitro and in vivo. Toxicol Appl Pharmacol. 2019;364:22-8.

237. Zhang H, Li N, Li K, Li P. Protective effect of Urtica dioica methanol extract against experimentally induced urinary calculi in rats. Mol Med Rep. 2014;10(6):3157-62.

238. Li J, Wen Q, Feng Y, Zhang J, Luo Y, Tan T. Characterization of the multiple chemical components of Glechomae Herba using ultra high performance liquid chromatography coupled to quadrupole-time-of-flight tandem mass spectrometry with diagnostic ion filtering strategy. J Sep Sci. 2019;42(7):1312-22.

239. Olayeriju OS, Papetti A, Colombo R, Mannucci B, Olaleye MT, Akindahunsi AA.

Phytochemical profiling of aqeous methanolic leaf extract of Triclisia gilletii by gas chromatography (GC/MS) and liquid chromatography (HPLC-PDA-ESI/MS(n)) tandem mass spectroscopy (MS): a pointer to its nephroprotection. Nat Prod Res. 2022;36(8):2171-6.

240. Xu X, Chen J, Lv H, Xi Y, Ying A, Hu X. Molecular mechanism of Pyrrosia lingua in the treatment of nephrolithiasis: Network pharmacology analysis and in vivo experimental verification. Phytomedicine. 2022;98:153929.

241. Anders HJ, Suarez-Alvarez B, Grigorescu M, Foresto-Neto O, Steiger S, Desai J, et al. The macrophage phenotype and inflammasome component NLRP3 contributes to nephrocalcinosis-related chronic kidney disease independent from IL-1-mediated tissue injury. Kidney Int. 2018;93(3):656-69.

242. Xi J, Chen Y, Jing J, Zhang Y, Liang C, Hao Z, et al. Sirtuin 3 suppresses the formation of renal calcium oxalate crystals through promoting M2 polarization of macrophages. J Cell Physiol. 2019;234(7):11463-73.

243. Naghii MR, Babaei M, Hedayati M. Androgens involvement in the pathogenesis of renal stones formation. PLoS One. 2014;9(4):e93790.

244. Zand RS, Jenkins DJ, Diamandis EP. Steroid hormone activity of flavonoids and related compounds. Breast Cancer Res Treat. 2000;62(1):35-49.

245. Wang H, Gao M, Wang J. Kaempferol inhibits cancer cell growth by antagonizing estrogen-related receptor α and γ activities. Cell Biol Int. 2013;37(11):1190-6.

246. Da J, Xu M, Wang Y, Li W, Lu M, Wang Z. Kaempferol Promotes Apoptosis While Inhibiting Cell Proliferation via Androgen-Dependent Pathway and Suppressing Vasculogenic Mimicry and Invasion in Prostate Cancer. Anal Cell Pathol (Amst). 2019;2019:1907698.

Attachment

Important detailed information on reagents and equipment can be found in the “2. Materials and methods” section.

One publication resulting from the dissertation: Yuan P, Sun X, Liu X, Hutterer G, Pummer K, Hager B, et al. Kaempferol alleviates calcium oxalate crystal-induced renal injury and crystal deposition via regulation of the AR/NOX2 signaling pathway. Phytomedicine. 2021; 86:153555.